THE THEORY OF ELECTRON HEATING IN COLLISIONLESS PLASMA SHOCK WAVES

A. J. F. Buckner

A Thesis Submitted for the Degree of PhD
at the
University of St Andrews

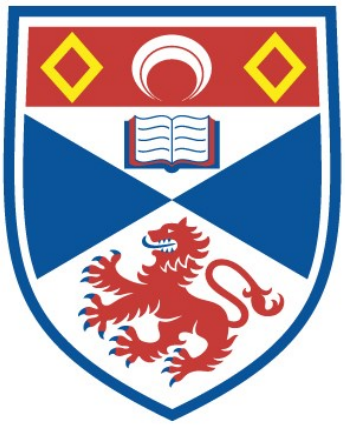

1993

THE THEORY OF ELECTRON HEATING IN COLLISIONLESS PLASMA SHOCK WAVES.

A.J.F.BUCKNER

THESIS SUBMITTED IN SEPTEMBER 1992 TO THE FACULTY OF SCIENCE OF THE UNIVERSITY OF ST. ANDREWS FOR THE DEGREE OF DOCTOR OF PHILOSOPHY

ProQuest LLC.
789 East Eisenhower Parkway
P.O. Box 1346
Ann Arbor, MI 48106 – 1346

To Lisa, my wife

Abstract

Equations are derived to describe the evolution of an electron distribution function under the action of electromagnetic instabilities in a non-uniform plasma using an extension of the quasilinear theory of Kennel and Engelmann. Variations in both the electron density and temperature and the background magnetic field are taken into account. These equations are simplified in the limit of small electron beta so that an electrostatic approximation is justified. Methods are then presented which allow the solution of these equations (or, in principle, the more complex electromagnetic equations). In particular, a method of solving the kinetic dispersion relation for an arbitrary background (first-order) distribution function with the minimum of additional asumptions and approximations is described in detail. The electrostatic equations are solved for a number of different cases in order to study the action of the modified two stream instability on the electron distribution function. Throughout, realistic values of the ratios of electron to ion mass and electron plasma to cyclotron frequency ratio are used. The applications to collisionless plasma shock waves are discussed, and it is found that the modified two stream instability can produce the (relatively small) amounts of electron heating observed at quasi-perpendicular terrestrial bow shocks, and the flat-topped electron distribution functions seen to evolve.

Extensions to the model which would greatly improve its applicability and accuracy, as well as the amount of computational effort required, are discussed.

Acknowledgements

It gives me great pleasure to thank the following people:

My supervisor, Professor R. A. Cairns, for his help, guidance and encouragement over the last four years;

Dr. R. Bingham for his hospitality and seemingly unbounded enthusiasm for plasma physics;

All the denizens of Room 226 over the years I have been a postgraduate student in the mathematics department: Alastair McGowan, Amin, Andy Miller, Helen Holt, David Johnson and Darren McDonald;

The staff of the Computing Laboratory at St. Andrews (especially Drs. John Henderson and Hania Allen and Dave Crust) for their advice and help;

Everbody in the Child Health Department at Ninewells Medical School and the Department of Mangement in St. Andrews for their support and encouragement;

The VAX and SUN computers of the Unviversity of St. Andrews, but especially the VAXs: I miss you.

The Science and Engineering Research Council, for financial assistance;

Lisa, without whom I could and would never have written this thesis.

Certificate

I certify that A.J.F.Buckner has satisfied the conditions of the Ordinance and Regulations and is thus qualified to submit the accompanying application for the Degree of Doctor of Philosophy.

Postgraduate career

I was admitted into the University of St. Andrews as a research student under Ordinance General No. 12 in October 1988 to work on collisionless plasma shock waves under the supervision of Professor R. A. Cairns. I was admitted under the above resolution as a candidate for the Degree of Doctor of Philosophy in October 1989.

Declaration

I declare that the following thesis is a record of research work carried out by me, that the thesis is my own composition, and that it has not been previously submitted in application for a higher degree.

In submitting this thesis to the University of St. Andrews, I understand that I am giving permission for it to be made available for use in accordance with the regualations of the University Library for the time being in force, subject to any copyright vested in the work not being affected thereby. I also understand that the title and abstract will be published, and that a copy of the work may be made and supplied to any *bona fide* library or research worker.

Contents

Chapter 1

Introduction

1.1 Shock waves

A shock wave is a transition layer across which the properties of a medium change from one set of values to another, different, set. Viewed from a frame of reference which moves with the shock, the medium flows into the shock from one side (the upstream side), is slowed down, deflected (in general), and heated up: the medium's ordered streaming energy on the upstream side is partially converted into random thermal energy on the downstream side. Shocks arise from the steepening of a finite amplitude wave due to nonlinear effects; the speed at which a point on the wave travels increases with the amplitude of the wave at that point, [29] so that the crest of the wave tends to catch up with the trough: it must be prevented from overtaking the trough by some physical mechanism, since otherwise quantities such as density, velocity and pressure would become multiply-valued functions of position. For a steady state structure to exist, there must be some mechanism present to counteract the nonlinear wave steepening, so that, eventually, a transition layer of finite thickness will be formed. In shock waves occurring in fluids, this mechanism is viscosity, which is due to the collisions between the molecules that make up the fluid. Dimensional arguments suggest

that the thickness of the shock should be of the order of the mean free path of the fluid [45], as is found to be the case.

If we attempt to apply these ideas to collisionless plasmas (that is to say, most plasmas of interest), then we find that the width of the shock region is implausibly high: for example, in the solar wind plasma, the mean free path λ is of the order of an Astronomical Unit (1 A.U. $\approx 1.5 \times 10^{11}$ m.), whereas the width of the shock transition layer may only be tens of kilometres thick. In the laboratory, shocks are observed in devices whose dimensions are smaller than λ. Thus we must identify a mechanism capable of producing dissipation in a collisionless plasma.

In a neutral fluid, the only means by which energy and momentum can be transported are by binary collisions between molecules. These are 'short range' interactions in the sense that particles can only affect the motion of other particles when they are in close proximity to one another. In a plasma, on the other hand, because the individual particles possess non-zero electrical charge, variations in their density and mean velocity can set up fluctuating electric and magnetic fields capable of propagating large distances. Other particles may 'collide' with these waves, resulting in energy and momentum transfer. In other words, particles can interact collectively as well as on an individual basis, and hence 'dissipation' is still possible without any classical collisions.

1.2 Governing equations

To describe the behaviour of a collisionless magnetised plasma, we will use the Vlasov-Maxwell system of equations. This employs a statistical description with a continuous six-dimensional phase fluid of density F_s for each particle species s ($s = i$ for positive ions, i.e. protons, and $s = e$ for electrons). The quantity $F_s(\mathbf{r}, \mathbf{v}, t)d\mathbf{r}d\mathbf{v}$ gives the number of particles with velocity between $\mathbf{v}$ and $\mathbf{v} + d\mathbf{v}$ and position between $\mathbf{r}$ and $\mathbf{r} + d\mathbf{r}$ at time t. F_s, the distribution function, obeys

a continuity-type equation:

$$\frac{\partial F_s}{\partial t} + \mathbf{v}.\frac{\partial F_s}{\partial \mathbf{r}} + \frac{q_s}{m_s}\left(\mathbf{E} + \mathbf{v} \wedge \mathbf{B}\right).\frac{\partial F_s}{\partial \mathbf{v}} = 0 \tag{1.1}$$

This expresses the fact that, in the absence of collisions, the rate of change of F_s along a particle trajectory is zero.

The electric and magnetic fields $\mathbf{E}$ and $\mathbf{B}$ are determined from the charge and current densities ρ and $\mathbf{j}$ by Maxwell's equations:

$$\frac{\partial}{\partial \mathbf{r}} \wedge \mathbf{B} = \mu_0 \mathbf{j} + \frac{1}{c^2}\frac{\partial \mathbf{E}}{\partial t} \tag{1.2}$$

$$\frac{\partial}{\partial \mathbf{r}} \wedge \mathbf{E} = -\frac{\partial \mathbf{B}}{\partial t} \tag{1.3}$$

$$\frac{\partial}{\partial \mathbf{r}} \cdot \mathbf{B} = 0 \tag{1.4}$$

$$\frac{\partial}{\partial \mathbf{r}} \cdot \mathbf{E} = \frac{\rho}{\varepsilon_0} \tag{1.5}$$

and the charge and current densities are obtained from the distribution functions by

$$\rho = \sum_s q_s \int F_s d\mathbf{v} \tag{1.6}$$

$$\mathbf{j} = \sum_s q_s \int \mathbf{v} F_s d\mathbf{v} \tag{1.7}$$

These equations constitute a closed, but hopelessly intractable, set.

We can take the average of equation(1.1) to obtain

$$\frac{\partial f_s}{\partial t} + \mathbf{v}.\frac{\partial f_s}{\partial \mathbf{r}} + \frac{q_s}{m_s}\left(\mathbf{E}_0 + \mathbf{v} \wedge \mathbf{B}_0\right).\frac{\partial f_s}{\partial \mathbf{v}} = C_s \tag{1.8}$$

where

$$C_s = -\frac{q_s}{m_s}\frac{\partial}{\partial \mathbf{v}} \cdot \left\langle \left(\delta\mathbf{E} + \mathbf{v} \wedge \delta\mathbf{B}\right) \delta f_s \right\rangle \tag{1.9}$$

The angle brackets denote that the quantity within is to be averaged in some way, and $f_s = \langle F_s \rangle$ and $\delta f_s = F_s - \langle F_s \rangle$. $\mathbf{E}_0$ and $\mathbf{B}_0$ are the averaged electric and

magnetic fields, and $\delta\mathbf{E}$ and $\delta\mathbf{B}$ are the fluctuations of the fields around their average values. Equation (1.8) now looks like the *collisional* Vlasov equation, with C_s acting like a classical term. However, C_s describes not the effect of (short range) particle-particle interactions (as would, for example, a Krook or Fokker-Planck term), but the influence on particles of fields set up by the collective motions of those particles. One important property of C_s is that it does not, in general, lead to the relaxation of an initial, arbitrary, distribution function to a Maxwellian. For example, with no background fields and no perturbed magnetic field we can recover the quasilinear equations of Drummond and Pines ([10]): in the case of an initially Maxwellian background plasma with a weak beam (the bump-on-tail instability), the resulting distribution has a flat 'plateau' in the region of velocity space in which particles have interacted most strongly with waves.

It is easy to show that the 'collision' term C_s satisfies the following identities:

$$\int C_s \, d\mathbf{v} = 0 \tag{1.10}$$

$$\begin{aligned} \frac{\partial}{\partial t}\left[\frac{1}{\mu_0}\langle \delta\mathbf{E} \wedge \delta\mathbf{B}\rangle\right] &+ \frac{\partial}{\partial \mathbf{r}}\left[\frac{1}{2}\varepsilon_0\langle \delta\mathbf{E}^2\rangle + \frac{1}{2\mu_0}\langle \delta\mathbf{B}^2\rangle\right] + \\ \frac{\partial}{\partial \mathbf{r}} \cdot \left[\varepsilon_0\langle \delta\mathbf{E}\delta\mathbf{E}\rangle + \frac{1}{\mu_0}\langle \delta\mathbf{B}\delta\mathbf{B}\rangle\right] &+ \sum_s \int m_s \mathbf{v} C_s \, d\mathbf{v} \\ &= 0 \end{aligned} \tag{1.11}$$

$$\frac{\partial}{\partial t}\left[\frac{1}{2}\varepsilon_0\langle \delta\mathbf{E}^2\rangle + \frac{1}{2\mu_0}\langle \delta\mathbf{B}^2\rangle\right] + \frac{\partial}{\partial \mathbf{r}} \cdot \left[\frac{1}{\mu_0}\langle \delta\mathbf{E} \wedge \delta\mathbf{B}\rangle\right] + \sum_s \int \frac{1}{2} m_s \mathbf{v}^2 C_s \, d\mathbf{v} = 0 \tag{1.12}$$

The first relation simply expresses the fact that particles are neither created nor destroyed by the collision operator, the other two express the rate at which momentum and energy respectively are transferred between fields and particles.

Another conservation relation that can be derived involves entropy. A collisional shock (for example a viscous hydrodynamic shock) will produce entropy. If we take equation (1.1), multiply it by $1 + \ln F_s$ and integrate over velocity, we

find that

$$\frac{\partial}{\partial t}\int F_s \ln F_s d\mathbf{v} + \frac{\partial}{\partial \mathbf{r}} \cdot \int \mathbf{v} F_s \ln F_s d\mathbf{v} = 0 \tag{1.13}$$

so that the entropy satisfies a conservation-type equation. However, if we define the entropy not in terms of the 'full' distribution function F_s but the averaged function f_s, that is $1 + \ln f_s$, then

$$\frac{\partial}{\partial t}\int f_s \ln f_s d\mathbf{v} + \frac{\partial}{\partial \mathbf{r}} \cdot \int \mathbf{v} f_s \ln f_s d\mathbf{v} = \int (1 + \ln f_s) C_s d\mathbf{v} \tag{1.14}$$

and it can be seen that there must be change of entropy across the shock layer, where $C_s \neq 0$.

1.3 Shock classification

When viewed in sufficient detail to be able to discern their small scale structure, collisionless plasma shocks can be seen to be different, dependinq on the values of a number of parameters. The size of the pseudo-collision term introduced above enables one to categorise shocks according to the level of turbulence present within the transition layer:-

1. Laminar shocks:

   Here, the pseudo-collision term C_s is zero, and so there is neither turbulence nor dissipation. In this case, the fluid equations do not have shock-like solutions, but only admit infinite wave-trains or single pulses (solitons) [48]. However, the Vlasov system can be shown to allow shocks [38], [39], since in the kinetic picture, the inclusion of finite Larmor radius effects means that particle reflection is allowed: ions can be bounced off the potential barrier across the shock, thus upsetting the symmetry between the up and downstream sides of the transition layer.

2. Quasi-laminar shocks:

The collision term is non-zero, but the amplitude of the turbulent fluctuations is small, i.e. $|\delta f_s| \ll f_s$. The shock has the appearance of a smooth transition layer, upon which are superimposed lower amplitude, smaller length-scale fluctuations.

3. Turbulent shocks:

   Here, $|\delta f_s| \approx f_s$, and there is no smooth transition layer.

There are various factors which determine into which class a particle shock should fall: below we list some of the most important, and their definitions:-

- ϑ_{Bn}: The angle between the outward pointing normal to the plane of the shock front and the direction of the upstream magnetic field.
- M_{Ms}: Fast magnetosonic Mach number $= V_1/\sqrt{(c_A^2 + c_S^2)}$, where V_1 is the upstream fluid velocity, c_A is the Alfvén wave speed and c_s the sound speed.
- β: This is the ratio of plasma pressure to magnetic pressure, that is:

$$\beta = \frac{n_0 k_B (T_e + T_i)}{B_0^2/(2\mu_0)} \tag{1.15}$$

- α: Ratio of electron plasma and cyclotron frequencies: $\omega_{pe}/\omega ce$
- ρ: Ratio of ion and electron temperatures: T_i/T_e

The level of shock turbulence is very closely related to ϑ_{Bn}. For $\vartheta_{Bn} \leq 10°$, shocks are said to be parallel, and are generally highly turbulent, highly complex structures; for $\arccos(\sqrt{m_e/m_i}) \leq \vartheta_{Bn} \leq 90°$, shocks are said to be perpendicular, and are more laminar; those shocks with values of ϑ_{Bn} inbetween are classed as oblique.

Turbulence increases with both the β and and Mach number of the upstream flow. There is a value of M, the *critical Mach number*, above which purely resistive effects (i.e. those due to anomalous resistivity) are unable to produce

the dissipation necessary to produce a shock, and some phenomenon producing anomalous viscosity must be invoked. As β tends to infinity, the critical Mach number tends to 1, and so all high-β shocks must be supercritical.

1.4 Quasi-Laminar perpendicular shock waves

When the upstream Mach number and plasma beta are both low, and the upstream magnetic field is in the plane of the shock, the physical mechanisms responsible for the shock can be understood, qualitatively speaking at least, fairly easily [6]. Suppose that there is a region in space in which the magnetic field increases over a distance L_s such that

$$a_{the} \ll L_s \ll a_{thi} \tag{1.16}$$

where $a_{th\alpha}$ is the thermal Larmor radius of particle species α. The electrons will perform many gyrations around the magnetic field direction as they drift through the shock with speed

$$u_E = \frac{E_y}{B(x)} \tag{1.17}$$

where $B(x)$ is the magnetic field, which points in the z-direction, perpendicular to the shock normal, E_y is the electric field in the plane of the shock, and x measures distance through the shock. By Maxwell's equations, E_y must be constant, and so the electrons will be slowed down. The ions, however, will not feel the gradient in the magnetic field because of their large Larmor radii, and so an electric field will develop in the x-direction pointing upstream in order to slow them down. This will cause the electrons to drift across the magnetic field (as will the field gradient), the current thus formed being of precisely the correct size to give rise (by Ampere's law) to the increase in the magnetic field that we postulated initially. It would thus seem possible for a steady state structure to exist.

In the absence of any dissipational mechanism, the magnetic field would increase smoothly and monotonically to a maximum value, and then decrease again.

Depending on the boundary conditions imposed upstream of the shock, either the magnetic field will return to its initial value, in which case we will have a solitary pulse propagating through the plasma, or for the field to oscillate, giving a large amplitude wave train. Neither of these situations is a shock. If, however, the cross-field drift current is sufficiently large, it is possible for waves propagating in the plane of the ramp to become unstable. They would then be expected to grow to some level, and then saturate, producing a steady level of anomalous dissipation. It would then be possible for a collisionless shock to form.

Since the ions will in fact have a thermal spread, the electric field pointing out of the shock will be able to reflect those ions with sufficiently small kinetic energy. These are then turned round by the magnetic field and accelerated by the tangential electric field. Usually they will re-enter the shock with sufficient energy to be transmitted. At lower Mach numbers, the proportion of ions reflected is small, but at high Mach numbers the proportion is large enough to enhance the magnetic field upstream of the main magnetic ramp and so to produce a broad 'foot' structure. At high Mach numbers it is this reflected ion population which is responsible for most shock dissipation.

1.5 The Earth's bow shock

It has been known since the late 1950's that the Sun is not in a state of static equilibrium with its surroundings, but is in fact incapable of retaining its hot, tenuous outer atmosphere (the 'Corona') by gravitational attraction. Thus, the whole of the solar system is pervaded by a plasma flowing rapidly away from the surface of the Sun. At the Earth's orbit, the parameters of this solar wind are:

Parameter	*description*	*typical value*
n_i	proton density	$5 \times 10^6 m^{-3}$
V_i	bulk speed	250 - 800 km/s
T_i	ion temperature	$7 \times 10^4 K$
T_e	electron temperature	$1.5 \times 10^5 K$
c_A	Alfvén speed	50 - 100 km/s
$c_{MS} = V_1/\sqrt{(c_A^2 + c_S^2)}$	Magnetosonic speed	60 - 150 km/s

The electron density and flow velocity are roughly equal to the proton values.

The pressure of the solar wind tends to compress the sunward (daytime) side of the Earth's magnetic field and stretch out the nightside field into a long tail (see Fig 1.1). A magnetic cavity, the magnetosphere, is formed around the Earth, extending out to a distance of about 10-11 Earth radii, with the solar wind flow pressure being approximately balanced by the magnetic pressure of the Earth's field. The solar wind is forced to flow around the boundary (the magnetopause) of the cavity. This flow is clearly supersonic with respect to the sound, Alfvén and magnetosonic wave speeds, and so a stand-off shock wave forms about 2-5 Earth radii upstream of ther magnetopause, just as happens when a blunt body travels supersonically through a fluid medium. The region between the shock wave and the magnetopause is known as the magnetosheath, and consists of shocked, subsonic, heated, turbulent plasma.

It was first hypothesised that shocks could in fact occur in the solar wind in order to explain the apparently paradoxically rapid onset of magnetic storms caused by solar flares. It seemed that otherwise the particles produced by the flare would have to have an implausibly narrow velocity spread ($\delta v/v \sim 10^{-3}$) in order to account for the observed rise time of the storm, about a minute. The first actual experimental observation of the bow shock seems to have been made by the magnetometer carried on board the IMP-1 spacecraft in 1963 [40]. Because the

solar wind parameters can vary by several orders of magnitude over a period of several months, the terrestrial bow shock is a valuable 'laboratory' for the study of shock physics. Multiple satellite missions, such as ISEE (International Sun-Earth Explorer) and AMPTE (Active Magnetospheric Particle Tracer Explorers), have made it possible to distinguish between time and space variations in plasma quantities, and the degree of sophistication of the instrumentation carried on board has made it possible to to make highly accurate measurements on both plasma and field quantities.

1.6 Numerical Studies of Collisionless Shock waves

Although the terrestrial bow shock does provide an excellent opportunity to study collisionless shocks, it does have a number of drawbacks, not least the cost and complication of transporting measuring equipment up into space. More fundamentally, it is impractical to make simultaneous observations on the shock at more than a few locations. As in other branches of plasma physics, the difficulty of experiment and the intractability of the governing equations has made the numerical simulation of plasma phenomena an attractive option. The first attempt to model a shock numerically was due to Colgate and Hartman [7] who used the charged sheet of Dawson [9] to simulate an electrostatic shock. The majority of computer codes written to study shock physics fall into three categories [34]:

Fluid codes: The multi-species fluid equations (conservation of mass, momentum, energy) are augmented by 'phenomenological' terms describing microscopic effects, which are outwith a purely fluid description;

Particle codes:	The motions of a sufficiently large number of particles are followed;
Hybrid codes:	A particle description is used for the ions, and a fluid description for the electrons.

Fluid codes have the virtue of requiring the least computational effort of the methods, but the description is clearly not self-consistent in that microinstablities cannot be modelled directly, and so anomalous transport terms must be included (recall that without viscosity or resistivity, classical or otherwise, the fluid equations do not support shock solutions). Other physical effects, such as particle reflection and trapping, are also absent.

These disadvantages would seem to be solved by full particle simulations [23]. The principle behind them is in fact very simple: given the positions and velocities of the particles at time t, charge and current are assigned to a mesh of points in configuration space. Maxwell's equations are solved for the electric and magnetic fields, which are then given on the mesh. The force at each particle is calculated by interpolation, and Newton's law of motion is then integrated for each particle to give its position and velocity at time $t + \delta t$, where δt is a time step. This process is repeated many times to follow the evolution of the plasma over a time of perhaps a few tens of ion gyroperiods. For a realistic result, a large number of particles must be employed, the number becoming successively larger as the number of dimensions is increased. For the numerical integration scheme to be stable, the code must be able to follow the motions of the electrons, so that the size of the electron plasma frequency imposes an upper limit on the time step. This problem is often alleviated by using an unphysically large value of the electron-ion mass ratio and/or the electron cyclotron-plasma frequency ratio. Both of these can limit the applicability of the results when the identification of a specific plasma instablility is to be made. Again, hybrid codes are much

more economical in terms of computer time and storage space, but the detailed electron dynamics cannot be studied.

1.7 Outline of Contents

In chapter two we outline the principle features of the various instabilities that have been proposed to account for the anomalous resistive dissipation in collisionless plasma shock waves, and review their applicability. We then derive a linear dispersion relation relating the complex frequency of an electromagnetic wave to its wavenumber. We simplify this dispersion relation to the case of electrostatic waves.

Chapter three contains a derivation of the quasilinear equations, which extends the theory of chapter two to allow for the reaction of the unstable electromagnetic waves on the electron distribution function. It is shown that an asymptotic steady state must be reached in which all the waves excited evolve towards a state of marginal stability. Again, the electrostatic limit is recovered. In the next chapter we discuss in some detail the numerical methods that we chose to solve the system of quasilinear equations, and the rationale behind their choice. Although the equations were only solved for electrostatic waves, it is possible to extend the methods to electromagnetic waves: however, the complexity of the equations would mean that considerable computational resources would be required.

In chapter five we present results obtained by the numerical computer code, and discuss their applicability to the shock problem.

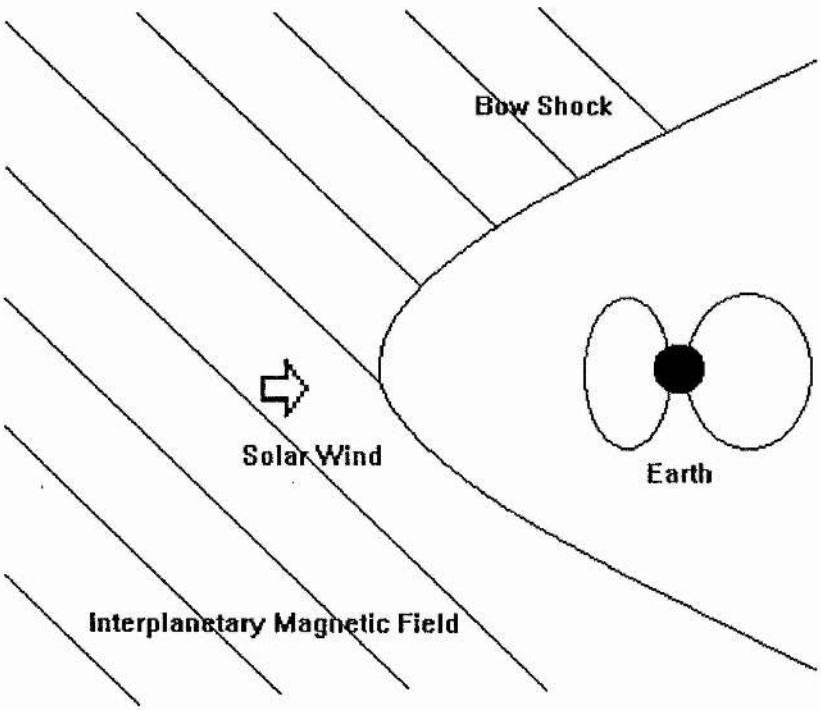

Figure 1.1: The near Earth environment

Chapter 2

Linear stability theory

2.1 Current driven instabilities in collisionless plasma shock waves

There are several different instabilities that could conceivably occur in the ramp of a low Mach number perpendicular collisionless shock wave, and here we intend to review the properties of some of them. In order to be a likely contender as a mechanism for producing the "dissipation" required for a resistive shock wave, an instability must satisfy a number of criteria [13],[34]:-

1. Any threshhold value above which the instability occurs must be satisfied;
2. The growth rate must be large enough for the instability to grow to a significant level in the time it takes for the plasma to flow through the shock;
3. The instability must not saturate at too low a level;
4. The excited waves must be able to heat the plasma.

Clearly, the first stage of any study of resistive heating must be a linear stability analysis to ascertain whether or not a specific instability mechanism will satisfy

the first two criteria under realistic physical conditions. Analysis of the other two criteria is necessarily nonlinear.

Among those instabilities that could occur are [13], [34],[41]:-

1. The Buneman (Two Stream) Instability

   This is the simplest of the streaming instabilities, and does not include the effects of the background magnetic field. Since it requires a relative electron-ion drift velocity greater than the electron thermal velocity, it seems unlikely to occur in a collisionless shock.

2. The Ion Acoustic Instability

   Ion acoustic waves can propagate through an unmagnetised plasma at phase velocities larger than the ion thermal velocity but smaller than the electron thermal velocity. If the ions are sufficiently cold, then the wave phase velocity lies on a virtually flat region of the ion distribution function, and there is little damping. For wavelengths much larger than the electron Debye length, the dispersion relation is similar to that for an acoustic wave, hence the name. Its nonlinear heating effects were studied early on [26], [27]. For typical bow shock parameters, where usually the ion and electron temperatures are roughly the same, the cross-field currents generated in the shock ramp are not large enough to give rise to the ion acoustic instability.

3. Bernstein Wave Instabilities

   Bernstein waves are electron waves that can propagate at right angles to the background magnetic field of a plasma at multiples of the electron cyclotron frequency without damping or growth [5]. If ion dynamics are included and the electrons are allowed to drift across the field, then at the points where the dispersion curves of the ion acoustic and Bernstein waves cross instability can occur [16],[14]. The waves have short wavelengths ($ka_{the} \gg 1$) and high frequencies ($\omega > \omega_{ce}$). The main attraction of these instabilities is

the fact that they can exist for arbitrary values of the electron-ion temperature ratio: however they are stabilised by the effects of either a magnetic field gradient or of orbit modifications by turbulent fields, both of which tend to 'smear out' the cyclotron resonances on which the instabilities are critically dependent. Very closely related is the beam cyclotron instability [30],[31], where the difference seems to be that the analysis is carried out in the electron, rather than the ion, rest frame. This class of instabilities is probably unimportant in shocks, because the instability saturates at too low a level to produce a high enough level of anomalous resistivity.

Lashmore-Davies [32] [33] has pointed out that in the presence of drifts the Bernstein waves have negative energy, so that the ions can absorb energy from the electron waves through the Landau resonance, causing the amplitude of the wave to grow.

4. The Lower Hybrid Drift Instability

Low frequency instabilities propagating perpendicularly to an inhomogeneous magnetic field have been studied for electrostatic [28] and electromagnetic waves [8],[17]. The instability propagates perpendicularly with wavenumber $ka_{the} \approx 1$) and frequency and growth rate both of the order of the lower hybrid frequency $\omega_{LH} = \omega_{pi}\,[1 + \omega_{pe}/\omega_{ce}]^{-1/2}$. The ions can be taken to be unmagnetised, but the electrons are strongly magnetised. There are gradients in the magnetic field, the density and the temperature. Despite a relatively low growth rate and long wavelength, it does seem to be able to heat both ions and electrons [43]. For non-perpendicular propagation, the instability is termed the generalised lower hybrid drift instability[24]: for electrons with finite temperature, the behaviour of the instability is complex.

5. The Modified Two Stream Instability

The modified two stream [35]is similar in nature to the lower hybrid drift instability. However, the analysis of the modified two stream instability generally neglects density gradient effects but includes a component of the wavenumber vector parallel to the magnetic field. Like the lower hybrid drift instability, it is a low frequency instability ($\omega \ll \omega_{ce}$). The effect of a magnetic field gradient is to reduce the growth rate slightly [13]. Its properties are insensitive the the ion-electron temperature ratio and the electron plasma to cyclotron frequency ratio. Electromagnetic effects tend to stabilise it for low beta and near perpendicular propagation when the relative ion-electron drift speed is greater then the Alfvén wave speed. Analysis of the instability under conditions typical of a laboratory shock experiment [13], using an estimate of the expected anomalous resistivity [15] suggest that it is unlikely to produce significant electron heating. The heating rates of the modified two-stream and ion acoustic instabilities have been compared under conditions in space shocks [51] using a model based on second-order Vlasov theory. It was found that the shock widths, amounts of anomalous heating, and electric field energy predicted by the modified two stream instability were in good agreement with observations of a number of subcritical bow shock crossings, whereas the ion acoustic gave rise to much narrower shocks than observed in order to generate the larger cross-field drifts it required for the given electron-ion temperature ratios. For finite electron beta, the instability becomes the kinetic cross-field streaming instability: this is not necessarily stabilised by electromagnetic effects for large drift velocities.

6. Parallel Drift-driven Instabilities

In non-perpendicular shock waves there will be a component of the background electric field parallel to the background magnetic field. This can

accelerate a portion of the electron population parallel along the electric field, producing an offset peak in the electron distribution function, which can then become unstable to parallel propagating ion and electron acoustic waves[46], possibly leading to parallel electron heating. The height of the offset peak is observed to decrease through the shock, suggesting the action of wave-particle interactions.

2.2 The linearised Vlasov equation

In order to determine whether a given electron equilibrium distribution is stable or unstable to small perturbations, we split all particle and field quantities into time-independent background parts and rapidly varying fluctuating parts. In all of what follows, we shall use a Cartesian co-ordinate system with the z axis aligned along the magnetic field, which is assumed to have no curvature or shear, and the x axis to be in the direction in which the background quantities vary, with the magnetic field increasing with increasing x. The y axis is chosen so that the axes form a right-handed set (see figure 2.1). Thus:-

$$F_e(\mathbf{r},\mathbf{v},t) = f_e(\mathbf{r},\mathbf{v}) + \delta f_e(\mathbf{r},\mathbf{v},t) \tag{2.1}$$

$$\mathbf{H}(\mathbf{r},t) = \mathbf{H}_0(x) + \delta\mathbf{H}(\mathbf{r},t) \tag{2.2}$$

where H is any of the field quantities. It is a consequence of our assumption of slab geometry that the background fields vary with x only. The background magnetic field is taken to be:

$$\mathbf{B}_0 = B_0(x)\hat{\mathbf{e}}_{\|} = B_0(1+\epsilon_B x)\hat{\mathbf{e}}_{\|}$$

and the background electric field to be:

$$\mathbf{E}_0 = (E_x, 0, 0)$$

The value of E_x is not independent, but is related to the background gradients by Ampére's law:-

$$\nabla \wedge \mathbf{B_0} = \mu_0 \mathbf{j_0} = \mu_0 n_0 \left(v_E + v_N\right) \hat{\mathbf{e}}_y \tag{2.3}$$

where $v_N = -\epsilon_N v_{the}^2/\omega_{ce}$ is the drift velocity in the y-direction due to the density gradient. This gives:

$$E_x = -\frac{B_0^2}{\mu_0 n_0 e}\epsilon_B - \frac{\epsilon_N v_{the}^2}{\omega_{ce}} \tag{2.4}$$

The quantity ϵ_B is of the order of the reciprocal of the length of the shock. We shall assume that the quantity $\epsilon_B v_{the}/\omega_{ce}$ is small, as the electrons will perform many gyro-orbits as they travel through the shock.

On assuming that the perturbed quantities are much smaller then the background quantities, and neglecting products of small quantities, the Vlasov equation becomes:-

$$v_x \cdot \frac{\partial f_e}{\partial x} - \frac{e}{m_e}\left[\mathbf{E_0} + \mathbf{v} \wedge \mathbf{B_0}\right] . \frac{\partial f_e}{\partial \mathbf{v}} = 0 \tag{2.5}$$

and

$$\frac{\partial}{\partial t}\delta f_e + \mathbf{v} . \frac{\partial}{\partial \mathbf{r}}\delta f_e - \frac{e}{m_e}\left[\mathbf{E_0} + \mathbf{v} \wedge \mathbf{B_0}\right] . \frac{\partial}{\partial \mathbf{v}}\delta f_e = \frac{e}{m_e}\left[\delta\mathbf{E} + \mathbf{v} \wedge \delta\mathbf{B}\right] . \frac{\partial f_e}{\partial \mathbf{v}} \tag{2.6}$$

Equation 2.5 can be shown to be satisfied if f_e is of the form:

$$f_e = f_e(\Lambda, v_\perp, v_\parallel)$$

where $\Lambda = \omega_{ce} x - (v_y - v_E)$, $v_\perp^2 = v_x^2 + (v_y - v_E)^2$, and $v_E = -E_x/B_0$ is the 'E cross B' drift velocity in the y-direction.

2.3 The perturbed electron distribution function

We now solve (2.6): its left-hand side is the derivative of f_e along the particle orbits in the unperturbed fields. Thus, we can integrate both sides with respect to t:

$$\delta f_e = \frac{e}{m_e}\int_{-\infty}^{t} [\delta\mathbf{E}(\mathbf{r}',t') + \mathbf{v}' \wedge \delta\mathbf{B}(\mathbf{r}',t')] \cdot \frac{\partial}{\partial \mathbf{v}'} f_e(\mathbf{v}',\mathbf{r}',t')\, dt' \qquad (2.7)$$

The lower limit of the integral has been taken to be $-\infty$, that is, we have ignored the effects of the initial values of the perturbed quantities. This integral will only converge for growing modes: damped waves may be dealt with by analytic continuation of the final dispersion relation. The perturbed Vlasov equation should be solved by a Laplace transform method, yielding the dispersion relation in the limit of large time, but this method is considerably more complicated mathematically. The dashed quantities satisfy the unperturbed orbit equations, viz.:

$$\frac{d\mathbf{v}'}{dt'}(t') = -\frac{e}{m_e}[\mathbf{E}_0(\mathbf{r}',t') + \mathbf{v}'(t') \wedge \mathbf{B}(\mathbf{r}',t')] \qquad (2.8)$$

$$\frac{d\mathbf{r}'}{dt'}(t') = \mathbf{v}'(t') \qquad (2.9)$$

with the initial conditions that $\mathbf{v}'(t'=t) = \mathbf{v}$ and $\mathbf{r}'(t'=t) = \mathbf{r}$. With the background magnetic fields of the form used here, equation (2.8) can be solved exactly in terms of elliptic integrals. However, on our assumption of weak inhomogeneity, we only need the first-order solutions, namely:

$$v_x'(t') = v_\perp \cos(\omega_{ce}(t'-t) + \vartheta)$$

$$v_y'(t') = v_\perp \sin(\omega_{ce}(t'-t) + \vartheta) + v_D$$

$$v_\parallel'(t') = v_\parallel$$

$$
\begin{aligned}
x'(t') &= x(t) + \frac{v_\perp}{\omega_{ce}}\left[\sin(\omega_{ce}(t'-t)+\vartheta) - \sin(\vartheta)\right] \\
y'(t') &= y(t) - \frac{v_\perp}{\omega_{ce}}\left[\cos(\omega_{ce}(t'-t)+\vartheta) - \cos(\vartheta)\right] + v_D(t'-t) \\
z'(t') &= z(t) + v_{||}(t'-t)
\end{aligned}
$$

Here, $v_D = v_E + v_B$ is the total drift velocity in the y-direction due to the 'E cross B' drift v_E and the magnetic field gradient drift $v_B = -\frac{1}{2}\epsilon_B v_\perp^2/\omega_{ce}$. All perturbed quantities are now assumed to vary harmonically, so that:

$$
\begin{aligned}
\delta\mathbf{B}(\mathbf{r},\mathbf{t}) &= \delta\tilde{\mathbf{B}}_\mathbf{k}(x)\exp[i(\mathbf{k}.\mathbf{r} - \Omega_\mathbf{k} t)] && (2.10)\\
\delta\mathbf{E}(\mathbf{r},\mathbf{t}) &= \delta\tilde{\mathbf{E}}_\mathbf{k}(x)\exp[i(\mathbf{k}.\mathbf{r} - \Omega_\mathbf{k} t)] && (2.11)\\
\delta\mathbf{f_e}(\mathbf{r},\mathbf{v},\mathbf{t}) &= \delta\tilde{\mathbf{f}}_{\mathbf{ek}}(x,\mathbf{v})\exp[i(\mathbf{k}.\mathbf{r} - \Omega_\mathbf{k} t)] && (2.12)
\end{aligned}
$$

We only consider waves in the y-z plane, so that $\left(0, k_\perp, k_{||}\right)$. Waves thus propagate perpendicularly to both the background magnetic field and the direction in which the quantities have been taken to vary. $\Omega_\mathbf{k} = \omega_\mathbf{k} + i\gamma_\mathbf{k}$, where $\omega_\mathbf{k}$ is the frequency, and $\gamma_\mathbf{k}$ the growth rate. Faraday's law can now be used to write the perturbed magnetic field in terms of the perturbed electric field in (2.7), giving

$$
\delta\tilde{\mathbf{B}}_\mathbf{k} = \frac{\mathbf{k}\wedge\delta\tilde{\mathbf{E}}_\mathbf{k}}{\Omega_\mathbf{k}} \qquad (2.13)
$$

and the solutions to the orbit equations can be used to write the derivative of f_e with respect to the primed velocity co-ordinates in terms of Λ, $v_\perp$ and $v_{||}$, all of which are constants of the motion. After changing the integration variable from t' to $\tau = t' - t$, we find:

$$
\begin{aligned}
\delta f_e &= \exp[-i(\mathbf{k}.\mathbf{r} - \Omega_\mathbf{k} t)] \\
&\times \frac{e}{m_e}\int_{-\infty}^{0} \exp\left\{i\left[-a_\perp\cos(\omega_{ce}\tau+\vartheta) + a_\perp\cos\vartheta - \bar{\Omega}_\mathbf{k}\tau\right]\right\}\hat{Q}_\mathbf{k} f_e d\tau \qquad (2.14)
\end{aligned}
$$

where $a_\perp = k_\perp v_\perp/\omega_{ce}$, $\bar{\Omega}_\mathbf{k} = \Omega_\mathbf{k} - k_\perp v_D - k_{||}v_{||}$.The operator $\hat{Q}$ is given by:

$$
\hat{Q}_\mathbf{k} = \frac{1}{\Omega_\mathbf{k}}\left[\hat{A}_{0,\mathbf{k}} + e^{-i(\omega_{ce}\tau+\vartheta)}\hat{A}_{-,\mathbf{k}} + e^{i(\omega_{ce}\tau+\vartheta)}\hat{A}_{+,\mathbf{k}}\right] \qquad (2.15)
$$

$$\hat{A}_{0,\mathbf{k}} = \delta\tilde{E}_y\left[(\omega_{\mathbf{k}} - k_\parallel v_\parallel)\left(-\frac{\partial}{\partial\Lambda} + \frac{v_D}{v_\perp}\frac{\partial}{\partial v_\perp}\right) + k_\parallel v_D\frac{\partial}{\partial v_\parallel}\right] \tag{2.16}$$

$$+ \delta\tilde{E}_\parallel\left[k_\perp v_\parallel\left(-\frac{\partial}{\partial\Lambda} + \frac{v_D}{v_\perp}\frac{\partial}{\partial v_\perp}\right) + (\omega_{\mathbf{k}} - k_\perp v_D)\frac{\partial}{\partial v_\parallel}\right]$$

$$\hat{A}_{\pm,\mathbf{k}} = \mp\frac{i}{2}\left[\pm i\delta\tilde{E}_{x,\mathbf{k}}\hat{U}_{\mathbf{k}} + \delta\tilde{E}_{y,\mathbf{k}}\hat{G}_{\mathbf{k}} + \delta\tilde{E}_{\parallel,\mathbf{k}}\hat{H}\right]$$

$$\hat{U}_{\mathbf{k}} = -k_\perp v_\perp\frac{\partial}{\partial\Lambda} + (\omega_{\mathbf{k}} - k_\perp v_E - k_\parallel v_\parallel)\frac{\partial}{\partial v_\perp} + k_\parallel v_\perp\frac{\partial}{\partial v_\parallel} \tag{2.17}$$

$$\hat{G}_{\mathbf{k}} = \left(\Omega_{\mathbf{k}} - k_\parallel v_\parallel\right)\frac{\partial}{\partial v_\perp} + k_\parallel v_\perp\frac{\partial}{\partial v_\perp} \tag{2.18}$$

$$\hat{H} = v_\parallel\frac{\partial}{\partial v_\perp} - v_\perp\frac{\partial}{\partial v_\parallel} \tag{2.19}$$

For this integral to converge, we must have $\Re\{\Omega_{\mathbf{k}}\} > 0$. In order to perform the integration, we use the Bessel function generating function to obtain the identity

$$e^{ia\sin\vartheta} = \sum_{n=-\infty}^{\infty} J_n(a)\, e^{in\vartheta}$$

and thus to write the right-hand side of (2.14) in terms of known integrals. The recurrence relations for the Bessel functions may then be employed to simplify the resulting expression to the following form:

$$\delta\tilde{f}_{e,\mathbf{k}} = i\frac{e}{m_e}\sum_{m=-\infty}^{\infty}\sum_{n=-\infty}^{\infty} e^{-i(m-n)(\vartheta-\pi/2)}\Omega_{n,\mathbf{k}}^{-1}J_m(a_\perp)\hat{F}_{n,\mathbf{k}}f_e \tag{2.20}$$

where

$$\Omega_{n,\mathbf{k}} = \Omega_{\mathbf{k}} - k_\perp v_D - k_\parallel v_\parallel - n\omega_{ce} \tag{2.21}$$

$$\hat{F}_{n,\mathbf{k}} = \frac{1}{\Omega_{\mathbf{k}}}\left[iJ_n'\delta\tilde{E}_{x,\mathbf{k}}\hat{U}_{\mathbf{k}} + J_n\delta\tilde{E}_{y,\mathbf{k}}\hat{V}_{n,\mathbf{k}} + J_n\delta\tilde{E}_{\parallel,\mathbf{k}}\hat{W}_{n,\mathbf{k}}\right] \tag{2.22}$$

$$\hat{V}_{n,\mathbf{k}} = -(\Omega_{\mathbf{k}} - k_\parallel v_\parallel)\frac{\partial}{\partial\Lambda} + (\Omega_{\mathbf{k}} - k_\parallel v_\parallel)\frac{(n\omega_{ce} + k_\perp v_B)}{k_\perp v_\perp}\frac{\partial}{\partial v_\perp}$$

$$+ \frac{k_\parallel}{k_\perp}(n\omega_{ce} + k_\perp v_D)\frac{\partial}{\partial v_\parallel} \tag{2.23}$$

$$\hat{W}_{n,\mathbf{k}} = -k_\perp v_\parallel\frac{\partial}{\partial\Lambda} + v_\parallel\frac{(n\omega_{ce} + k_\perp v_B)}{v_\perp}\frac{\partial}{\partial v_\perp}$$

$$+ (\Omega_{\mathbf{k}} - k_\perp v_D - n\omega_{ce})\frac{\partial}{\partial v_\parallel} \tag{2.24}$$

2.4 The perturbed ion distribution function

As they travel through the shock layer, the ions will be virtually unaffected by the magnetic field, since the ion gyroradius is much larger than the shock thickness. Their orbits can thus be approximated by straight lines. Also, since the frequency of the waves in the shock is much larger than the ion cyclotron frequency, they will behave as if the perturbations are electrostatic. Hence, we can take the perturbed Vlasov equation for the ions to be:

$$\frac{\partial \delta \tilde{f}_{i,\mathbf{k}}}{\partial t} + \mathbf{v}.\frac{\partial \delta \tilde{f}_{i,\mathbf{k}}}{\partial \mathbf{r}} = -\frac{e}{m_i}\delta \tilde{\mathbf{E}}_{\mathbf{k}}.\frac{\partial f_i}{\partial \mathbf{v}}$$

The perturbed ion equation then gives:

$$\delta \tilde{f}_{i,\mathbf{k}} = -i\frac{e}{m_i}\frac{\delta \tilde{\mathbf{E}}_{\mathbf{k}}}{(\Omega_{\mathbf{k}} - \mathbf{k}.\mathbf{v})}\frac{\partial f_i}{\partial \mathbf{v}} \tag{2.25}$$

2.5 The dispersion relation

From Maxwell's curl-B equation, we can derive a wave equation for the Fourier transformed perturbed electric field $\delta \tilde{\mathbf{E}}_{\mathbf{k}}$

$$\mathbf{k} \wedge \left(\mathbf{k} \wedge \delta \tilde{\mathbf{E}}_{\mathbf{k}}\right) = -\frac{\Omega_{\mathbf{k}}^2}{c^2}\delta \tilde{\mathbf{E}}_{\mathbf{k}} - i\Omega_{\mathbf{k}}\mu_0 \sum_s \delta \tilde{\mathbf{j}}_{s,\mathbf{k}} \tag{2.26}$$

where $\delta \tilde{\mathbf{j}}_{s,\mathbf{k}}$ is the Fourier transform of the perturbed current density due to particle species s. The sum is over all particle species. The current density is given in terms of the perturbed distribution function by

$$\delta \tilde{\mathbf{j}}_{s,\mathbf{k}} = q_s \int \mathbf{v} \delta \tilde{f_{s,\mathbf{k}}}\, d\mathbf{v} \tag{2.27}$$

The electron current density can be calculated since we know the perturbed electron distribution function (2.20). Thus, if $\hat{\mathbf{e}_x}$, $\hat{\mathbf{e}_y}$ and $\hat{\mathbf{e}_{||}}$ are unit vectors in the x, y and z directions, then:

$$\begin{aligned}\delta\tilde{\mathbf{j}}_{e,\mathbf{k}} &= -i\frac{e^2}{m_e}\sum_m\sum_n\int\left[v_\perp\cos\vartheta\hat{\mathbf{e}_x}+(v_\perp\sin\vartheta+v_D)\hat{\mathbf{e}_y}+v_\parallel\hat{\mathbf{e}_\parallel}\right]e^{-i(m-n)(\vartheta-\pi/2)}\\ &\qquad \Omega_{n,\mathbf{k}}^{-1}J_m(a_\perp)\hat{F}_{n,\mathbf{k}}f_e\,d\mathbf{v}\\ &= -i\frac{e^2}{m_e}\sum_m\sum_n\int\left[\frac{1}{2}(\hat{\mathbf{e}_x}-i\hat{\mathbf{e}_y})v_\perp e^{i\vartheta}+\frac{1}{2}(\hat{\mathbf{e}_x}+i\hat{\mathbf{e}_y})v_\perp e^{-i\vartheta}+v_D\hat{\mathbf{e}_y}+v_\parallel\hat{\mathbf{e}_\parallel}\right]\\ &\qquad e^{-i(m-n)(\vartheta-\pi/2)}\Omega_{n,\mathbf{k}}^{-1}J_m(a_\perp)\hat{F}_{n,\mathbf{k}}f_e\,d\mathbf{v}\end{aligned}\tag{2.28}$$

Since we have:

$$\frac{1}{2\pi}\int_0^{2\pi}e^{-i(m-n-p)\vartheta}d\vartheta=\delta_{m,n+p}=\begin{cases}1 & m=n+p\\ 0 & \text{otherwise}\end{cases}\tag{2.29}$$

the double summation over m and n collapses to a single summation over n when the theta integration is carried out. Using the Bessel function recurrence relations once again, we finally obtain the following expression for the perturbed electron current density:

$$\begin{aligned}\delta\tilde{\mathbf{j}}_{e,\mathbf{k}} &= -\frac{ie^2}{m_e\Omega_{\mathbf{k}}}\sum_n\int\left[-iv_\perp J_n'(a_\perp)\hat{\mathbf{e}_x}+(n\omega_{ce}+k_\perp v_D)J_n(a_\perp)\hat{\mathbf{e}_y}+k_\parallel J_n(a_\perp)\hat{\mathbf{e}_\parallel}\right]\\ &\qquad \Omega_{n,\mathbf{k}}^{-1}J_m(a_\perp)\hat{F}_{n,\mathbf{k}}f_e\,d\mathbf{v}\end{aligned}\tag{2.30}$$

The perturbed current density for each species can be related to the perturbed electric field through a conductivity tensor $\sigma_{s,\mathbf{k}}$:

$$\delta\tilde{\mathbf{j}}_{s,\mathbf{k}}=\sigma_{s,\mathbf{k}}\cdot\delta\tilde{\mathbf{E}}_{\mathbf{k}}\tag{2.31}$$

The ion conductivity tensor is simply

$$\sigma_{i,\mathbf{k}}=i\frac{e^2}{m_i\Omega_{\mathbf{k}}}\int\frac{\mathbf{v}}{(\Omega_{\mathbf{k}}-\mathbf{k}.\mathbf{v})}\frac{\partial f_i}{\partial\mathbf{v}}\,d\mathbf{v}\tag{2.32}$$

and the electron conductivity is given by:

$$\sigma_{e,\mathbf{k}}=-i\frac{e^2}{m_e\Omega_{\mathbf{k}}}\sum_{n=-\infty}^{+\infty}\int\frac{1}{(\Omega_{\mathbf{k}}-k_\perp v_D-k_\parallel v_\parallel-n\omega_{ce})}\hat{\mathbf{S}}_{n,\mathbf{k}}f_e\,d\mathbf{v}\tag{2.33}$$

where

$$\hat{\mathsf{S}}_{n,\mathbf{k}} = \begin{bmatrix} v_\perp J_n'^2 \hat{U}_\mathbf{k} & -iv_\perp J_n J_n' \hat{V}_{n,\mathbf{k}} & -iv_\perp J_n J_n' \hat{W}_{n,\mathbf{k}} \\ iv_\perp J_n J_n' \hat{V}_{n,\mathbf{k}} & \frac{(n\omega_{ce}+k_\perp v_D)}{k_\perp} J_n^2 \hat{V}_{n,\mathbf{k}} & \frac{(n\omega_\mathbf{k}+k_\perp v_D)}{k_\perp} J_n^2 \hat{W}_{n,\mathbf{k}} \\ iv_\parallel J_n J_n' \hat{U}_\mathbf{k} & v_\parallel J_n^2 \hat{V}_{n,\mathbf{k}} & v_\parallel J_n^2 \hat{W}_{n,\mathbf{k}} \end{bmatrix} \tag{2.34}$$

To obtain the dispersion relation, we simply insert (2.31) into (2.26), to give $\mathsf{M} \cdot \delta\tilde{\mathbf{E}}_\mathbf{k} = 0$. In order that the electric field has non-zero value, the determinant of the tensor M must be zero, so that the dispersion relation is:

$$\left| \mathsf{I} + \frac{c^2}{\Omega_\mathbf{k}^2} \left(\mathbf{k}\,\mathbf{k} - k^2 \mathsf{I} \right) + \sum_s \varepsilon_{s,\mathbf{k}} \right| = 0 \tag{2.35}$$

where

$$\varepsilon_{s,\mathbf{k}} = \frac{i}{\varepsilon_0 \Omega_\mathbf{k}} \sigma_{s,\mathbf{k}} \tag{2.36}$$

2.6 Simplifications of the dispersion relation

The dispersion relation just derived is intractable in its present form, and must be solved by numerical methods. Even so, a number of simplifications can be made, to make numerical solution an easier and more efficient task. If, as we will do later, we only take into consideration electrostatic waves, then we can make drastic simplifications. This should be valid provided that the plasma beta is small: in this case the shock will be laminar or quasilaminar. We can obtain the electrostatic form from the electromagnetic by taking the limit $c \to \infty$, although it is in fact much simpler to return to the perturbed electron function (2.20) and write the perturbed electric field in terms of a potential function. For waves in the y-z plane, we have

$$\delta\tilde{\mathbf{E}}_\mathbf{k} = -i\mathbf{k}\delta\tilde{\varphi}_\mathbf{k}$$

so that (2.20) becomes:

$$\delta\tilde{f}_{e,\mathbf{k}} = \frac{e}{m_e}\delta\tilde{\varphi}_{\mathbf{k}} \sum_{m=-\infty}^{\infty}\sum_{n=-\infty}^{\infty} e^{-i(m-n)(\vartheta-\pi/2)}\Omega_{n,\mathbf{k}}^{-1} J_m(a_\perp)J_n(a_\perp)\hat{F}_{n,\mathbf{k}}f_e \qquad (2.37)$$

where the operator $\hat{F}_{n,\mathbf{k}}$ is given by:

$$\hat{F}_{n,\mathbf{k}} = -k_\perp\frac{\partial}{\partial\Lambda} + \frac{(n\omega_{ce}+k_\perp v_B)}{v_\perp}\frac{\partial}{\partial v_\perp} + k_\parallel\frac{\partial}{\partial v_\parallel}$$

This new form of the perturbed electron function is used to calculate the current density, which is then substituted into Poisson's equation. The dispersion relation will now have the form:

$$K = 1 + \chi_i + \chi_e \qquad (2.38)$$

where χ_i and χ_e are the ion and electron susceptibilities respectively.

$$\chi_i = \frac{e^2}{m_e\varepsilon_0 k}\int\frac{1}{\Omega-\mathbf{k}\cdot\mathbf{v}}\frac{\partial f_i}{\partial\mathbf{v}}\,d\mathbf{v} \qquad (2.39)$$

$$\chi_e = \frac{e^2}{m_e\varepsilon_0 k^2}\sum_{n=-\infty}^{\infty}\int\frac{J_n^2(a_\perp)}{\Omega_k - k_\perp v_D - k_\parallel v_\parallel - n\omega_{ce}}\hat{F}_{n,\mathbf{k}}f_e\,d\mathbf{v} \qquad (2.40)$$

The fact that the frequency $\omega_{\mathbf{k}}$ is much less than the electron cyclotron frequency means that we can ignore all the terms in the summation in (2.40) apart from that with $n = 0$. For the case when the electron distribution function is an isotropic Maxwellian with a density gradient (but no temperature gradient) and the ion distribution function is simply an isotropic Maxwellian, that is:

$$\begin{aligned} f_e(\Lambda, v_\perp, v_\parallel) &= \frac{n_0(\Lambda)}{(2\pi)^{\frac{3}{2}}}\frac{1}{v_{the}^3}\exp\left[-\frac{1}{2}\left(v_\perp^2+v_\parallel^2\right)/v_{the}^2\right] \\ f_i(\mathbf{v}) &= \frac{n_0}{(2\pi)^{\frac{3}{2}}}\frac{1}{v_{thi}^3}\exp\left[-\frac{1}{2}v^2/v_{thi}^2\right] \end{aligned} \qquad (2.41)$$

where $v_{ths} = k_B T_s/m_s$ is the thermal velocity, the susceptibilities have the form:

$$\chi_i = \frac{1}{k^2\lambda_{Di}^2}\left[1+\xi_i Z\left(\xi_i\right)\right] \qquad (2.42)$$

$$\begin{aligned}
\xi_i &= \frac{\Omega_{\mathbf{k}}}{\sqrt{2}k_{\|}v_{thi}} \\
\chi_e &= \frac{1}{k^2\lambda_{De}^2}\left[1+2\frac{(\Omega_{\mathbf{k}}-k_{\perp}v_E-k_{\perp}v_N)}{\sqrt{2}k_{\|}v_{the}}\int_0^{\infty} xJ_0^2(a_{\perp})Z(\xi_0)\exp\left(-x^2\right)dx\right] \\
\xi_0 &= \frac{\Omega_{\mathbf{k}}-k_{\perp}v_D}{\sqrt{2}k_{\|}v_{the}}
\end{aligned} \tag{2.43}$$

where λ_{Ds} is the Debye length for particles of species s, $v_N = -\epsilon_N v_{the}^2/\omega_{ce}$ is the drift velocity induced by the density gradient. Z is the plasma dispersion function [12], defined by

$$Z(\xi) = \frac{1}{\sqrt{\pi}}\int_{-\infty}^{\infty}\frac{\exp\left(-x^2\right)}{x-\xi}\,dx \tag{2.44}$$

Because v_B depends upon $v_{\perp}$, ξ_0 will depend upon x, and so the integral in (2.43) must be evaluated numerically. If we ignore the effects of the magnetic field gradient (which should be less important than those of the electric field for low beta plasmas) but retain the electric field, the integral may be evaluated analytically using the relation:

$$\int_0^{\infty} xJ_n^2(sx)e^{-x^2}\,dx = \frac{1}{2}e^{-s^2/2}I_n(s^2/2) \tag{2.45}$$

to give:

$$\chi_e = \frac{1}{k^2\lambda_{De}^2}\left[1+\frac{(\Omega_{\mathbf{k}}-k_{\perp}v_E-k_{\perp}v_N)}{\sqrt{2}k_{\|}v_{the}}\exp\left(-\lambda^2\right)I_0(\lambda^2)Z(\xi_0)\right] \tag{2.46}$$

where $\lambda = k_{\perp}v_{the}/\omega_{ce}$. When $v_N = 0$,this is the same as the dispersion relation for the modified two stream instability (for example equation (4) of [35]).

Finally, in cases where the ions are cold, that is to say, $\Omega_{\mathbf{k}} \gg \mathbf{k}\cdot\mathbf{v}$, by expanding the denominator of (2.42) and retaining only the lowest order term, we obtain:

$$\chi_i = -\frac{\omega_{pi}^2}{\Omega_{\mathbf{k}}^2} \tag{2.47}$$

2.7 Numerical solutions of the dispersion relation

Since the literature on the linear stability analysis of cross field current- driven instabilities is substantial, we do not propose to devote a large amount of space to the solutions of the linear dispersion relations derived. However, it is interesting to consider an anisotropic distribution function, that is with $T_{e\perp} \neq T_{e\parallel}$, where $T_{e\perp}$ and $T_{e\parallel}$ are the electron temperatures perpendicular and parallel to the background magnetic field, and to study the dependence of the growth rate of the instability on the temperature anisotropy $\vartheta = T_{e\perp}/T_{e\parallel}$. If we define $u_{e\parallel}^2 = k_B T_{e\parallel}/m_e$ and $u_{e\perp}^2 = k_B T_{e\perp}/m_e$, then an appropriate background distribution function is

$$f_e(v_\perp, v_\parallel) = \frac{1}{(2\pi)^{3/2}} \frac{n_0}{u_{e\perp}^2 u_{e\parallel}} \exp\left[-\frac{1}{2}\left(\frac{v_\perp^2}{u_{e\perp}^2} + \frac{v_\parallel^2}{u_{e\parallel}^2}\right)\right] \tag{2.48}$$

from which we can derive the following relation for the electron susceptibility:

$$\chi_e = \frac{\omega_{pe}^2}{k^2 u_{e\parallel}^2}\left\{1 + 2\int_0^\infty x J_0^2(sx)\left[\frac{(\omega - k_\perp v_E)}{\sqrt{2}k_\parallel u_{e\parallel}} + \left(1 - \frac{u_{e\parallel}^2}{u_{e\perp}^2}\right)\frac{k_\perp \epsilon_B {u_{e\perp}}^2 x^2}{\sqrt{2}k_\parallel u_{e\parallel}}\right] Z(\xi_0) e^{-x^2}\, dx\right\} \tag{2.49}$$

Figures 2.2 and 2.3 show plots of the real frequency and growth rate (measured in units of the electron cyclotron frequency) respectively for the mode with $k_\perp u_{e\perp}/\omega_{ce} = 1.0$ and $k_\parallel u_{e\perp}/\omega_{ce} = 0.1$ as $T_{e\perp}$ is held fixed and $T_\parallel$ increased, as would happen during a period of parallel electron heating.

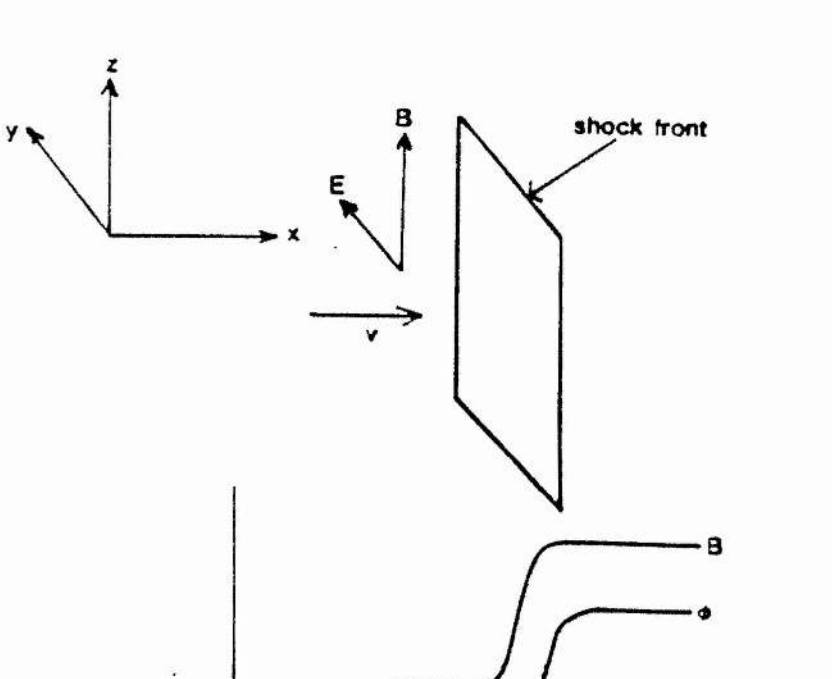

Figure 2.1: Perpendicular shock, showing coordinate sytem used.

Figure 2.2: Frequency versus temperature ratio

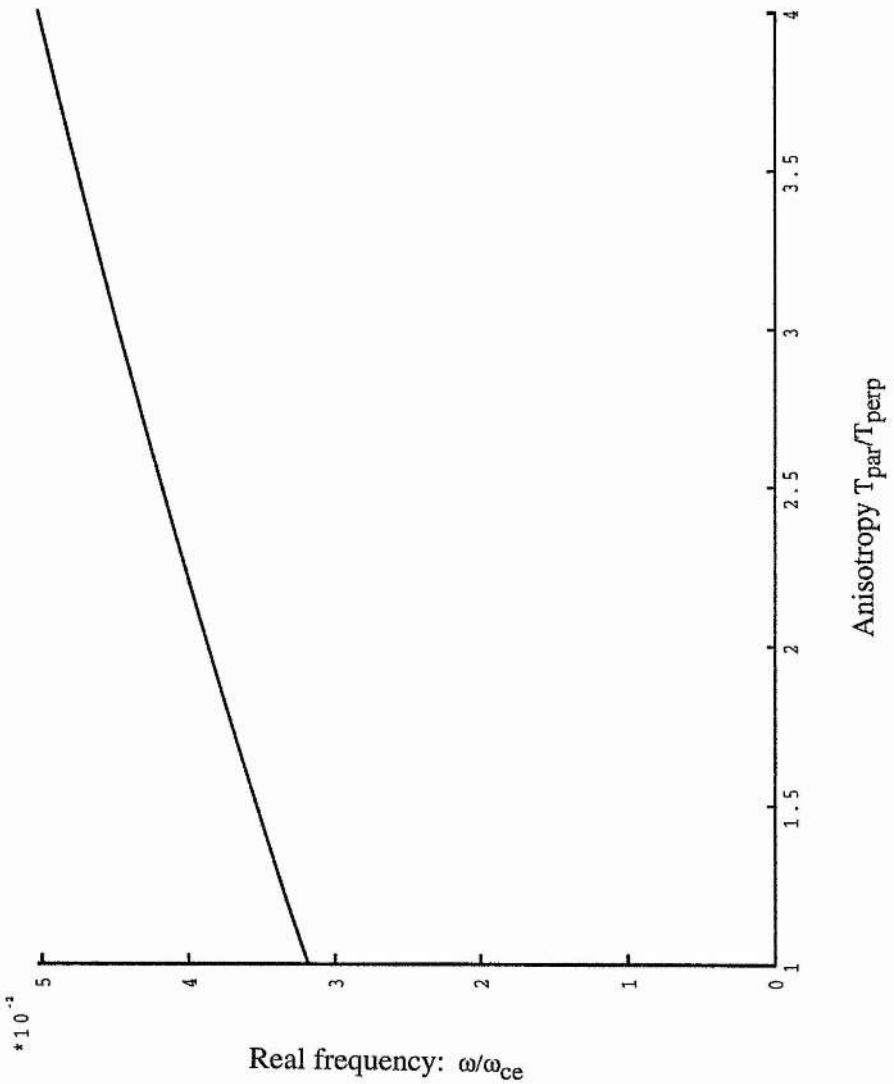

Figure 2.3: Growth rate versus temperature ratio

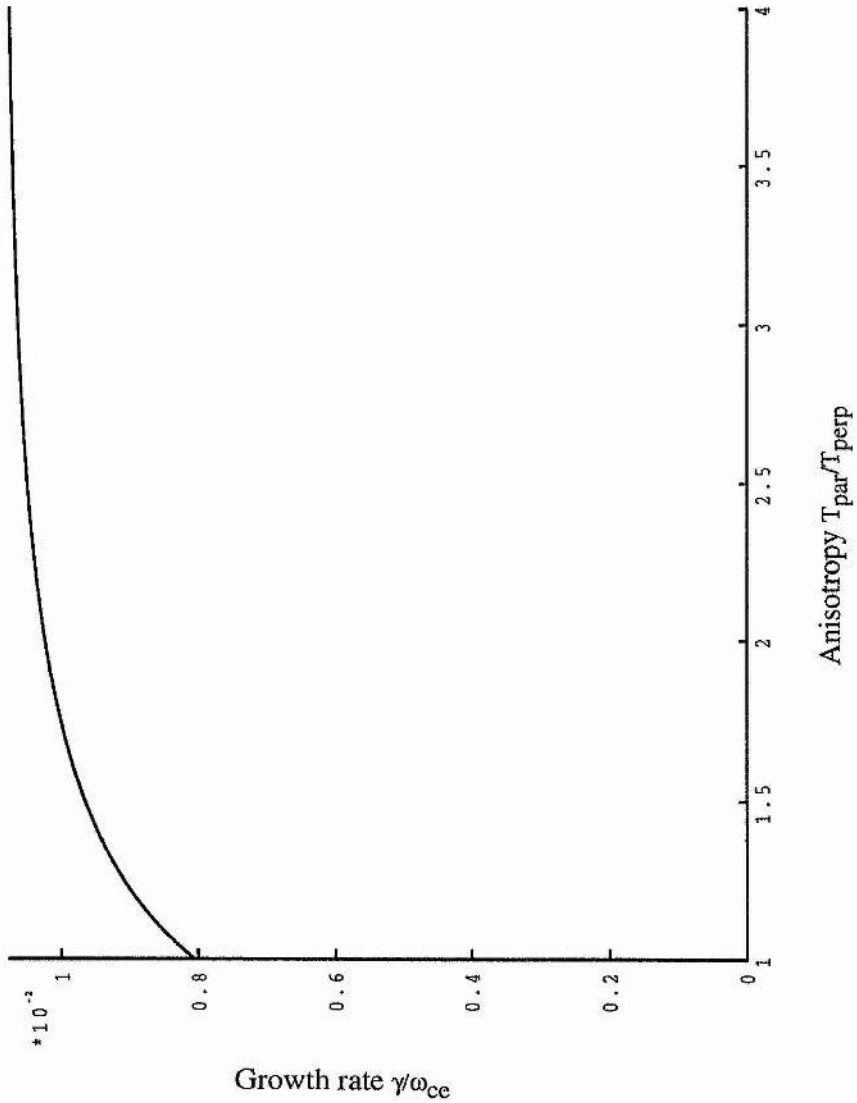

Chapter 3

Derivation of the Quasilinear Equations

3.1 Quasilinear theory

In the last chapter, we linearised the Vlasov equation about an unstable equilibrium, and subsequently solved for the perturbed electron distribution function. On using Maxwell's equations this yielded a linear dispersion relation, so that given the value of the wave vector $\mathbf{k}$, we could calculate the value of the complex frequency $\Omega_k = \omega_k + i\gamma_k$. We now want to be able to determine the change in the background electron distribution function caused by the growth of the waves in the system over a time-scale larger than that for which linear theory is valid. To achieve this, we employ quasilinear theory. This is the simplest non-linear theory of plasma instabilities, and was first developed for unmagnetised plasmas by Drummond and Pines [10] and Vedenov, Velikov and Sagdeev [49], and later generalised to electromagnetic instabilities in a homogeneous magnetic field by Kennel and Engelmann [25], and also to the case of electrostatic waves propagating through an inhomogeneous plasma [4].

The principles of quasilinear theory are as follows: the Vlasov equation is, as

before, divided into a background part, which describes the action of the waves on the slowly varying unperturbed distribution function, and a fluctuating part to describe the rapidly varying behaviour of the system due to the influence of the waves. To solve the latter equation we decompose the perturbed quantities into a set of Fourier modes, and ignore interactions between the different wave modes, so that the perturbed distribution function satisfies a *linear* equation, which can then be solved. The perturbed distribution function is then substituted into the unperturbed equation, yielding a diffusion-type equation. In general, particles will diffuse in velocity space in such a way so as to push the system into a stable (or marginally stable) state. Not surprisingly, diffusion is strongest for those particles with velocities close to the phase velocities of the waves ('resonant diffusion'), and weaker for the remaining particles.

3.2 The electron quasilinear diffusion equation

We now derive an equation to follow the evolution of the electron distribution function. The derivation substantially follows that of [25]: however, we have allowed the background magnetic field to vary slowly in the x-direction. We start by averaging the Vlasov equation in order to remove all rapidly varying terms. However, we allow the background distribution function to vary (slowly) in time and retain the second order term involving the wave field and the perturbed distribution function. This was neglected in the linear theory, but is retained here as it describes the action of the wave spectrum on the background distribution. The averaged Vlasov equation is:

$$\frac{\partial f_e}{\partial t} + \mathbf{v}.\frac{\partial f_e}{\partial \mathbf{r}} - \frac{e}{m_e}\left(\mathbf{E}_0 + \mathbf{v} \wedge \mathbf{B}_0\right).\frac{\partial f_e}{\partial \mathbf{v}} = \frac{e}{m_e}\left\langle (\delta\mathbf{E} + \mathbf{v} \wedge \delta\mathbf{B}) \cdot \frac{\partial \delta f_e}{\partial \mathbf{v}} \right\rangle \qquad (3.1)$$

The angled brackets denote that the quantity they enclose is to be averaged in some way. The exact form of the averaging process is not critical, as long as it

removes all terms linear in the perturbed quantities. Since the situation under consideration is time-dependent with waves in the y-z plane, we could take:

$$\langle f(y,z)\rangle = \frac{1}{4L_yL_z}\int_{-\frac{L_y}{2}}^{\frac{L_y}{2}}\int_{-\frac{L_z}{2}}^{\frac{L_z}{2}} f(y,z)\,dydz \tag{3.2}$$

where L_y and L_z measure the periodicity length of the system in the y and z directions respectively.

We now need to derive an expression for the perturbed distribution function. To do this we Fourier analyse the perturbed quantities in time and space:

$$\delta B(\mathbf{r},t) = \sum_{\mathbf{k}} \delta\tilde{B}_{\mathbf{k}}(x)\exp[i(\mathbf{k}.\mathbf{r}-\Omega_{\mathbf{k}}t)] \tag{3.3}$$

$$\delta E(\mathbf{r},t) = \sum_{\mathbf{k}} \delta\tilde{E}_{\mathbf{k}}(x)\exp[i(\mathbf{k}.\mathbf{r}-\Omega_{\mathbf{k}}t)] \tag{3.4}$$

$$\delta f_e(\mathbf{r},\mathbf{v},t) = \sum_{\mathbf{k}} \delta\tilde{f}_{e\mathbf{k}}(x,\mathbf{v})\exp[i(\mathbf{k}.\mathbf{r}-\Omega_{\mathbf{k}}t)] \tag{3.5}$$

We have assumed that the system is periodic in the y and z directions, so that the wave number vector is forced to take on a number of discrete values. This is purely for algebraic convenience, and later we will let the periodicity lengths L_y and L_z become infinite, in which case the wave number spectrum becomes continuous, and the sums in our expressions become integrals.

The time-independent distribution function used in the linear stability theory of the previous chapter was necessarily independent of the gyroangle theta (defined by $\tan\vartheta = \frac{v_y - v_E}{v_x}$). Since the fundamental idea of quasilinear theory is that the background distribution changes slowly compared to the perturbed distribution function, then its variation with the gyroangle should also be weak. If we then expand the background distribution function in terms of the reciprocal of the electron cyclotron frequency [25]:

$$f_e(\Lambda, v_\perp, \vartheta, v_\parallel, t) = f_e^{[0]}(\Lambda, v_\perp, \vartheta, v_\parallel, t) + \frac{1}{\omega_{ce}} f_e^{[1]}(\Lambda, v_\perp, \vartheta, v_\parallel, t) + O(\frac{1}{\omega_{ce}^2}) \tag{3.6}$$

Using 3.1, and remembering that the rate of change of f_e due to the waves is small, we see that:

$$\frac{\partial f_e^{[0]}}{\partial \vartheta} = 0$$

This valid as long as the growth rates of the waves are all much smaller than the cyclotron frequency. For the instabilities considered in this thesis, we have:

$$\Im\{\Omega\} < \Re\{\Omega\}$$

and

$$\Re\{\Omega\} \ll \omega_{ce}$$

so that we are clearly justified in making this assumption. The higher order terms in (3.6) can be removed by integrating (3.1) over the gyroangle (gyroaverging) and noting that the terms $f_e^{[n]}$ are all periodic in theta. We are left with an evolution equation for $f_e^{[0]}$. We will drop the superscript so as not to overburden the notation.

Since all the perturbed quantities are real, a number of symmetry relations has to be obeyed:

$$\delta\tilde{\mathbf{B}}_{-\mathbf{k}} = \delta\tilde{\mathbf{B}}_{\mathbf{k}}^{\star} \tag{3.7}$$

$$\delta\tilde{\mathbf{E}}_{-\mathbf{k}} = \delta\tilde{\mathbf{E}}_{\mathbf{k}}^{\star} \tag{3.8}$$

$$\delta\tilde{f}_{e-\mathbf{k}} = \delta\tilde{f}_{e\mathbf{k}}^{\star} \tag{3.9}$$

$$\Omega_{-\mathbf{k}} = -\Omega_{\mathbf{k}}^{\star} \tag{3.10}$$

A star (*) denotes that the complex conjugate is to be taken. We can solve the perturbed Vlasov equation exactly as was done in chapter 2, and deduce a dispersion relation, only now the background distribution function is changing slowly with time. If we substitute the Fourier expansions for $\delta\tilde{B}_{\mathbf{k}}$, $\delta\tilde{E}_{\mathbf{k}}$ and $\delta\tilde{f}_{e\mathbf{k}}$ into (3.1), then we find that products of different Fourier components are rapidly varying, and disappear under the average. We are then left with:

$$\frac{\partial f_e}{\partial t} + \mathbf{v}.\frac{\partial f_e}{\partial \mathbf{r}} - \frac{e}{m_e}\left(\mathbf{E}_0 + \mathbf{v} \wedge \mathbf{B}_0\right).\frac{\partial f_e}{\partial \mathbf{v}} = \frac{e}{m_e}\sum_{\mathbf{k}}\left(\delta\tilde{B}_{-\mathbf{k}} + \mathbf{v} \wedge \delta\tilde{E}_{-\mathbf{k}}\right) \cdot \frac{\partial \delta\tilde{f}_{e\mathbf{k}}}{\partial \mathbf{v}} \tag{3.11}$$

The right-hand side is necessarily real, on account of the symmetry relations (3.7) to (3.10).

From chapter 2, the perturbed electron distribution function can be written as:

$$\delta\tilde{f}_{e,\mathbf{k}} = \sum_m \sum_n e^{-(m-n)\vartheta} G_{mn\mathbf{k}} \tag{3.12}$$

where

$$G_{mn\mathbf{k}} = i\frac{e}{m_e} e^{-(m-n)\pi/2} J_m(a_\perp)\Omega_{n,\mathbf{k}}^{-1}\hat{F}_{n,\mathbf{k}} f_e \tag{3.13}$$

We now substitute this into the right-hand side of (3.11), use (2.13) to eliminate $\delta\tilde{B}_{\mathbf{k}}$, and change velocity co-ordinates to cylindrical polars. The gyro-averaged background Vlasov equation is then:

$$\frac{\partial f_e}{\partial t} = \Re\left\{\frac{e}{m_e}\sum_{\mathbf{k}}\frac{1}{2\pi}\int_0^{2\pi}\hat{P}_{\mathbf{k}}\delta\tilde{f}_{e,\mathbf{k}}d\vartheta\right\} \tag{3.14}$$

with

$$\hat{P}_{\mathbf{k}} = \hat{A}_0 + C_0\frac{\partial}{\partial\vartheta} + e^{i\vartheta}\left[\hat{A}_+ + iC_+\frac{\partial}{\partial\vartheta}\right] + e^{-i\vartheta}\left[\hat{A}_- + iC_-\frac{\partial}{\partial\vartheta}\right] \tag{3.15}$$

$$C_\pm = \frac{1}{2v_\perp}\left[\left(\Omega_{\mathbf{k}} - k_\perp v_D - k_\perp v_B - k_\parallel v_\parallel\right)\delta\tilde{E}_{x,\mathbf{k}} \mp i\left(\Omega_{\mathbf{k}} - k_\parallel v_\parallel\right)\delta\tilde{E}_{y,\mathbf{k}} \mp i\, k_\perp v_\parallel \delta\tilde{E}_{\parallel,\mathbf{k}}\right] \tag{3.16}$$

The operators $\hat{A}_0$ and $\hat{A}_\pm$ were defined in chapter 2. The form of C_0 is not important; we shall see later that when the θ integration is carried out it disappears.

To calculate the right-hand side of 3.14, we need to evaluate the term:

$$\frac{1}{2\pi}\int_0^{2\pi}\hat{P}_{\mathbf{k}}^{\star}\delta\tilde{f}_{e,\mathbf{k}}d\vartheta \tag{3.17}$$

If we substitute for $\hat{P}_{\mathbf{k}}$ from 3.15 and for $\delta\tilde{f}_{e,\mathbf{k}}$ from 3.12, then:

$$\begin{aligned}\frac{1}{2\pi}\int_0^{2\pi}\hat{P}^{\star}_{\mathbf{k}}\delta\tilde{f}_{e,\mathbf{k}}d\vartheta &= \frac{1}{2\pi}\int_0^{2\pi}\left\{\hat{A}_0+C_0\frac{\partial}{\partial\vartheta}+e^{i\vartheta}\left[\hat{A}_+ + iC_+\frac{\partial}{\partial\vartheta}\right]\right.\\ &\left.+e^{-i\vartheta}\left[\hat{A}_- + iC_-\frac{\partial}{\partial\vartheta}\right]\right\}^{*}\delta\tilde{f}_{e,\mathbf{k}}d\vartheta\end{aligned} \tag{3.18}$$

The $\hat{A}$ operators and $C_{\pm}$ are all independent of theta, so that we can integrate the terms proportional to $e^{\pm i\vartheta}$ by parts, that is:

$$\frac{1}{2\pi}\int_0^{2\pi} ie^{\pm i\vartheta}\frac{\partial g}{\partial\vartheta}d\vartheta = \pm e^{\pm i\vartheta}g$$

and

$$\frac{1}{2\pi}\int_0^{2\pi}\frac{\partial g}{\partial\vartheta}d\vartheta = 0 \tag{3.19}$$

thus:

$$\begin{aligned}\frac{1}{2\pi}\int_0^{2\pi}\hat{P}^{\star}_{\mathbf{k}}\delta\tilde{f}_{e,\mathbf{k}}d\vartheta &= \frac{1}{2\pi}\int_0^{2\pi}\left\{\hat{A}_0+e^{i\vartheta}\left(\hat{A}_+ + C_+\right)+e^{-i\vartheta}\left(\hat{A}_- + C_-\right)\right\}^{*}\\ &\qquad\delta\tilde{f}_{e,\mathbf{k}}d\vartheta\\ &= \sum_m\sum_n\frac{1}{2\pi}\int_0^{2\pi}\left\{e^{i(m-n)\vartheta}\hat{A}_0+e^{i(m-n+1)\vartheta}\left(\hat{A}_+ + C_+\right)\right.\\ &\qquad\left.+e^{i(m-n-1)\vartheta}\left(\hat{A}_- + C_-\right)\right\}^{*}G_{mn\mathbf{k}}d\vartheta\end{aligned} \tag{3.20}$$

We can now use (2.29) to perform the theta integration. As before, the double summation reduces to a single summation over n. Thus:

$$\frac{1}{2\pi}\int_0^{2\pi}\hat{P}^{\star}_{\mathbf{k}}\delta\tilde{f}_{e,\mathbf{k}}d\vartheta = \sum_n\left\{\left[\hat{P}^{[1]}_{n,\mathbf{k}}\right]^{*}+\left[\hat{P}^{[2]}_{n,\mathbf{k}}\right]^{*}+\left[\hat{P}^{[3]}_{n,\mathbf{k}}\right]^{*}\right\} \tag{3.21}$$

where

$$\hat{P}^{[1]}_{n,\mathbf{k}} = \hat{A}_0G_{n,n,\mathbf{k}} \tag{3.22}$$

$$\hat{P}^{[2]}_{n,\mathbf{k}} = \left(\hat{A}_+G_{n-1,n,\mathbf{k}}+\hat{A}_-G_{n+1,n,\mathbf{k}}\right) \tag{3.23}$$

$$\hat{P}^{[3]}_{n,\mathbf{k}} = \left(C_+G_{n-1,n,\mathbf{k}}+C_-G_{n+1,n,\mathbf{k}}\right) \tag{3.24}$$

On substituting in $\delta\tilde{f}_{e,\mathbf{k}}$ from 3.12, it is possible to perform the theta-integration, reducing the double sum to a single sum.

We now expand the right-hand sides of equations (3.22) to (3.24) in turn:

$$\begin{aligned}
\left[\hat{P}^{[2]}_{n,\mathbf{k}}\right]^* &= \left[-\frac{i}{2}\left(i\delta\tilde{E}_{x,\mathbf{k}}\hat{U}_{\mathbf{k}} + \delta\tilde{E}_{y,\mathbf{k}}\hat{G}_{\mathbf{k}} + k_\perp\delta\tilde{E}_{\|,\mathbf{k}}\hat{H}_{\mathbf{k}}\right)\right]^* \left[\frac{e}{m_e}J_{n-1}\Omega^{-1}_{n,\mathbf{k}}\hat{F}_{n,\mathbf{k}}f_e\right] \\
&- \left[\frac{i}{2}\left(-i\delta\tilde{E}_{x,\mathbf{k}}\hat{U}_{\mathbf{k}} + \delta\tilde{E}_{y,\mathbf{k}}\hat{G}_{\mathbf{k}} + k_\perp\delta\tilde{E}_{\|,\mathbf{k}}\hat{H}_{\mathbf{k}}\right)\right]^* \left[\frac{e}{m_e}J_{n+1}\Omega^{-1}_{n,\mathbf{k}}\hat{F}_{n,\mathbf{k}}f_e\right] \\
&= \frac{e}{m_e}\left\{-\delta\tilde{E}_{x,\mathbf{k}}\hat{U}_{\mathbf{k}}\left(\frac{J_{n+1}-J_{n-1}}{2}\right) - i\delta\tilde{E}_{y,\mathbf{k}}\hat{G}_{\mathbf{k}}\left(\frac{J_{n+1}+J_{n-1}}{2}\right)\right. \\
&- \left. ik_\perp\delta\tilde{E}_{\|,\mathbf{k}}\hat{H}_{\mathbf{k}}\left(\frac{J_{n+1}+J_{n-1}}{2}\right)\right\}^* \times \Omega^{-1}_{n,\mathbf{k}}\hat{F}_{n,\mathbf{k}}f_e \\
&= i\frac{e}{m_e}\left\{\delta\tilde{E}_{x,\mathbf{k}}\hat{U}_{\mathbf{k}}J'_n + \delta\tilde{E}_{y,\mathbf{k}}\hat{G}_{\mathbf{k}}\frac{n\omega_{ce}}{k_\perp v_\perp}J_n + \delta\tilde{E}_{\|,\mathbf{k}}\frac{n\omega_{ce}}{v_\perp}J_n\right\}^* \\
&\times\Omega^{-1}_{n,\mathbf{k}}\hat{F}_{n,\mathbf{k}}f_e \qquad (3.25)
\end{aligned}$$

A similar process gives:

$$\begin{aligned}
\left[\hat{P}^{[3]}_{n,\mathbf{k}}\right]^* &= \frac{1}{2v_\perp}\left[\left(\bar{\Omega}_{\mathbf{k}} - k_\perp v_B\right)\delta\tilde{E}_{x,\mathbf{k}} - i\left(\Omega_{\mathbf{k}} - k_\perp v_\|\right)\delta\tilde{E}_{y,\mathbf{k}} - k_\perp v_\|\delta\tilde{E}_{\|,\mathbf{k}}\right]^* \\
&\times\left[\frac{e}{m_e}J_{n-1}\Omega^{-1}_{n,\mathbf{k}}\hat{F}_{n,\mathbf{k}}f_e\right] \\
&= -\frac{i}{2v_\perp}\left[-i\left(\bar{\Omega}_{\mathbf{k}} - k_\perp v_B\right)\delta\tilde{E}_{x,\mathbf{k}}J'_n - \frac{n\omega ce}{k_\perp v_\perp}\left(\Omega_{\mathbf{k}} - k_\perp v_\|\right)\delta\tilde{E}_{y,\mathbf{k}}\right. \\
&\left. -n\omega_{ce}\frac{v_\|}{v_\perp}\delta\tilde{E}_{\|,\mathbf{k}}J_n\right]^* \frac{e}{m_e}\Omega^{-1}_{n,\mathbf{k}}\hat{F}_{n,\mathbf{k}}f_e \qquad (3.26)
\end{aligned}$$

and finally:

$$\begin{aligned}
\left[\hat{P}^{[1]}_{n,\mathbf{k}}\right]^* &= \left\{\left[-\left(\Omega_{\mathbf{k}} - k_\perp v_\|\right)\left(\frac{\partial}{\partial\Lambda} - v_B\frac{1}{v_\perp}\frac{\partial}{\partial v_\perp}\right) + k_\| v_D\frac{\partial}{\partial v_\|}\right]\delta\tilde{E}_{y,\mathbf{k}}\right. \\
&+ \left.\left[k_\perp v_\|\left(\frac{\partial}{\partial\Lambda} - v_B\frac{1}{v_\perp}\frac{\partial}{\partial v_\perp}\right) + \left(\Omega_{\mathbf{k}} - k_\perp v_D\right)\frac{\partial}{\partial v_\|}\right]\delta\tilde{E}_{\|,\mathbf{k}}\right\}^* \\
&\times i\frac{e}{m_e}\Omega^{-1}_{n,\mathbf{k}}\hat{F}_{n,\mathbf{k}}f_e \qquad (3.27)
\end{aligned}$$

We now substitute (3.25), (3.26) and (3.27) into (3.21), to get:

$$\hat{A}^*_0 G_{n,n,\mathbf{k}} + \hat{A}^*_+ G_{n-1,n,\mathbf{k}} + \hat{A}^*_- G_{n+1,n,\mathbf{k}} + C^*_+ G_{n-1,n,\mathbf{k}} + C^*_- G_{n+1,n,\mathbf{k}}$$

$$
\begin{aligned}
&= \left\{ i\delta\tilde{E}_{x,\mathbf{k}} \left[\hat{U}_{\mathbf{k}} + \frac{(\Omega_{\mathbf{k}} - k_\perp v_B)}{v_\perp} \right] J_n' \right. \\
&+ \delta\tilde{E}_{y,\mathbf{k}} \left[-\left(\Omega_{\mathbf{k}} - k_\perp v_\parallel\right) \left(\frac{\partial}{\partial \Lambda} - v_B \frac{1}{v_\perp} \frac{\partial}{\partial v_\perp} \right) + k_\parallel v_D \frac{\partial}{\partial v_\parallel} \right. \\
&\quad \left. + \frac{n\omega_{ce}}{k_\perp} \left(\hat{G} \frac{1}{v_\perp} + \frac{\left(\Omega_{\mathbf{k}} - k_\perp v_\parallel\right)}{v_\perp^2} \right) \right] J_n \\
&+ \delta\tilde{E}_{\parallel,\mathbf{k}} \left[-k_\perp v_\parallel \frac{\partial}{\partial \Lambda} + n\omega_{ce} \left(\hat{H} \frac{1}{v_\perp} + \frac{v_\parallel}{v_\perp^2} \right) \right. \\
&\quad \left. \left. + k_\perp v_\parallel \frac{v_B}{v_\perp} \frac{\partial}{\partial v_\perp} + \left(\Omega_{\mathbf{k}} - k_\perp v_D\right) \frac{\partial}{\partial v_\parallel} \right] J_n \right\}^\star \\
&\quad \times i\frac{e}{m_e} \Omega_{n,\mathbf{k}}^{-1} \hat{F}_{n,\mathbf{k}} f_e
\end{aligned}
\tag{3.28}
$$

We now use the operator identities:

$$
\begin{aligned}
\hat{G}_{\mathbf{k}} \frac{1}{v_\perp} &= \frac{1}{v_\perp} \hat{G}_{\mathbf{k}} - \frac{(\Omega_{\mathbf{k}} - k_\perp v_D)}{v_\perp^2} \\
\hat{H}_{\mathbf{k}} \frac{1}{v_\perp} &= \frac{1}{v_\perp} \hat{H}_{\mathbf{k}} - \frac{v_\parallel}{v_\perp^2}
\end{aligned}
$$

in (3.28) to write (3.21) as:

$$
\begin{aligned}
\frac{1}{2\pi} \int_0^{2\pi} \hat{P}_{\mathbf{k}}^\star \delta\tilde{f}_{e,\mathbf{k}} d\vartheta &= i\frac{e}{m_e} \sum_n \left\{ i\delta\tilde{E}_{x,\mathbf{k}} \left[\hat{U}_{\mathbf{k}} + \frac{(\Omega_{\mathbf{k}} - k_\perp v_B)}{v_\perp} \right] J_n' \right. \\
&+ \left. \delta\tilde{E}_{y,\mathbf{k}} \hat{V}_{n,\mathbf{k}} J_n + \delta\tilde{E}_{\parallel,\mathbf{k}} \hat{W}_{n,\mathbf{k}} J_n \right\}^\star \\
&\quad \times \Omega_{n,\mathbf{k}}^{-1} \hat{F}_{n,\mathbf{k}} f_e
\end{aligned}
\tag{3.29}
$$

The evolution equation for the electron distribution function is thus:

$$
\frac{\partial f_e}{\partial t} = \Re \left\{ i\frac{e^2}{m_e^2} \sum_n \sum_{\mathbf{k}} \left[\frac{\left(\bar{\Omega}_{\mathbf{k}} - k_\perp v_B\right)}{\Omega_{\mathbf{k}} v_\perp} + \hat{F_{n,\mathbf{k}}} \right]^* \Omega_{n,\mathbf{k}}^{-1} \hat{F_{n,\mathbf{k}}} f_e \right\}
\tag{3.30}
$$

This equation can be written in the form of a quasilinear diffusion equation:-

$$
\frac{\partial f_e}{\partial t} = \frac{\partial}{\partial \mu} \cdot \left[\mathsf{D}_e \cdot \frac{\partial f_e}{\partial \mu} \right]
\tag{3.31}
$$

$$
\mathsf{D}_\mathbf{e} = \Re \left\{ i\frac{e^2}{m_e} \sum_n \sum_{\mathbf{k}} \mathbf{a}_{n,\mathbf{k}}^* \Omega_{n,\mathbf{k}}^{-1} \mathbf{a}_{n,\mathbf{k}} \right\}
\tag{3.32}
$$

$$\mathbf{a}_{n,\mathbf{k}} = a_{n,\Lambda,\mathbf{k}}\hat{\mathbf{e}}_\Lambda + a_{n,\perp\mathbf{k}}\hat{\mathbf{e}}_\perp + a_{n,\|,\mathbf{k}}\hat{\mathbf{e}}_\|$$

$$\begin{aligned} a_{n,\Lambda,\mathbf{k}} = -\frac{1}{\Omega_\mathbf{k}}\Big[& ik_\perp v_\perp J_n' \delta\tilde{E}_{x,\mathbf{k}} + \\ & \left(\Omega_\mathbf{k} - k_\| v_\|\right) J_n \delta\tilde{E}_{y,\mathbf{k}} + k_\perp v_\| J_n \delta\tilde{E}_{\|,\mathbf{k}}\Big] \end{aligned} \tag{3.33}$$

$$\begin{aligned} a_{n,\perp,\mathbf{k}} = \frac{1}{\Omega_\mathbf{k}}\Big[& i\left(\Omega_\mathbf{k} - k_\perp v_E - k_\| v_\|\right) J_n' \delta\tilde{E}_{x,\mathbf{k}} + \\ & \frac{(n\omega_{ce} + k_\perp v_B)}{k_\perp v_\perp}\left(\Omega_\mathbf{k} - k_\| v_\|\right) J_n \delta\tilde{E}_{y,\mathbf{k}} + \\ & v_\| \frac{(n\omega_{ce} + k_\perp v_B)}{v_\perp} J_n \delta\tilde{E}_{\|,\mathbf{k}}\Big] \end{aligned} \tag{3.34}$$

$$\begin{aligned} a_{n,\|,\mathbf{k}}\hat{\mathbf{e}}_\| = \frac{1}{\Omega_\mathbf{k}}\Big[& ik_\| v_\perp J_n' \delta\tilde{E}_{x,\mathbf{k}} + \\ & (n\omega_{ce} + k_\perp v_D)\frac{k_\|}{k_\perp} J_n \delta\tilde{E}_{y,\mathbf{k}} + \\ & (\Omega_\mathbf{k} - k_\perp v_D - n\omega_{ce}) J_n \delta\tilde{E}_{\|,\mathbf{k}}\Big] \end{aligned} \tag{3.35}$$

$$\mu = \Lambda\hat{\mathbf{e}}_\Lambda + v_\perp\hat{\mathbf{e}}_\perp + v_\|\hat{\mathbf{e}}_\| \tag{3.36}$$

If there are no spatial gradients in the background quantities then the above equations are equivalent to equations (2.26) and (2.27) of [25]. It can be shown (see Appendix) that equation (3.31) conserves energy.

3.3 The Quasi-H Theorem

We can apply the arguments of Kennel and Engelmann [25] to (3.31) to show that the system must tend to some marginally stable state as t tends to infinity. We accomplish this by defining the functional

$$H_e = \frac{1}{2}\int f_e^2 d\mu \tag{3.37}$$

Differentiating this with respect to time, using (3.31) and integrating by parts gives us:

$$\begin{aligned}\frac{dH_e}{dt} &= -\frac{e^2}{m_e^2}\sum_{\mathbf{k}}\sum_{n}\int\left|\mathbf{a}_{n,\mathbf{k}}\cdot\frac{\partial f_e}{\partial\mu}\right|^2\frac{\gamma_{\mathbf{k}}}{\left(\omega_{\mathbf{k}}-k_\perp v_D-k_{\|}v_{\|}-n\omega_{ce}\right)^2+\gamma_{\mathbf{k}}^2}d\mu \\ &\leq 0 \end{aligned} \tag{3.38}$$

Since H_e is clearly positive definite, and $\frac{dH_e}{dt}$ is negative semi-definite, H must decrease monotonically in time until it reaches a steady state with $\frac{dH_e}{dt}=0$. This must occur either when $\gamma_{\mathbf{k}}=0$ or, since H_e is a sum of positive definite terms,

$$\mathbf{a}_{n,\mathbf{k}}\cdot\frac{\partial f_e}{\partial\mu}=0 \tag{3.39}$$

In the latter case we arrive at a contradiction, as the perturbed distribution would have to be identically zero, in which case no waves would be excited. Thus, in the limit of infinite time the electron distribution function must tend to form such that all the waves excited are stable.

3.4 Evolution of field amplitudes

On the long timescale, the electric fields will change in time according to:

$$E_{\alpha,\mathbf{k}}(t)E^{\star}_{\beta,\mathbf{k}}(t)=E_{\alpha,\mathbf{k}}(0)E^{\star}_{\beta,\mathbf{k}}(0)\exp\left[\int_0^t 2\gamma_{\mathbf{k}}(t')dt'\right] \tag{3.40}$$

This expression can be written as a differential equation, giving:

$$\frac{\partial E_{\alpha,\mathbf{k}}(t)E^{\star}_{\beta,\mathbf{k}}(t)}{\partial t}=2\gamma_{\mathbf{k}}(t)E_{\alpha,\mathbf{k}}(t)E^{\star}_{\beta,\mathbf{k}}(t) \tag{3.41}$$

3.5 Quasilinear diffusion equation for electrostatic waves

In the same way that we simplified the dispersion equation by assuming that the electric field was derivable from a potential, we can write the diffusion tensor as:

$$\mathsf{D}_{\mathrm{e}} = \frac{e^2}{m_e^2} \sum_n \sum_{\mathbf{k}} \mathbf{b}_{n,\mathbf{k}} \frac{J_n^2(a_\perp) I_{\mathbf{k}} \gamma_{\mathbf{k}}}{(\omega_{\mathbf{k}} - k_\perp v_D - k_{\|} v_{\|} - n\omega_{ce})^2 + \gamma_{\mathbf{k}}^2} \mathbf{b}_{n,\mathbf{k}} \tag{3.42}$$

where

$$\mathbf{b}_{n,\mathbf{k}} = -k_\perp \hat{\mathbf{e}}_\Lambda + \frac{(n\omega_{ce} + k_\perp v_B)}{v_\perp} \hat{\mathbf{e}}_\perp + k_{\|} \hat{\mathbf{e}}_{\|} \tag{3.43}$$

$$I_{\mathbf{k}}(t) = |\delta\tilde{\varphi}_{\mathbf{k}}(t)|^2 \tag{3.44}$$

$I_{\mathbf{k}}$ is the intensity of the wave with wavelength $\mathbf{k}$. This quantity will evolve in time according to:

$$\frac{\partial I_{\mathbf{k}}}{\partial t} = 2\gamma_{\mathbf{k}} I_{\mathbf{k}} \tag{3.45}$$

It is possible to simplify both (3.32) and (3.42) by ignoring the $n \neq 0$ terms, as was done in the dispersion relation.

3.6 Quasilinear diffusion of the ions

If we make the assumption of negligible ion temperature again, we can derive equations to describe the evolution of the bulk ion parameters under the action of the turbulence. Because of the large mass of the ions, we can neglect the effect of the magnetic field on them. The quasilinear diffusion equation for the ions under the last assumption is:

$$\frac{\partial}{\partial t} f_i = \frac{\partial}{\partial \mathbf{v}} \cdot \left[\mathsf{D}_{\mathrm{i}} \cdot \frac{\partial}{\partial \mathbf{v}} \mathbf{f}_{\mathrm{i}} \right] \tag{3.46}$$

where:

$$\mathsf{D}_{\mathrm{i}} = \Re \left\{ \mathrm{i} \frac{\mathrm{e}^2}{\mathrm{m}_{\mathrm{i}}^2} \sum_{\mathbf{k}} \mathbf{k} \frac{|\delta\tilde{\varphi}_{\mathbf{k}}|^2}{(\Omega_{\mathbf{k}} - \mathbf{k} \cdot \mathbf{v})} \mathbf{k} \right\} \tag{3.47}$$

To derive an equation for the rate of change of the ion thermal velocity, we multiply (3.46) my $\frac{1}{2}m_i v^2$ and integrate over velocity:

$$\begin{aligned}\frac{d}{dt}\int \frac{1}{2}m_i v^2 f_i d\mathbf{v} &= -\int m_i \mathbf{v}\cdot \mathsf{D_i}\cdot \frac{\partial}{\partial \mathbf{v}}\mathbf{f_i} d\mathbf{v} \\ &= \Re\left\{-i\frac{e^2}{m_i}\sum_{\mathbf{k}}\int \mathbf{k}\cdot\mathbf{v}\frac{|\delta\tilde{\varphi}_{\mathbf{k}}|^2}{(\Omega_{\mathbf{k}}-\mathbf{k}\cdot\mathbf{v})}\mathbf{k}\cdot\frac{\partial}{\partial\mathbf{v}}f_i d\mathbf{v}\right\} \quad (3.48)\end{aligned}$$

If the ions are cold enough, i.e. $kv_{thi} < \Omega_{\mathbf{k}}$, then we can expand the denominator in the above:

$$\begin{aligned}\frac{1}{(\Omega_{\mathbf{k}}-\mathbf{k}\cdot\mathbf{v})} &= \frac{1}{\Omega_{\mathbf{k}}}\left[1-\frac{\mathbf{k}\cdot\mathbf{v}}{\Omega_{\mathbf{k}}}\right]^{-1} \\ &= \frac{1}{\Omega_{\mathbf{k}}}\left[1+\frac{\mathbf{k}\cdot\mathbf{v}}{\Omega_{\mathbf{k}}}+\left(\frac{\mathbf{k}\cdot\mathbf{v}}{\Omega_{\mathbf{k}}}\right)^2+...\right]\end{aligned}$$

and so

$$\begin{aligned}\frac{d}{dt}\int \frac{1}{2}m_i v^2 f_i d\mathbf{v} &= \Re\left\{-i\frac{e^2}{m_i}\sum_{\mathbf{k}}|\delta\tilde{\varphi}_{\mathbf{k}}|^2\int\frac{\mathbf{k}\cdot\mathbf{v}}{\Omega_{\mathbf{k}}}\left[1+\frac{\mathbf{k}\cdot\mathbf{v}}{\Omega_{\mathbf{k}}}+\left(\frac{\mathbf{k}\cdot\mathbf{v}}{\Omega_{\mathbf{k}}}\right)^2+...\right]\right. \\ &\qquad \left.\mathbf{k}\cdot\frac{\partial}{\partial\mathbf{v}}f_i d\mathbf{v}\right\} \\ &= \Re\left\{i\frac{e^2}{m_i}\sum_{\mathbf{k}}|\delta\tilde{\varphi}_{\mathbf{k}}|^2\frac{k^2}{\Omega_{\mathbf{k}}}\right. \\ &\qquad \left.\int\left[1+2\frac{\mathbf{k}\cdot\mathbf{v}}{\Omega_{\mathbf{k}}}+3\left(\frac{\mathbf{k}\cdot\mathbf{v}}{\Omega_{\mathbf{k}}}\right)^2+...\right]f_i d\mathbf{v}\right\}\end{aligned}$$

$$\begin{aligned}\Rightarrow \frac{1}{2}n_0 m_i\frac{d}{dt}v_{thi}^2 &= \Re\left\{i\frac{e^2}{m_i}\sum_{\mathbf{k}}|\delta\tilde{\varphi}_{\mathbf{k}}|^2\frac{k^2}{\Omega_{\mathbf{k}}}n_0\left(1+3\frac{k^2v_{thi}^2}{\Omega_{\mathbf{k}}^2}+...\right)\right\} \\ &= n_0\frac{e^2}{m_i}\sum_{\mathbf{k}}\frac{k^2|\delta\tilde{\varphi}_{\mathbf{k}}|^2\gamma_{\mathbf{k}}}{\left(\omega_{\mathbf{k}}^2+\gamma_{\mathbf{k}}^2\right)}\left(1+3\frac{k^2v_{thi}^2}{\Omega_{\mathbf{k}}^2}+...\right) \quad (3.49)\end{aligned}$$

Thus, the rate of change of the ion thermal velocity is given entirely in terms of bulk ion parameters and field quantities. The term linear in the velocity integrates out to zero, as if the ions have no drift velocity initially, then by (3.46) they must have no drift velocity for all time. Neglect of the term in $3k^2v_{thi}^2/\Omega_{\mathbf{k}}^2$, and of higher order thermal corrections, is consistent with the use of the cold ion approximation in the dispersion relation.

Chapter 4

Solution of the Quasilinear Equations

4.1 The quasilinear equations

The system of equations for the evolution of the electron distribution function under the action of electrostatic turbulence is:

$$K = 1 - \frac{\omega_{pi}^2}{\Omega_{\mathbf{k}}^2} + \frac{2\pi e^2}{m_e \varepsilon_0 k^2} \int_{-\infty}^{\infty} \int_0^{\infty} \frac{J_0^2(a_\perp)}{\Omega_{\mathbf{k}} - k_\perp v_D - k_{\|} v_{\|}} \mathbf{b}_0 . \frac{\partial f_e}{\partial \mu} v_\perp dv_\perp dv_{\|} = 0 \tag{4.1}$$

$$\frac{\partial f_e}{\partial t} = \frac{\partial}{\partial \mu} \cdot \left[\mathsf{D}_e \cdot \frac{\partial f_e}{\partial \mu} \right] \tag{4.2}$$

$$\mathsf{D}_\mathbf{e} = \Re \left\{ i \frac{e^2}{m_e^2} \int \mathbf{b}_0 \frac{J_0^2(a_\perp) I_\mathbf{k}}{\Omega_\mathbf{k} - k_\perp v_D - k_{\|} v_{\|}} \mathbf{b}_0 \, d\mathbf{k} \right\} \tag{4.3}$$

$$\mathbf{b}_0 = -k_\perp \hat{\mathbf{e}}_\Lambda + \frac{k_\perp v_B}{v_\perp} \hat{\mathbf{e}}_\perp + k_{\|} \hat{\mathbf{e}}_{\|}$$

$$\frac{\partial I_\mathbf{k}}{\partial t} = 2\gamma_\mathbf{k} I_\mathbf{k} \tag{4.4}$$

$$\mu = \Lambda \hat{\mathbf{e}}_\Lambda + v_\perp \hat{\mathbf{e}}_\perp + v_{\|} \hat{\mathbf{e}}_{\|} \tag{4.5}$$

Only the electron distribution function has been allowed to evolve in time: the ions are taken to have a constant temperature $T_i \ll T_e$.

In order to follow the evolution of the system, the folowing scheme is used to advance the ysytem through a small time interval:

1. Given the distribution function f_e, the dispersion relation is solved for a range of values of $k_\perp$ and $k_\parallel$ to give the complex frequency Ω_k;
2. The diffusion tensor $\mathsf{D_e}$ is calculated;
3. The electron distribution function is advanced to the next time level;
4. Finally, the wave intensity function is advanced.

This process is repeated until either a prespecified time value is reached or all waves in the system have stabilised.

4.2 Solution of the dispersion relation

The numerical solution of the dispersion equation poses not inconsiderable problems. Normally, one is able to represent the distribution function by a known, analytical function: usually one chooses a Maxwellian distribution with appropriately chosen temperature and density, as was done above. This has the great advantage that the singular $v_\parallel$ integral can be written in terms of a tabulated function, the plasma dispersion function.

In the situation under consideration here, however, the electron distribution will evolve in time, and even if it were initially Maxwellian, it would soon cease to be so. This change in form is crucial to the theory, since the growth rate is dependent on the shape of the distribution, and we are hoping that the distribution function will change so that the instability will cease.

In non-dimensional form, the $v_\parallel$ integral in (4.1) will be of the form

$$F(\xi) = \frac{1}{\sqrt{\pi}} \int_L \frac{g(u)}{u - \xi} du \tag{4.6}$$

where L is the Landau contour, that is, from minus infinity to infinity underneath any singularities of the integrand. To evaluate such an integral numerically (as does the Ferguson subroutine for the evaluation of the plasma dispersion function), one would have to be able to evaluate $g(u)$ off the real axis. For a Maxwellian plasma, $g(u) = \exp(-u^2)$, and this process poses no problems, but we intend to solve the diffusion equation using a finite difference method, which means that $f_e(x, v_\perp, v_{||}, t)$ may only be calculated for real $v_{||}$.

In order to obtain an approximation to $\omega_{\mathbf{k}}$ and $\gamma_{\mathbf{k}}$, we considered the use of two different strategies, a small growth rate approximation method (method 1) and an orthogonal polynomial expansion method (method 2).

4.2.1 Method 1

Split K into its real and imaginary parts $K = K_r + iK_i$, then, assuming that

$$\begin{aligned} K_i &\ll K_r \\ \gamma_{\mathbf{k}} &\ll \omega_{\mathbf{k}} \end{aligned} \tag{4.7}$$

we can Taylor-expand K about $\omega_{\mathbf{k}}$, and get, on dropping small terms:

$$K_r(\omega_{\mathbf{k}}) = 0 \tag{4.8}$$

$$\gamma_{\mathbf{k}} = -K_i \left[\frac{\partial K_r}{\partial \omega_{\mathbf{k}}}\right]^{-1} \tag{4.9}$$

In other words, we find the solution of the real part of the dispersion relation for real $\Omega_{\mathbf{k}}$, and then calculate the growth rate from the imaginary part of the dispersion relation and the gradient of the real part, both of which are to be evaluated at $\omega_{\mathbf{k}}$. The problem of evaluating f_e off the real axis is now solved, since K_r now involves the Cauchy principal part of the $v_{||}$ integral, which can be evaluated by putting f_e to be a Maxwellian with density and temperature equal to those of the true distribution function. In K_i the smallness of $\gamma_{\mathbf{k}}$ means that

we can replace the resonant denominator by the Dirac delta function:

$$K_r = 1 + \chi_i^{[r]} + \chi_e^{[r]}$$

$$\chi_i^{[r]} = -\left(\frac{\omega_{pi}}{\omega_{\mathbf{k}}}\right)^2$$

$$\chi_e^{[r]} = \frac{2\pi e^2}{m_e \varepsilon_0 k^2} \int_0^\infty P \int_{-\infty}^\infty \frac{J_0^2(a_\perp)}{\omega_{\mathbf{k}} - k_\perp v_D - k_{||} v_{||}} \mathbf{b}_0 \cdot \frac{\partial f_e}{\partial \mu} v_\perp dv_\perp dv_{||}$$

$$= \frac{2\pi\omega_{pe}^2}{v_{the}^2 k^2} \left\{ 1 + 2\frac{(\omega_{\mathbf{k}} - k_\perp v_E - k_\perp v_N)}{\sqrt{2} k_{||} v_{the}} \int_0^\infty x J_0^2(sx) Z_r(\xi_0) e^{-x^2} dx \right\} \quad (4.10)$$

$$K_i = \frac{2\pi^2 e^2}{m_e \varepsilon_0 k^2} \int_0^\infty \int_{-\infty}^\infty J_0^2(a_\perp)\, \delta(\omega_{\mathbf{k}} - k_\perp v_D - k_{||} v_{||})\, \mathbf{b}_0 \cdot \frac{\partial f_e}{\partial \mu} v_\perp dv_\perp dv_{||} \quad (4.11)$$

where $s = \sqrt{2} k_\perp v_{the}/\omega_{ce}$, $v_N = -\epsilon_N v_{the}^2/\omega_{ce}$, $\epsilon_N = (1/n_0) dn_0/dx$

$$\xi_0 = \frac{(\omega_{\mathbf{k}} - k_\perp v_D)}{\sqrt{2} k_{||} v_{the}} \quad (4.12)$$

and

$$Z_r(\xi) = \frac{1}{\sqrt{\pi}} P \int_{-\infty}^\infty \frac{e^{-z^2}}{z - \xi} dx$$
$$= -2e^{-\xi^2} \int_0^\xi e^{z^2} dz \quad (4.13)$$

The function here denoted $Z_r(\xi)$ is related to Dawson's integral [1]

Equation (4.8) is solved using the Van WijnGaarden-Dekker-Brent method [42]. This is an iterative method, so that the derivative term in (4.9) can be calculated from the last two iterated $\omega_{\mathbf{k}}$ values and the known values of K_r at those points. Calculation of $\frac{\partial K_r}{\partial \omega_{\mathbf{k}}}$ directly (by differentiating 4.10 analytically) did not seem to be any more accurate, and involved the computational expense of another numerical integration.

4.2.2 Method 2

We shall go back to the dispersion relation (2.38),(2.40) and (2.40), but we have not specified any particular distribution function. We now expand the distribution function in terms of a set of known functions, namely the Hermite polynomials [1].

$$f_e(\Lambda, v_\perp, v_\parallel, t) = \frac{1}{(2\pi)^{\frac{3}{2}}} \sum_{m=-\infty}^{\infty} f_m(\Lambda, v_\perp, t) H_m(v_\parallel / v_{the}) \exp\left(-\frac{1}{2} v_\parallel^2 / v_{the}^2\right) \tag{4.14}$$

It turns out that a similar expansion in the perpendicular velocity component is not necessary. Such polynomial expansions have been used in analytical and numerical studies of the non-linear Vlasov equation [22],[2],[3]. However, to our knowledge, they have not been used to solve the linear dispersion relation for an arbitrary distribution function, as here. The Hermite polynomials are defined by the generating function:

$$\exp(-s^2 + 2sv) = \sum_{m=-\infty}^{m=\infty} H_m(v) \frac{s^m}{m!} \tag{4.15}$$

We now substitute the expansion 4.14 into the dispersion relation. The electron susceptibility χ_e is then:

$$\begin{aligned}
\chi_e &= \frac{1}{\sqrt{2\pi}} \frac{n_0 e^2}{m_e \varepsilon_0 k^2} \sum_{n=-\infty}^{\infty} \int_{-\infty}^{\infty} \int_0^{\infty} \frac{J_n^2(a_\perp)}{\omega_n - k_\parallel v_\parallel} \\
&\qquad \left[-k_\perp \frac{\partial}{\partial \Lambda} + \frac{(n\omega_{ce} + k_\perp v_B)}{v_\perp} \frac{\partial}{\partial v_\perp} + k_\parallel \frac{\partial}{\partial v_\parallel}\right] f_e(v_\perp, v_\parallel, t)\, v_\perp dv_\perp dv_\parallel \\
&= \frac{1}{\sqrt{2\pi}} \frac{\omega_{pe}^2}{k^2} \sum_m \sum_n \int_{-\infty}^{\infty} \int_0^{\infty} \frac{J_n^2(a_\perp)}{\omega_n - k_\parallel v_\parallel} \\
&\qquad \left[-k_\perp \frac{\partial f_m}{\partial \Lambda} H_m + \frac{(n\omega_{ce} + k_\perp v_B)}{v_\perp} \frac{\partial f_m}{\partial v_\perp} H_m + k_\parallel f_m \left(\frac{H_m'}{v_{the}} - \frac{v_\parallel}{v_{the}^2} H_m\right)\right]
\end{aligned}$$

$$\exp\left(-\frac{1}{2}v_{\|}^2/v_{the}^2\right)\frac{v_\perp dv_\perp dv_{\|}}{v_{the}^3}$$

$$= \frac{1}{\sqrt{2\pi}}\frac{\omega_{pe}^2}{k^2}\sum_m\sum_n\int_{-\infty}^{\infty}\int_0^{\infty}\frac{J_n^2(a_\perp)}{\omega_n - k_{\|}v_{\|}}$$
$$\left[-k_\perp\frac{\partial f_m}{\partial\Lambda}H_m + \frac{(n\omega_{ce}+k_\perp v_B)}{v_\perp}\frac{\partial f_m}{\partial v_\perp}H_m + 2m\frac{k_{\|}}{v_{the}}f_m H_{m-1} + \frac{(\omega_n - k_{\|}v_{\|}-\omega_n)}{v_{the}^2}f_m H_m\right]$$
$$\exp\left(-\frac{1}{2}v_{\|}^2/v_{the}^2\right)\frac{v_\perp dv_\perp dv_{\|}}{v_{the}^3} \tag{4.16}$$

where $\omega_n = \omega_{\mathbf{k}} - k_\perp v_D - n\omega_{ce}$, and we have employed the relation:

$$\frac{dH_m}{dv} = 2mH_{m-1} \tag{4.17}$$

If we now define a set of functions ψ_m by

$$\psi_m(\xi) = \frac{1}{\sqrt{2\pi}}\int_{-\infty}^{\infty}\frac{H_m(z)}{z-\xi}\exp\left(-\frac{1}{2}z^2\right)dz \tag{4.18}$$

where $z = v_{\|}/v_{the}$ and $z_n = (\omega_{\mathbf{k}} - k_\perp v_D - n)/k_{\|}$, then we can write the electron susceptibility as

$$\chi_e = \frac{1}{k^2\lambda_{De}^2}\left\{1 - \frac{1}{k_{\|}v_{the}}\sum_m\sum_n\int_0^{\infty}J_n^2(a_\perp)\right.$$
$$\left[-k_\perp v_{the}^2\frac{\partial f_m}{\partial\Lambda}\psi_m(z_n) + (n\omega_{ce}+k_\perp v_B)\frac{v_{the}^2}{v_\perp}\frac{\partial f_m}{\partial v_\perp}\psi_m(z_n) + 2mk_{\|}v_{the}f_m\psi_{m-1}(z_n) - f_m\omega_n\psi_m(z_n)\right]\left.\frac{v_\perp dv_\perp}{v_{the}^2}\right\} \tag{4.19}$$

The function defined by (4.18) can be evaluated directly by numerical integration. However, this is extremely slow, and many psi-functions must be evaluated

for the same value of their argument, but successive values of m, each time we need to evaluate (4.19). A considerably more efficient method to achieve this is to use the two term recurrence relation satisfied by the Hermite polynomials to derive a recurrence relation for the psi-functions. We have:

$$H_{m+1}(v) = 2vH_m(v) - 2mH_{m-1}(v) \tag{4.20}$$

giving:

$$\begin{aligned} \frac{1}{\pi^{\frac{1}{2}}} \int_{-\infty}^{\infty} \frac{H_{m+1}(v)}{v-\xi} e^{-\frac{1}{2}v^2}\, dv &= \frac{2}{\pi^{\frac{1}{2}}} \int_{-\infty}^{\infty} \frac{(v-\xi+\xi)}{v-\xi} H_m(v) e^{-\frac{1}{2}v^2}\, dv \\ &\quad - \frac{2m}{\pi^{\frac{1}{2}}} \int_{-\infty}^{\infty} \frac{H_{m-1}(v)}{v-\xi} e^{-\frac{1}{2}v^2}\, dv \end{aligned} \tag{4.21}$$

and hence:

$$\psi_{m+1}(\xi) = 2\xi\psi_m(\xi) - 2m\psi_{m-1}(\xi) + 2\lambda_m \tag{4.22}$$

where

$$\lambda_m = \frac{1}{\pi^{\frac{1}{2}}} \int_{-\infty}^{\infty} H_m(v) e^{-\frac{1}{2}v^2}\, dv \tag{4.23}$$

Using the properties of the Hermite polynomials, it can be shown very easily that the λ's also satisfy a recurrence relation, namely:

$$\lambda_{m+1} = 2m\lambda_{m-1} \tag{4.24}$$

Clearly, the λ_m are all zero for m odd.

The starting values for ψ's and λ's are:

$$\begin{aligned} \psi_{-1} &= 0 \\ \psi_0 &= \frac{1}{\pi^{\frac{1}{2}}} \int_{-\infty}^{\infty} \frac{e^{-\frac{1}{2}v^2}}{v-\xi}\, dv = Z(\xi/\sqrt{2}) \end{aligned}$$

$$\begin{aligned}\lambda_{-1} &= 0 \\ \lambda_0 &= \sqrt{2}\end{aligned}$$

Hence (4.19) can be computed with only one evaluation of the plasma dispersion dispersion function, and repeated applications of (4.22) and (4.24).

Given the coefficients f_m, it is possible to evaluate the dispersion relation for arbitrary f_e. In order evaluate the former given the latter, we use the fact that the Hermite polynomials are othogonal, that is to say:

$$\int_{-\infty}^{\infty} H_m(v)H_n(v)\exp(-v^2)dv = \begin{cases} 2^n n!\sqrt{\pi} & m = n \\ 0 & \text{otherwise} \end{cases} \tag{4.25}$$

the coefficients f_m can be evaluated by use of the relation:

$$f_m(\Lambda, v_\perp, t) = \frac{1}{2^n n!\sqrt{\pi}} \int_{-\infty}^{\infty} f_e(\Lambda, v_\perp, v_\parallel, t)H_m(v)\exp(-\frac{1}{2}v^2)dv \tag{4.26}$$

In practice, the summation in (4.14) will be truncated to a finite number (perhaps a few tens) of terms.

Given that the f_m are known, it is necessary to solve the complex dispersion relation (4.19): this was achieved by employing Muller's method [44],[50],[42]. Like Brent's method, this is iterative and so requires an initial estimate for the root of the dispersion relation to start off the root-finding process. Initially, the lower hybrid frequency $\omega_{LH} \approx \sqrt{\omega_{ce}\omega_{ci}}$ is a good enough value: at each subsequent time that the dispersion relation is to be solved, the last root is used as an initial estimate.

4.2.3 Validation and comparison of the methods

In order to validate the arithmetic in the polynomial expansion method, we used it to solve the dispersion relation for a set of test distributions, and then compared

the results with those obtained when the distributions were substituted into the dispersion relation directly. In both cases Muller's method was used to solve the dispersion relation. The test distributions used were of the form

$$f_e(v_\perp, v_\parallel) = \frac{n_e}{v_{the}^3} \frac{1}{(2\pi)^{3/2}} \frac{1}{1.3...(2p-1)} \left(\frac{v_\parallel}{v_{the}}\right)^{2p} \exp\left[-\frac{1}{2}\frac{(v_\perp^2 + v_\parallel^2)}{v_{the}^2}\right] \qquad (4.27)$$

where p is a positive integer. After some algebra, it is possible to derive the following expression for the electron susceptibility:

$$\chi_e = \frac{1}{k^2\lambda_{De}^2}\left\{1 + \frac{2^{p+1}}{1.3...(2p-1)}\int_0^\infty J_0^2(sx)\left[cZ_{2p}(\xi_0) - pZ_{2p-1}(\xi_0)\right] e^{-x^2}\, x dx\right\} \qquad (4.28)$$

where

$$\begin{aligned} c &= \frac{\Omega_{\mathbf{k}} - k_\perp v_E - k_\perp v_N}{\sqrt{2}k_\parallel v_{the}} \\ Z_n(\xi) &= \frac{1}{\pi^{\frac{1}{2}}}\int_{-\infty}^{\infty} t^n \frac{e^{-t^2}}{(t-\xi)}\, dt \end{aligned}$$

The Z functions are simply generalisations of the plasma dispersion function, and were evaluated using a recurrence relation method [18]. The case p=0 just gives the Maxwellian dispersion relation. This dispersion relation is not meant to model any physically realistic situation, but it does provide a good check that the mechanics of the polynomial expansion method function correctly. The results are diplayed in the table.

p	Polynomial expansion method	Exact
1	$2.44535 \times 10^{-2} + i2.95537 \times 10^{-3}$	$2.44559 \times 10^{-2} + i2.96172 \times 10^{-3}$
2	$2.33234 \times 10^{-2} - i2.69325 \times 10^{-3}$	$2.33231 \times 10^{-2} - i2.69189 \times 10^{-3}$
3	$2.52640 \times 10^{-2} - i8.53585 \times 10^{-3}$	$2.52579 \times 10^{-2} - i8.53058 \times 10^{-3}$
4	$3.50951 \times 10^{-2} - i1.26392 \times 10^{-2}$	$3.50968 \times 10^{-2} - i1.26882 \times 10^{-2}$
5	$3.81804 \times 10^{-2} - i3.88605 \times 10^{-3}$	$3.82107 \times 10^{-2} - i3.89820 \times 10^{-3}$
6	$3.62416 \times 10^{-2} - i1.03653 \times 10^{-3}$	$3.62662 \times 10^{-2} + i1.03969 \times 10^{-2}$
10	$3.33103 \times 10^{-2} - i1.31651 \times 10^{-5}$	$3.33275 \times 10^{-2} - i1.46416 \times 10^{-5}$

The relative performance of the small growth rate and polynomial expansion methods was evaluated by comparing the values of $\omega_{\mathbf{k}}$ and $\gamma_{\mathbf{k}}$ obtained from (4.8) and (4.9) and the value of $\Omega_{\mathbf{k}}$ obtained by inserting a Maxwellian directly into (4.1). For $\beta_e = 0.1$, $\epsilon_B = 0.01$ and $\epsilon_N = 0$ we obtained:

$(k_\perp, k_\parallel)$	Brent	Muller
$(1.0, 0.01)$	$3.25 \times 10^{-2} + i7.37 \times 10^{-10}$	$3.23 \times 10^{-2} + i5.84 \times 10^{-10}$
$(1.0, 0.05)$	$3.54 \times 10^{-2} + i6.83 \times 10^{-5}$	$3.49 \times 10^{-2} + i8.05 \times 10^{-3}$
$(1.0, 0.1)$	$3.55 \times 10^{-2} + i1.04 \times 10^{-2}$	$3.18 \times 10^{-2} + i8.06 \times 10^{-3}$
$(1.0, 0.2)$	$2.79 \times 10^{-2} + i6.37 \times 10^{-3}$	$2.59 \times 10^{-2} + i5.80 \times 10^{-3}$
$(2.0, 0.1)$	$5.39 \times 10^{-2} + i2.55 \times 10^{-5}$	$5.38 \times 10^{-2} + i1.30 \times 10^{-2}$

The results in the Muller column are for both the 'exact' solution and for the results obtained by the polynomial expansion method, since these were vitually identical to the accuracy quoted. As can be seen, the agreement between the small growth rate method and the exact result is fairly good in most cases, but certainly not exceptional, even though the condition (4.7) is not always satisfied.

As a final test, the two methods were used to solve the dispersion relation for a non-Maxwellian plasma. The distribution function used was that for a 'resonance' distribution:

$$f_e(v_\perp, v_\parallel) = \frac{1}{2\pi^2} \frac{n_e}{v_{the}^3} \frac{e^{-\frac{1}{2}v_\perp^2/v_{the}^2}}{(1 + v_\parallel^2/v_{the}^2)} \tag{4.29}$$

from which we can derive:

$$\chi_e = \frac{1}{k^2\lambda_{De}^2} \left\{ 1 - 2\int_0^\infty x J_0^2(sx) \left[\frac{k_\perp v_B}{k_\parallel v_{the}} \frac{1}{(\xi_0 + i)} + \frac{\xi_0(\xi_0 + 2i)}{(\xi_0 + i)^2} \right] e^{-x^2}\, dx \right\} \tag{4.30}$$

The results were as follows:

$(k_\perp, k_\parallel)$	**Small growth rate**	**Polynomial expansion**	**Exact**
$(1.0, 0.1)$	$3.55 \times 10^{-2} +$	$3.16 \times 10^{-2} +$	$3.33 \times 10^{-2} +$
	$i2.35 \times 10^{-3}$	$i3.75 \times 10^{-3}$	$i3.93 \times 10^{-3}$
$(1.0, 0.05)$	$3.48 \times 10^{-2} +$	$3.19 \times 10^{-2} +$	$3.32 \times 10^{-2} +$
	$i2.12 \times 10^{-4}$	$i7.99 \times 10^{-4}$	$i8.02 \times 10^{-4}$
$(2.0, 0.1)$	$5.39 \times 10^{-2} +$	$5.24 \times 10^{-2} +$	$5.31 \times 10^{-2} +$
	$i1.19 \times 10^{-3}$	$i2.74 \times 10^{-3}$	$i3.36 \times 10^{-3}$
$(0.5, 0.1)$	$1.56 \times 10^{-2} +$	$1.41 \times 10^{-2} +$	$1.47 \times 10^{-2} +$
	$i5.52 \times 10^{-3}$	$i6.32 \times 10^{-3}$	$i7.45 \times 10^{-3}$
$(1.0, 0.2)$	$2.79 \times 10^{-2} +$	$2.81 \times 10^{-2} +$	$2.91 \times 10^{-2} +$
	$i4.67 \times 10^{-3}$	$i5.64 \times 10^{-3}$	$i6.20 \times 10^{-3}$

In this case, the Hermite polynomial expansion method gives a closer result than the small growth rate approximation, which consistently underestimates the growth rate.

In conclusion, The two two methods both perform reasonably well on a number of test problems. Although it is more complicated and computationally involved, the Hermite polynomial expansion does give better results. On the basis of experience with the two methods as part of the code to solve the complete set of quasilinear equations, it was found that the polynomial expansion method

produced more plausible results. Thus, the latter was used to produce all the results shown in the next chapter.

To evaluate the diffusion tensor, the dispersion relation is solved for a number of values of $\mathbf{k}$ defined on a regular grid, to give $\omega_{\mathbf{k}}$ and $\gamma_{\mathbf{k}}$. The integral in (4.3) is then evaluated numerically using standard techniques.

4.3 Solution of the wave and particle evolution equations

It is straightforward to advance the wave intensity function from one time level to the next. However, the diffusion equation currently has three 'space-like' independent variables on its right-hand side: to enable the computations to be carried out in a reasonable length of time on the computing resources available, some additional simplifications are required, which will be described below. In this section, we shall assume that we only need to solve a two-dimensional diffusion equation of the form:

$$\frac{\partial f}{\partial t}(\mathbf{r},t) = \frac{\partial}{\partial \mathbf{r}} \cdot \left[\mathsf{D}(\mathbf{r},t) \cdot \frac{\partial f}{\partial \mathbf{r}}(\mathbf{r},t) \right] = \hat{D} f(\mathbf{r},t) \tag{4.31}$$

where $\mathbf{r} = (x,y)$, $f = f(x,y,t)$ and t is time. We will also have an initial condition on f, namely $f(x,y,0) = f_0(x,y)$, and an appropriate set of boundary conditions. It is not necessarily the case that x and y are Cartesian co-ordinates. The diffusion coefficient D is a 2 by 2 matrix, all of whose elements will, in general, be non-zero, which means that there will be cross-derivative terms (proportional to $\frac{\partial^2 f}{\partial x \partial y}$) on the right-hand side of (4.31). The spatial derivatives were differenced on a regular mesh of points $(x_i, y_j) = (i\Delta x, j\Delta y)$ using standard techniques ([37]). The diffusion tensor was held constant between time steps. In order to advance the solution of (4.31) from one time step to the next, we have chosen to employ the line hopscotch method, [19], [20], [21], as it is capable of handling cross-derivative

terms very easily. It is also claimed to be fast and is easy to programme, as it only involves the solution of tridiagonal systems of linear equations. Since it is probably not a very widely used numerical method, we will outline its principles here.

The finite difference replacement of $\hat{D}$ is denoted $\hat{L}$, i.e.

$$\hat{D}f(x_i, y_j, t^n) = \hat{L}f_{ij}^n$$

where f_{ij}^n is an approximation to the solution value at the point (x_i, y_j, t^n). Since the diffusion tensor is space-dependent, the operator $\hat{L}$ will depend on i and j. Since the differential operator $\hat{D}$ only involves second derivatives at the highest, the difference operator $\hat{L}$ will only involve f at the point (x_i, y_j, t^n) and its immediate neighbours (in the notation of [19], $\hat{D}$ is said to be an 'E-operator'). This property is vital for the application of the hopscotch algorithm.

The two simplest ways to integrate (4.31) are the simple explicit and the implicit algorithms:

$$f_{ij}^{n+1} = f_{ij}^n + \Delta t \hat{L} f_{ij}^n \tag{4.32}$$

$$f_{ij}^{n+1} = f_{ij}^n + \Delta t \hat{L} f_{ij}^{n+1} \tag{4.33}$$

where Δt is the timestep. The first method has the advantage of simplicity: the only unknown in the equation is f_{ij}^{n+1}, and so we can calculate f at time level $n+1$ without having to solve any systems of equations. However, it has poor stability properties, with the result that Δt must be small in order that the numerical solution does not deviate wildly from the true one. The second method is unconditionally stable, but f_{ij}^{n+1} appears on both sides of the equation, and is thus only given implicitly by 4.33. It is thus necessary to solve a matrix equation at each time step (mercifully, the coefficient matrix is sparse: that is to say, although it may have a large number of elements, the vast bulk of them

will be zero), and although a variety of methods exists to accomplish this, such as successive over-relaxation, it is a potentially time-consuming process.

The class of hopscotch methods works by combing 4.32 and 4.33 in such a way that we only ever need to solve (at worst) tridiagonal systems of equations, a process which can be performed quickly and easily using Gaussian elimination (without pivoting). The recipe for line hopscotch is as follows:

- for all grid points such that j + n is odd, apply 4.32
- for all grid points such that j + n is even, apply 4.33

In the first step, we solve the diffusion equation (explicitly) along alternate lines parallel to one axis. The new (partial) solution can overwrite the old, so no new storage is required. After this process, the situation is as shown in figure 4.1.

The new solution ($f(x_i, y_j, t^n)$) is known at all the points with filled-in circles. The implicit scheme is now applied at all the remaining points: at point (i, j) at most nine points (those ringed) are required to evaluate ($f(x_i, y_j, t^{n+1})$), but six are already known. The three remaining unknown points give us our tridiagonal system.

On an $n \times n$ grid, line hopscotch will require the solution of $n/2$ sets of equations, whereas an alternating direction implicit (ADI) method, which requires a complicated splitting of $\hat{L}$ so that only tridiagonal equations must be solved, will require the solution of n equations per timestep. In order to achieve unconditional stability, the 'explicit' and 'implicit' lines swap over at successive time levels. Other varieties of the hopscotch algorithm exist, such as 'block' and 'ordered odd-even' hopscotch [37].

4.4 Conclusion

It is by no means claimed that the methods presented above represent the most economical or efficient way to solve the quasilinear equations. For example, al-

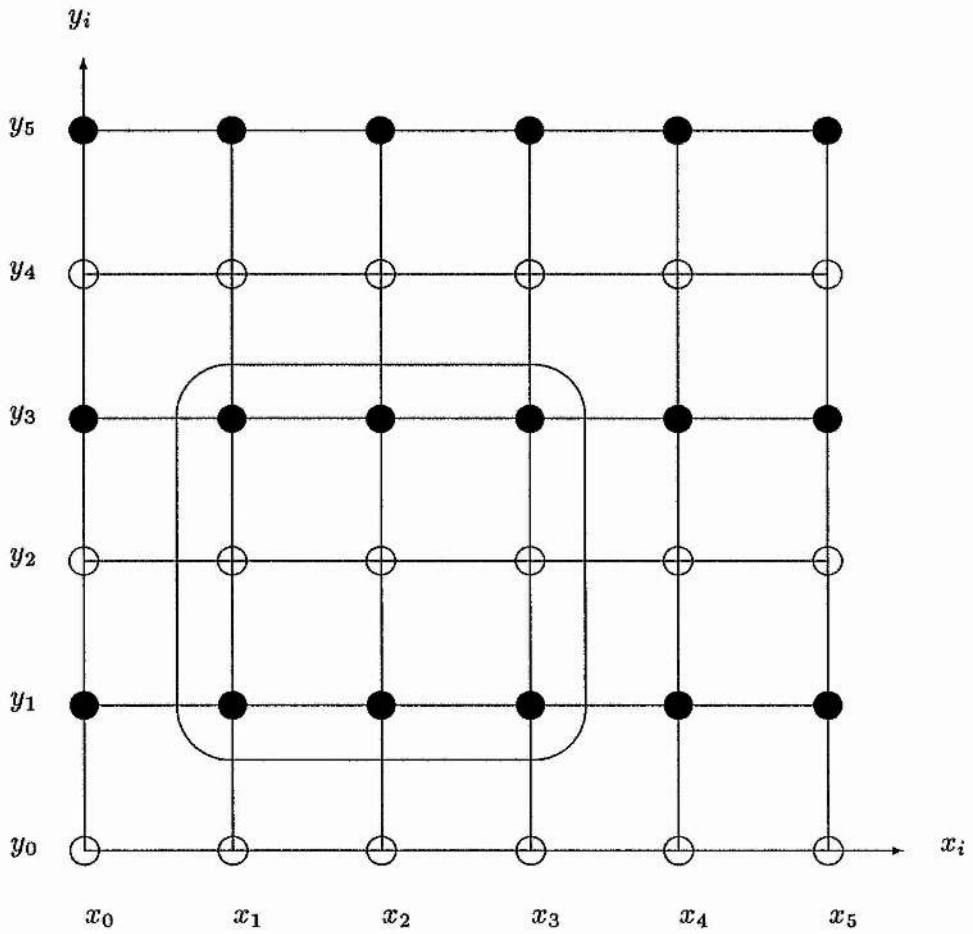

Figure 4.1: Line hopscotch after the explicit stage.

though the hopscotch method works well for two-dimensional diffusion equations, it is not readily generalisable to three dimensions, so that we cannot easily study the evolution of distribution functions with spatial and full velocity dependence with all possibly apposite physical processes included. This could be a problem if we wanted to study the evolution of an inhomgeneous plasma under the action of electromagnetic instabilities such as the kinetic cross field streaming instability or the generalised lower hybrid drift instability. Moreover, there is no way presented in the numerical analytical literature known to us of varying the time step so as to maintain within a pre-specified accuracy limit. This would allow integration of the diffusion equation to proceed in a much more efficient manner. Use of the 'method of lines', perhaps coupled with the expansion (4.14), to convert the partial differential equation into a large system of ordinary differential equations (which can then be solved numerically using an appropriate library routine), would perhaps be preferential. However, whichever numerical method one chooses for a particular problem, there is probably always a slighly better one around the corner.

The method we have used to solve the dispersion relation, by expanding the background distribution in terms of a set of orthogonal polynomials, is, on the hand, capable of being extended to a variety of other cases (for example, electromagnetic instabilities), and could be used in any application where the detailed shape of the distribution function must be taken into account.

Chapter 5

Numerical results

5.1 Solution of the quasilinear equations

In this set of results, we shall ignore all spatial gradients in (4.2) and (4.1), so that diffusion is only allowed to occur in $v_\perp$ and $v_\parallel$, and we have a two-dimensional diffusion equation to solve. The distribution evolves in time only, not in space, with the magnetic gradient inverse length scale held constant. Stabilisation is expected to occur solely due to the alteration of the shape of the distribution function on account of the reaction of the unstable waves.

The diffusion equation now reads:

$$\begin{aligned}\frac{\partial f_e}{\partial t} &= \frac{1}{v_\perp}\frac{\partial}{\partial v_\perp}\left[v_\perp D_{\perp,\perp}\frac{\partial f_e}{\partial v_\perp}\right] + \frac{1}{v_\perp}\frac{\partial}{\partial v_\perp}\left[v_\perp D_{\perp,\parallel}\frac{\partial f_e}{\partial v_\parallel}\right] + \frac{\partial}{\partial v_\parallel}\left[D_{\parallel,\perp}\frac{\partial f_e}{\partial v_\perp}\right] \\ &\quad + \frac{\partial}{\partial v_\parallel}\left[D_{\parallel,\parallel}\frac{\partial f_e}{\partial v_\parallel}\right] \\ 0 &\leq v_\perp \leq \infty \\ -\infty &\leq v_\parallel \leq \infty \end{aligned} \tag{5.1}$$

where the elements $D_{\alpha,\beta}$ of the diffusion tensor are:

$$D_{\perp,\perp} = \Re\left\{ i\frac{e^2}{m_e^2}\int J_0^2(a_\perp)\left(\frac{k_\perp v_B}{v_\perp}\right)^2 \frac{I_{\mathbf{k}}}{\Omega_{\mathbf{k}} - k_\perp v_D - k_{||}v_{||}}\, d\mathbf{k}\right\} \quad (5.2)$$

$$D_{\perp,||} = D_{||,\perp} = \Re\left\{ -i\frac{e^2}{m_e^2}\int J_0^2(a_\perp)\frac{k_\perp v_B k_{||}}{v_\perp} \frac{I_{\mathbf{k}}}{\Omega_{\mathbf{k}} - k_\perp v_D - k_{||}v_{||}}\, d\mathbf{k}\right\} \quad (5.3)$$

$$D_{||,||} = \Re\left\{ i\frac{e^2}{m_e^2}\int J_0^2(a_\perp)k_{||}^2 \frac{I_{\mathbf{k}}}{\Omega_{\mathbf{k}} - k_\perp v_D - k_{||}v_{||}}\, d\mathbf{k}\right\} \quad (5.4)$$

For (5.1) to have a regular solution, it is necessary that $D_{\perp,||} \longrightarrow 0$ as $v_\perp \longrightarrow 0$: this is clearly the case.

The boundary conditions are that:

$$f_e(v_\perp, v_{||}, t) \longrightarrow 0 \qquad v_\perp \longrightarrow \infty$$

$$f_e(v_\perp, v_{||}, t) \longrightarrow 0 \qquad v_{||} \longrightarrow \pm\infty$$

$$\frac{\partial f_e}{\partial v_\perp}(v_\perp, v_{||}, t) = 0 \qquad v_\perp = 0$$

The infinite range of $v_\perp$ and $v_{||}$ was truncated: in all numerical integrations we took $0 \leq v_\perp \leq 10v_{the0}$ and $-10v_{the0} \leq v_{||} \leq 10v_{the0}$, where v_{the0} is the thermal velocity of the initial electron distribution function.

The initial electron distribution function is taken to be an isotropic Maxwellian:-

$$f_e(v_\perp, v_{||}, 0) = \frac{1}{(2\pi)^{3/2}}\frac{n_0}{v_{the0}^3}\exp\left[-\frac{1}{2}\left(v_\perp^2 + v_{||}^2\right)/v_{the0}^2\right] \quad (5.5)$$

The initial form of the wave intensity spectrum is not particularly important, since initially the waves will grow exponentially. The range of wavenumber values

was chosen to span the region in k-space where growth is largest. Individual waves were given evenly distributed values of $k_\perp$ and $k_\parallel$. The actual number of waves used was not found to be critical, and since the dispersion relation must be solved for each wave this number was held fairly low in order to minimise the computational time required.

5.2 Time evolution of the modified two stream instability

We present the results of the solution of the quasilinear equations for two different values of ϵ_B, namely $a_{the}\epsilon_B = 0.01$ (Run 1) and $a_{the}\epsilon_B = 0.02$ (Run 2). The pages following 74 and 77 give a succession of plots of the electron distribution function at various stages in its evolution in time. The abscissae are measured in units of the initial electron thermal velocity, and the initial plot is normalised so that the volume under the surface is unity. The computer code conserves particles extremely well, so that each subsequent plot is, effectively, normalised in the same way. The main features of the evolution of the electron distribution functions are the same in each case: after a few hundred electron gyroperiods wings begin to form in the parallel direction as particles with parallel velocities of the order of one or two thermal velocities are accelerated to higher energies. The wings later develop into broader, more shoulder-like structures, at the expense of the central peak (as total particle number must be conserved). Eventually, the distribution function becomes a broad, low, roughly flat-topped structure. Figures 5.4 and 5.4 show the change of the parallel electron thermal velocity, as defined by

$$v_{the\parallel} = \left[\frac{\int v_\parallel^2 f_e d\mathbf{v}}{\int f_e d\mathbf{v}}\right]^{\frac{1}{2}} \tag{5.6}$$

with time for the two runs.

There is, in comparison, virtually no perpendicular heating observed. Because

they are highly magnetised, the electrons will be able to move much less freely across the magnetic field than along it. This is due to the essentially Landau nature of the resonance. It would be possible to produce more perpendicular heating by including cyclotron ($n \neq 0$) terms as well as the Landau ($n = 0$) term in the dispersion relation and diffusion coefficients: in other words, we would have to consider the Bernstein wave type instabilities as well.

Also shown after the plots of the distribution function are plots of the growth rates of the waves. It can be seen from figure 5.3 that in the first run the maximum growth rate does decreases monotonically in time, whereas in the run (figure 5.5) with the larger magnetic field gradient (and hence stronger instability) this is not so. The mode which is growing at the fastest rate at one point in time will not necessarily be doing so later on. What seems to happen in the latter case (Run 2) is that initially the most unstable mode will have the greatest effect on the electron distribution function (for a wave in resonance, $D \approx 1/\gamma$). This mode will then change the shape of the distribution function so that it will become more stable, presumably (in the nature of quasilinear theory) by flattening some portion of the distribution function. Schematically, one might expect the distribution function shown in figure 5.2 (upper panel) to become as shown in figure 5.2 (lower panel), that is, for a plateau to be formed, with

$$\frac{k_\perp v_B}{v_\perp}\frac{\partial f_e}{\partial v_\perp} + k_\parallel \frac{\partial f_e}{\partial v_\parallel} \approx 0 \tag{5.7}$$

However, the distribution function has now been steepened at other points, and so it is possible that another mode might be made more unstable, and may become the new dominant mode. It will then modify the distribution function in such a way as to reduce its own growth rate, and the process could then continue until all the modes are effectively stabilised. It should be borne in mind that the dispersion relation can only be solved at a finite set of points in $\mathbf{k}$ space, when in reality there will be a true continuum of waves excited. Thus, a real system might

move towards stability in a somewhat smoother fashion. However, the average growth rate, defined by

$$\bar{\gamma}(t) = \int \gamma(\mathbf{k}, t)\, d\mathbf{k} \tag{5.8}$$

is in fact a monotonically decreasing function of time in both cases.

The dependence in the rate of heating of the plasma on the electron beta is shown in figures 5.7 to 5.10. The larger beta is, the smaller is the amount of electron heating after the same length of time. This is because the larger beta is, the greater is the stabilising efect of the magnetic gradient drift.

At the end of both runs 1 and 2, it can be seen that all of the growth rates have been reduced substantially from their initial values. However, following the system to longer times becomes increasingly problematic numerically. As time progresses, the form of the diffusion tensor becomes more and more complex, so that numerical solution of the diffusion equation becomes increasingly more difficult. Even so, in a shock, the particles must traverse the ramp in a finite time, the gradients necessary to drive the instability will only be present for a finite period of time.

Moreover, in these runs we have fixed the value of the cross-field ion-electron drift velocity to be the same throughout the time span of the run. However, it would be more realistic to specify this quantity initially, and then allow it to vary in time under the action of the unstable wave spectrum. This would introduce another stabilisation mechanism on top of the quasilinear modification of the electron distribution function. It is the cross-field drift that provides the free energy source for the instability, and so we have been feeding energy into the system, resulting in wave growth and particle heating.

If we work now in the electron rest frame, the cross- field macroscopic drift due to the 'E cross B' force will be contained in the ion terms. Thus, the ion susceptibility is modified to

$$\chi_{i,\mathbf{k}} = \frac{1}{k^2 \lambda_{Di}^2} \left(1 + \xi_i Z\left(\xi_i\right)\right) \tag{5.9}$$

where $\xi_i = (\Omega - k_\perp v_0)/\sqrt{2} k v_{thi}$, or, assuming that the ions are cold,

$$\chi_e = -\frac{\omega_{pi}^2}{\left(\Omega - k_\perp v_0\right)^2} \tag{5.10}$$

Here, v_0 is the cross-field drift. The magnetic field gradient length scale can be related to the drift velocity (assuming a linear field profile) by Ampère's law, as was done above, to give:

$$\epsilon_B a_{the} = 0.5 \beta_e \frac{v_0}{v_{the}} \tag{5.11}$$

The magnetic drift velocity term in both the dispersion relation and the diffusion coefficients can thus be evaluated.

In order to follow the evolution of the drift velocity, we can take the first moment of the ion diffusion equation, to obtain:

$$n_0 \frac{dv_0}{dt} = -i \frac{\varepsilon_0}{m_i} \sum_{\mathbf{k}} k_\perp k^2 \left|\delta\varphi_{\mathbf{k}}\right|^2 \left\{\chi_{i,\mathbf{k}}\right\} \tag{5.12}$$

The neglect of spatial dependency (that is, variation with Λ) in the above has the effect of excluding effects due to the lower hybrid drift instability, which relies on gradients in density and temperature. Unfortunately, including spatial variation has the effect of increasing the number of independent variables on the left hand side of the electron diffusion equation from two to three, putting it beyond the scope of the code that we have written to solve the diffusion equation, as well as increasing the scale of the computational problem substantially. However, there are two ways in which we can include spatial effects without having to write a code to solve three-dimensional diffusion equations: due to lack of time, these computations have not been undertaken, but we feel that it is worthwhile to outline how the calculations could, in principle, proceed. First, we could study

only flute modes (that is, set $k_{\|} = 0$. This would leave us with a problem similar to that studied qualitatively by Krall and Book [26],[27]. We feel, though, that electron heating due to this would not be significant, and that it is necessary to retain a finite component of the wavenumber parallel to the magnetic field. We can do this by noting that in the low frequency ($\omega \ll \omega_{ce}$), low beta (and hence electrostatic) limit, we can remove the $v_{\perp}$ variation by neglecting the magnetic field gradient (from (5.11) it can be seen that for low electron beta the effect of the magnetic is going to be of secondary importance in comparison to the macroscopic drifts). It can be seen immediately from (4.3) that

$$D_{\perp,\perp} = D_{\perp,\|} = D_{\|,\perp} = 0 \tag{5.13}$$

since $v_B = 0$, and also the other diffusion coefficients become independent of $v_{\perp}$. We can then write

$$f_e(\Lambda, v_{\perp}, v_{\|}, t) = 2\pi \frac{n_e}{v_{the}^3} e^{-\frac{1}{2}v_{\perp}^2/v_{the}^2} f_{e,\|}(\Lambda, v_{\|}, t) \tag{5.14}$$

where

$$f_{e,\|}(\Lambda, v_{\|}, t) = \frac{1}{2\pi} \int_0^{\infty} f_e(\Lambda, v_{\perp}, v_{\|}, t) v_{\perp} dv_{\perp} \tag{5.15}$$

On integrating the electron quasilinear diffusion equation over $v_{\perp}$ we obtain:

$$\begin{aligned} \frac{\partial f_{e,\|}}{\partial t} &= \frac{\partial}{\partial \Lambda}\left[D_{\Lambda,\Lambda}\frac{\partial f_{e,\|}}{\partial \Lambda}\right] + \frac{\partial}{\partial \Lambda}\left[D_{\Lambda,\|}\frac{\partial f_{e,\|}}{\partial v_{\|}}\right] + \frac{\partial}{\partial v_{\|}}\left[D_{\|,\Lambda}\frac{\partial f_{e,\|}}{\partial \Lambda}\right] \\ &\quad + \frac{\partial}{\partial v_{\|}}\left[D_{\|,\|}\frac{\partial f_{e,\|}}{\partial v_{\|}}\right] \end{aligned} \tag{5.16}$$

The dispersion relation is now Λ-dependent, but it can be simplified, because the resonant denominator is now no longer dpendent on $v_{\perp}$, and so the integral in (4.19) can be evaluated analytically, using (2.45), to give:

$$\chi_e = \frac{1}{k^2\lambda_{De}^2}\left\{1 - \frac{1}{k_\parallel v_{the}}\exp -\lambda^2 I_0(\lambda^2) \right.$$
$$\left. \sum_m \left[-k_\perp v_{the}^2 \frac{\partial g_m}{\partial \Lambda}\psi_m + 2mk_\parallel v_{the} g_m \psi_{m-1} - \omega g_m \psi_m \right] \right\} \qquad (5.17)$$

where

$$g_m(\Lambda, t) = \frac{1}{2^{m-1/2}m!}\int_{-\infty}^{\infty} f_{e,\parallel}(\Lambda, v_\parallel, t) H_m\left(\frac{v_\parallel}{v_{the}}\right) \exp\left(-\frac{1}{2}\frac{v_\parallel}{v_{the}}^2\right) \frac{dv_\parallel}{v_{the}}$$

This dispersion relation now includes all drifts due to gradients in density and temperature.

The initial conditions would now have to be Λ-dependent, with the initial distribution function specified throughout a 'box' of finite length with appropriate boundary conditions at either end: specification that the spatial gradient of the electron distribution function be zero at both ends would have the effect of eliminating inflow or outflow of plasma through the ends of the box.

The analysis could be extended to include waves with finite wave number in the x-direction by a WKBJ-type method [4].

5.3 Applications to collisionless shock waves

In the results presented above we have effectively fixed attention to a point in space in an inhomogeneous plasma, and followed the evolution of the electron distribution function and waves in time. However, in a collisionless plasma shock wave, particles will be convected from a region of uniform properties through a region of non-zero field (and density) gradients to another uniform region. To model electron heating across a shock layer, we move to a frame of reference moving through the shock with a speed equal to the 'E cross B' drift velocity in the direction through the shock. Thus, the diffusion equation (neglecting Λ variation on the right hand side) becomes:

$$u_0\omega_{ce}\frac{\partial f_e}{\partial \Lambda} = \frac{\partial}{\partial v}\cdot\left[\mathsf{D}_e\cdot\frac{\partial f_e}{\partial v}\right] \tag{5.18}$$

where $u_0 = E_y/B_0$ is the drift speed of the electrons through the shock. We would end up with an initial value problem with the upstream conditions specified in advance. We should also, in this case, model the generation of waves by thermal excitation processes, by adding a term $S_{\mathbf{k}}$ to the wave intensity evolution equation:

$$\frac{\partial}{\partial x}\left[u_0 I_{\mathbf{k}}\right] = 2\gamma_{\mathbf{k}} + S_{\mathbf{k}} \tag{5.19}$$

since otherwise the upstream wave spectrum would damp out in the uniform region of the plasma. However, we have simply ignored thermal excitation processes ($S_{\mathbf{k}} = 0$), and set the right hand side of (5.19) to be zero for all waves with negative growth rates.

There are now several extra parameters to be specified in advance. The first is the upstream Alfvènic Mach number M_{A1}. Obviously, this must exceed unity, and it must also be less than the first critical Mach number to ensure that the shock is subcritical, and hence laminar. This fixes the upstream bulk flow velocity:

$$\frac{v_1}{v_{the1}} = M_{A1}\frac{v_{A1}}{v_{the1}} \tag{5.20}$$

We must also specify the magnetic field profile $B_0(x)$. We assumed that the field increases smoothly and monotonically from its upstream value to its downstream value, which was usually taken to be twice the upstream value. We are principally interested in laminar shocks, but a quasilaminar shock could perhaps be modelled by superimposing oscillations on the monotonic field profile. The upstream conditions that we have imposed have the implication that the proportion of reflected ions will be low, so that there will not be a magnetic 'foot' structure upstream of of the shock ramp, nor will there be a magnetic overshoot downstream. The magnetic field gradient length scale can then be evaluated using:

$$\epsilon_B = \frac{1}{B_0}\frac{dB_0}{dx} \tag{5.21}$$

Finally, we must specify the width of the shock. We used values consistent with a number of quasi-perpendicular shocks observed by the ISEE spacecraft [47]. These all had a width L_S such that:

$$L_S = a\frac{c}{\omega_{pi}} \tag{5.22}$$

where a is a dimensionless quantity of the order of unity. These shocks, being non-perpendicular, are in fact probably dispersive, rather than resistive, in character, and hence the amount of anomalous resistivity required is much smaller than that needed in much thinner perpendicular shocks, which tend to have thicknesses such that:

$$L_S = b\frac{c}{\omega_{pe}} \tag{5.23}$$

where b is another dimensionless quantity, but of order ten to twenty. For this class of shock, which is more often found in the laboratory than in the solar wind, it is more likely that the ion acoustic instability is dominant, since the cross-field currents will be larger.

Results for a run with parameters appropriate to a quasiperpendicular bow shock are presented in run 3. We have taken $a = 1$ and $\beta_e = 0.1$. The total amount of heating is fairly modest, about 40% of the upstream value, but this is in rough accordance with the amount of anomalous (that is, greater than adiabatic) heating observed. It should be recalled that our model does not include the heating caused by the direct compression of the plasma by the background fields, only the anomalous heating by the modified two stream instability.

The sequence of distribution functions shows that the downstream electron distribution function has a flat top. This is typical of magnetosheath electron distributions, though these particles will have passed through any of a large

variety of shocks. However, observations of electron distributions in the bow shock [11], [47] do actually show the progressive flattening of the electron distribution function as one moves progressively through the shock. This process is often accompanied by formation and subsequent erosion of an offset peak in the parallel direction. This is probably due to the action of the component of the background electric field along the background magnetic field, which will be present as the observed shocks were not exactly perpendicular. However, this has been neglected in our calculations.

Most of the activity can be seen to occur in the middle of the shock, as this is where the magnetic field gradient is largest. The parallel temperature lags behind the growth since it takes a while for the waves to build up to a large enough amplitude to be able to affect the bulk of the ditribution appreciably. The temperature levels off after the system has stabilised because we have only included growing waves in the calculation of the evolution of the electron distribution function. This is also why the intensity, defined by

$$I_{tot} = \sum_{\mathbf{k}} \frac{\frac{1}{2}\varepsilon_0 k^2 \left|\delta\varphi_{\mathbf{k}}\right|^2}{n_1 k_B T_{e1}} \tag{5.24}$$

does not damp away in the downstream portion of the shock. The maximum value of the wave intensity, about 10^{-5}, seems to be compare favourably with that obtained by Winske et al. [51], despite substantial differences in our model and theirs.

5.4 Extensions to the model

There are clearly many additional physical phenomena that could be included in the model. However, the philosophy behind the current work has been to attempt to generate and solve the simplest possible model capable of giving something approaching a reasonable description of the physical problem. Possible future

work could include modelling:

- warm ions
- electromagnetic waves
- inclusion of spatial gradients

Our results are valid provided $T_i \ll T_e$. However, it is more characteristic of the bow shock to have $T_i \approx T_e$. The consequence of having thermal ions is to include the effect of ion Landau damping. This alters the nature of the modified two stream instability by stabilising modes with wave numbers $ka_{the} \approx 1$, so that the modes with maximum growth rates are now such that $ka_{the} < 1$. Thus, the characteristic wavelength of the instability will be longer, and wave particle interactions more gentle. Hence, one might expect particle heating to be weaker. Particle simulation studies suggest that the ions retain their Maxwellian form throughout the lifetime of the instability, and hence an approach based on taking moments of the ion evolution equation would suffice. Ion heating by lower hybrid type instabilities can be quite considerable [43].

The inclusion of electromagnetic terms could also improve the model. As the electron beta increases the modified two stream instability becomes the kinetic cross field streaming instability: the oscillation frequency is still in the lower hybrid frequency range, but now the mode is essentially a whistler, with a mixed electrostatic/electromagnetic nature depending on the angle of propagation to the magnetic field, which is generally smaller than that for the modified two stream instability. Under certain conditions it is necessary to include $n \neq 0$ terms in the dispersion relation. The actual computation would be more difficult in this case since now the dispersion relation is the determinant of a three by three matrix, all the elements of which will, in general, have to be evaluated. The more oblique propagation of the unstable modes may mean that there will be a greater degree

of electron heating due to the larger values of the wave number vector along the magnetic field.

Taking into account the effects of the spatial variation of the distribution function in the quasilinear diffusion equation poses problems when the time dependent, inhomogeneous problem is considered, since now the spatial variable, Λ, occurs on both sides of the equation. This difficulty is purely numerical.

A criticism that could be levelled at the model is that it does not take into account the Rankine-Hugoniot relations that link the upstream state of the plasma to the downstream state. This could be achieved by using the method of Winske et al. [51] in their comparison of heating due to the ion acoustic and modified two stream instabilities. Essentially, a shock width is assumed, from which the cross field drift is estimated. The anomalous heating due to current-driven instabilities is then calculated (in their case by using second-order transport theory, in our case by solving the quasilinear equations). The amount of adiabatic heating is then evaluated, and then the shock width is adjusted so that the amount of total (adiabatic plus anomalous) heating is in closer agreement with that required by the Rankine-Hugoniot equations. The process is then repeated until a self-consistent result can be obtained. One difficulty is that the Rankine-Hugoniot equations require both the up and downstream distributions to be Maxwellian, whereas we have seen that the downstream electron distribution function will not be Maxwellian, even if the upstream distribution is. However, construction of such a model would in principle be straightforward.

In conclusion, this work should not be taken as the 'last word' on the subject, but rather a first step towards constructing a reasonably accurate, self-consistent model of electron heating in subcritical shockwaves which takes into account the non-Maxwellian nature of the electrons as they pass through a shock.

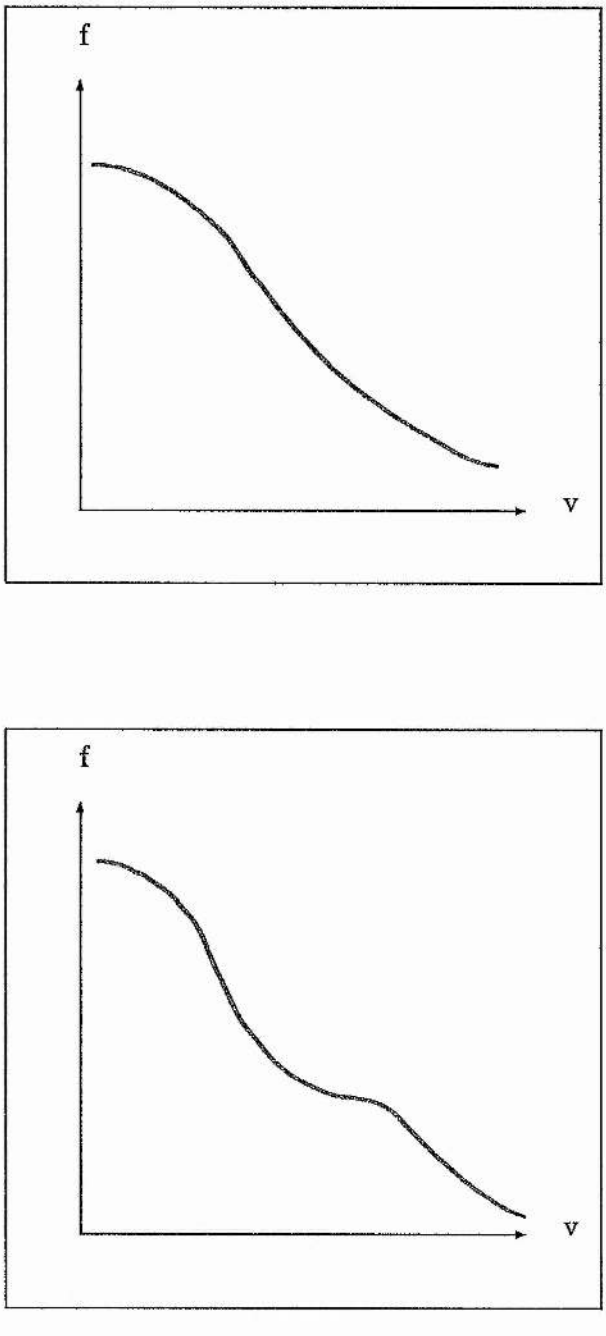

Figure 5.1: Velocity distribution function (f) before (top panel) and after (bottom panel) modification by wave particle interactions. Axes in arbitrary units.

Run 1

Parameter	*description*	*value*
$\epsilon_B a_{the}$	Inverse magnetic field scale	0.01
α	ω_{pe}/ω_{ce}	68
β_e	Electron beta	0.1
δ	Electron/ion mass ration	1/1836
T_i	Ion temperature	0

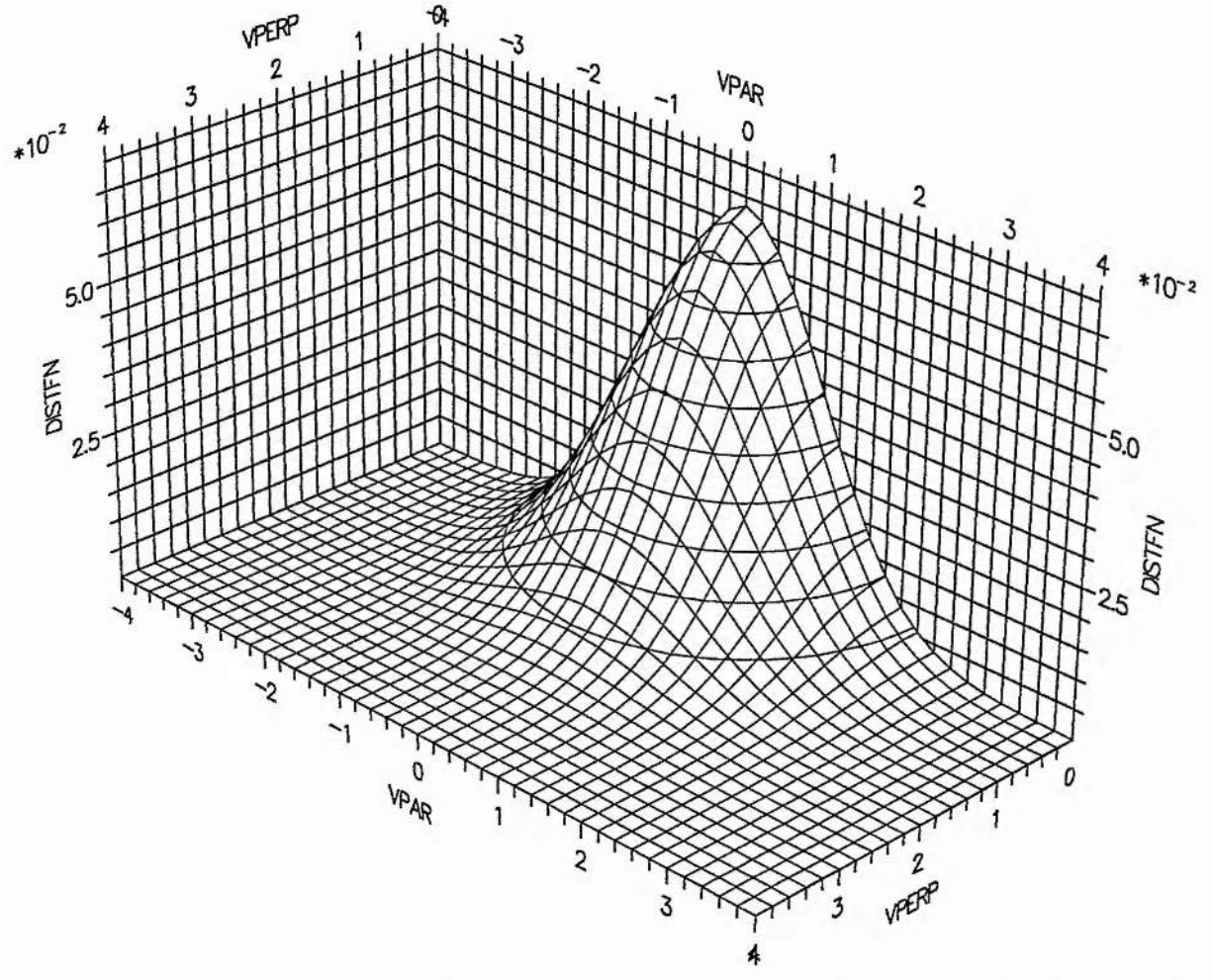

TIME = $0\omega_{ce}^{-1}$ ELECTRON DISTRIBUTION FUNCTION.

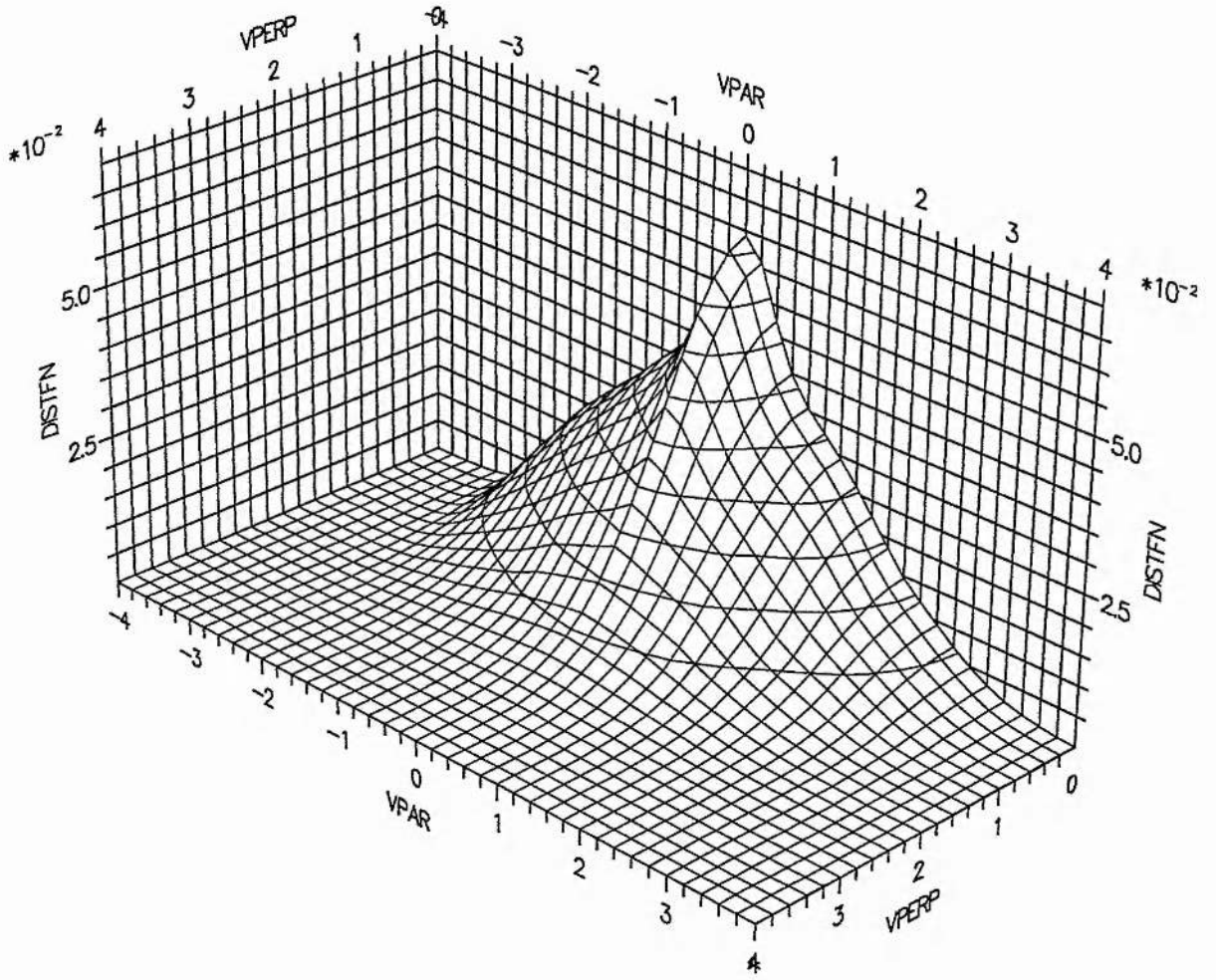

TIME = $375\omega_{ce}^{-1}$ ELECTRON DISTRIBUTION FUNCTION.

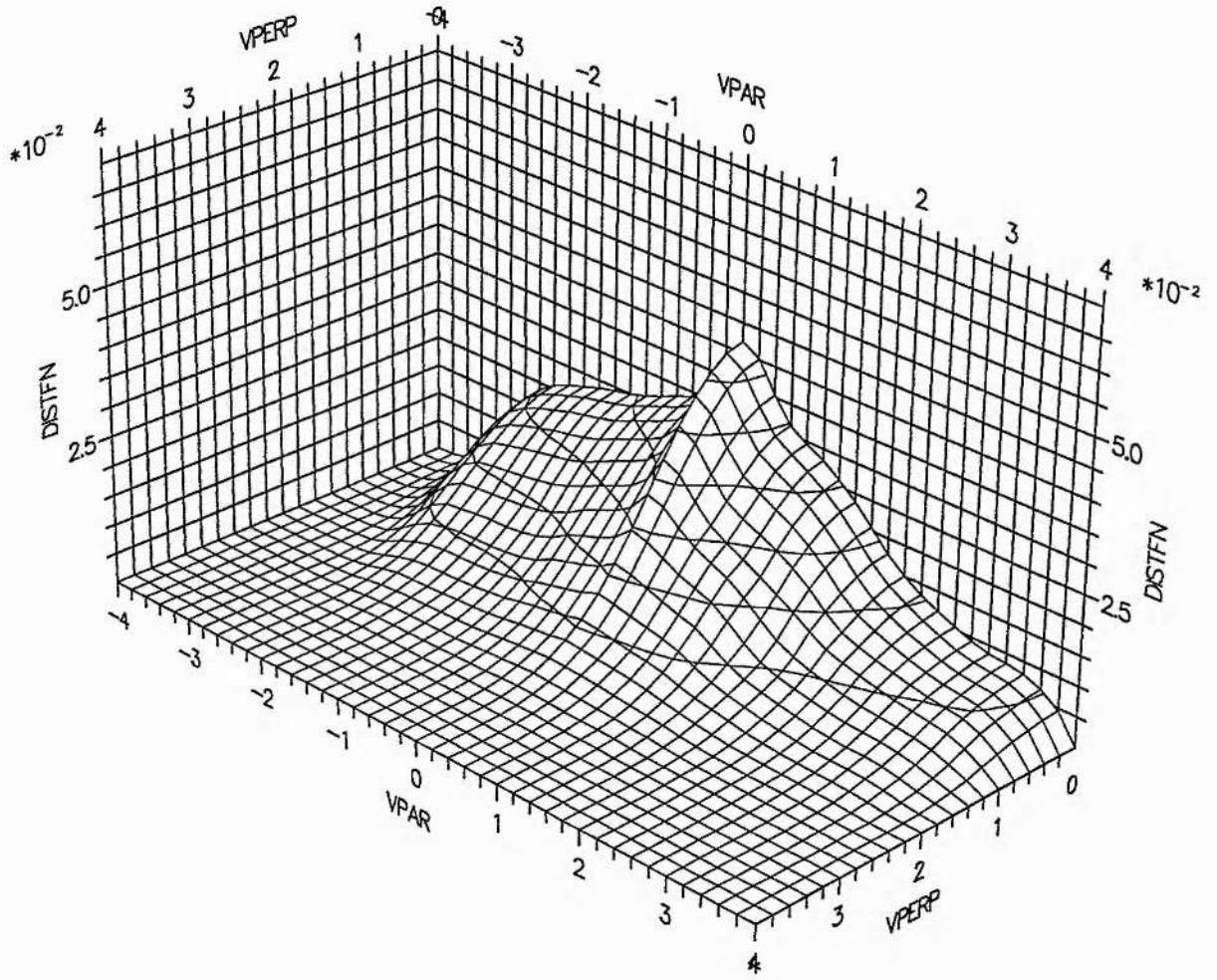

TIME = $500\omega_{ce}^{-1}$ ELECTRON DISTRIBUTION FUNCTION.

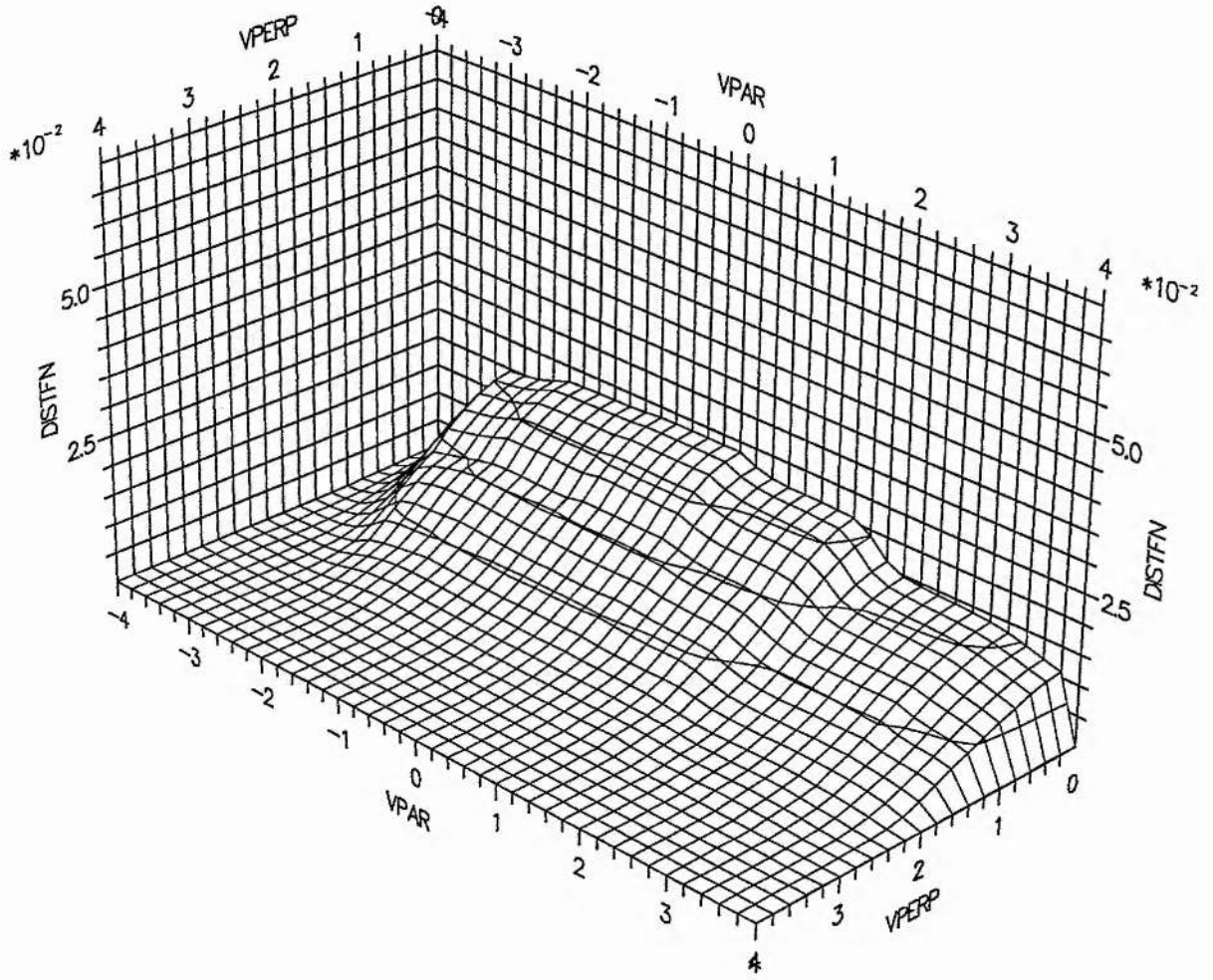

TIME = $750\omega_{ce}^{-1}$ ELECTRON DISTRIBUTION FUNCTION.

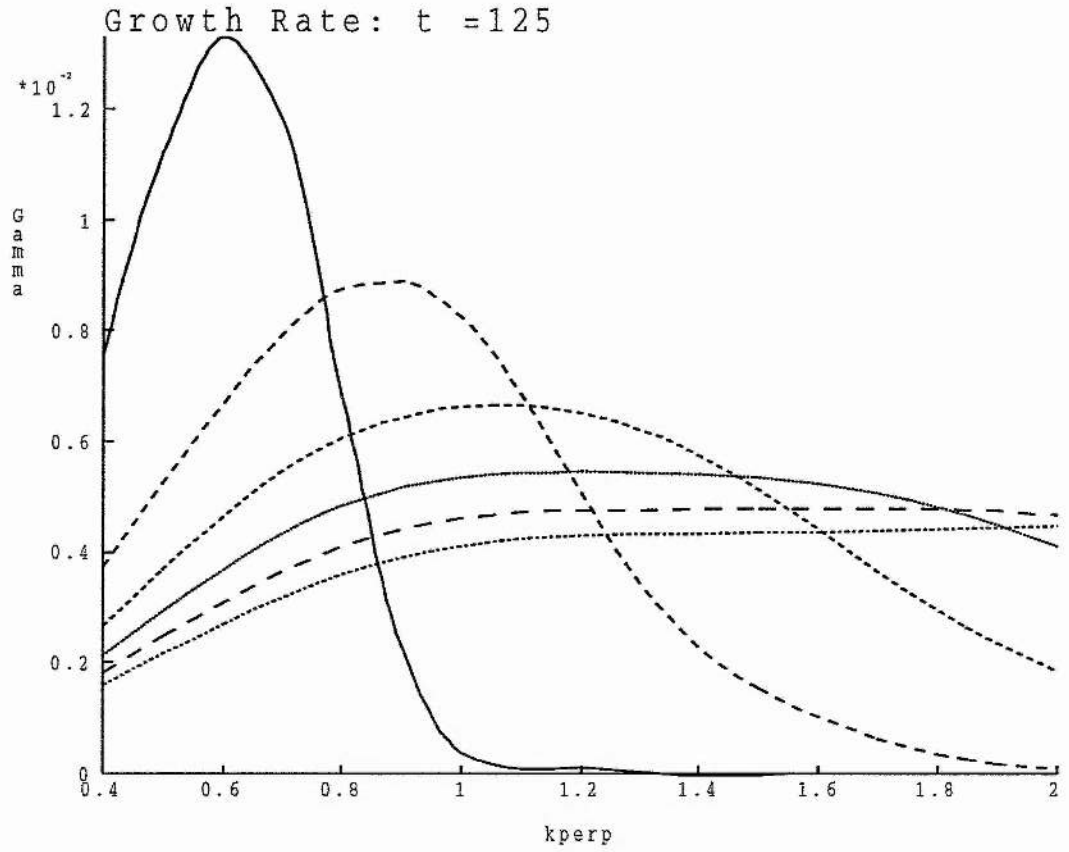
Growth Rate: t =125
*10^-2
1.2
1
0.8
0.6
0.4
0.2
0
Gamma
0.4
0.6
0.8
1
1.2
1.4
1.6
1.8
2
kperp

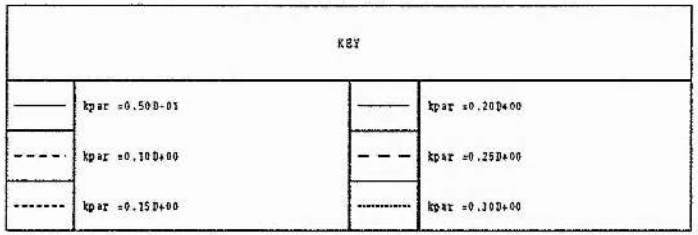
KEY
kpar =0.50D-01
kpar =0.20D+00
kpar =0.10D+00
kpar =0.25D+00
kpar =0.15D+00
kpar =0.30D+00

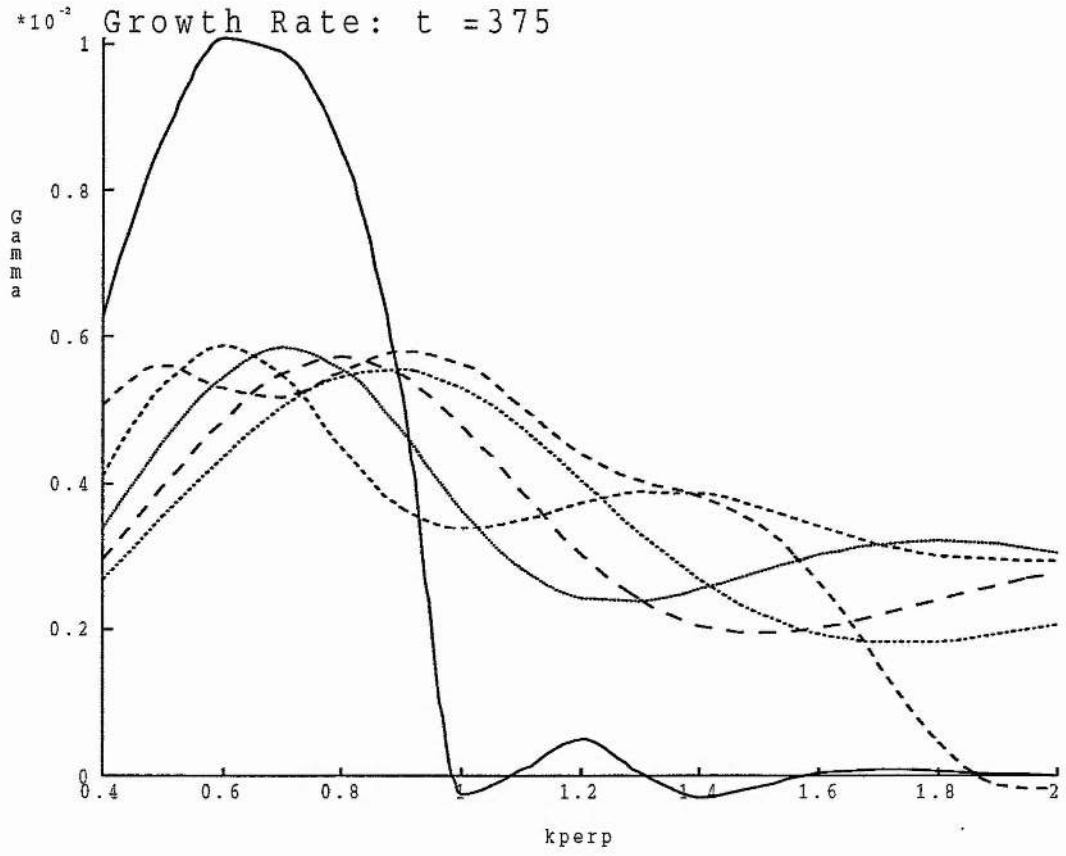

KEY			
———	kpar =0.50D-01	———	kpar =0.20D+00
- - - -	kpar =0.10D+00	— — —	kpar =0.25D+00
-------	kpar =0.15D+00	·····	kpar =0.30D+00

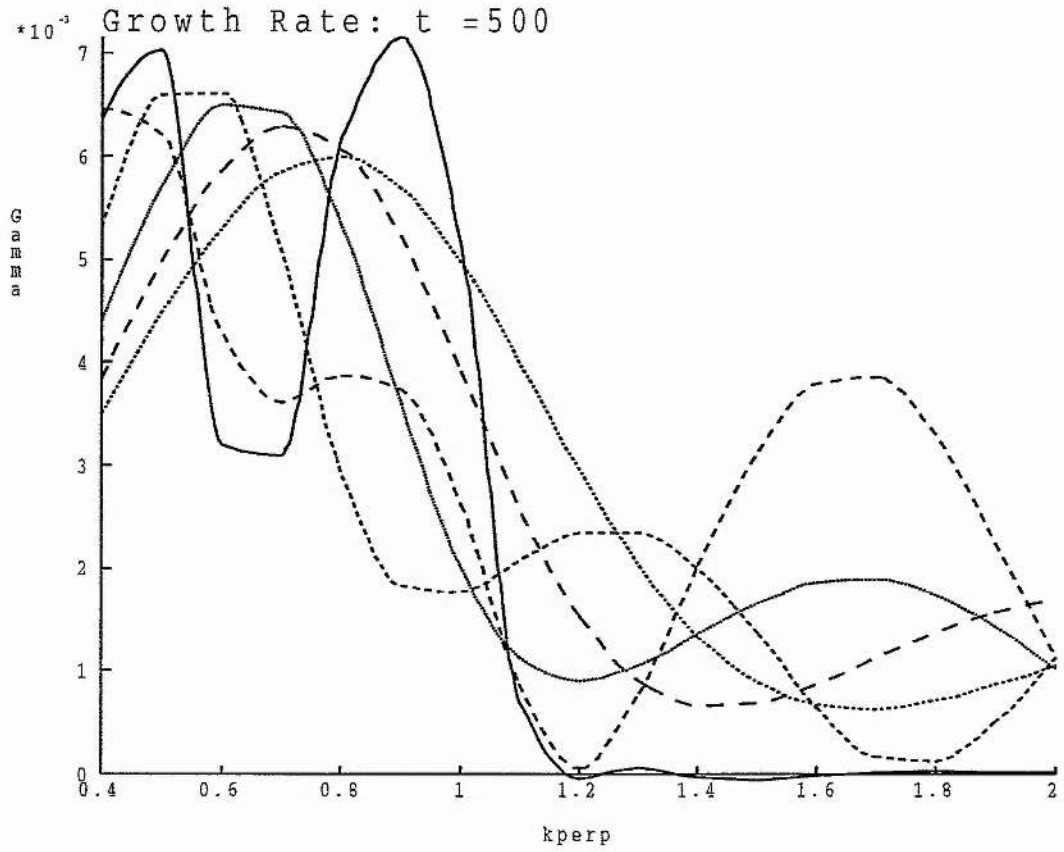

KEY			
———	kpar =0.50D-01	———	kpar =0.20D+00
- - - -	kpar =0.10D+00	— — —	kpar =0.25D+00
------	kpar =0.15D+00	·····	kpar =0.30D+00

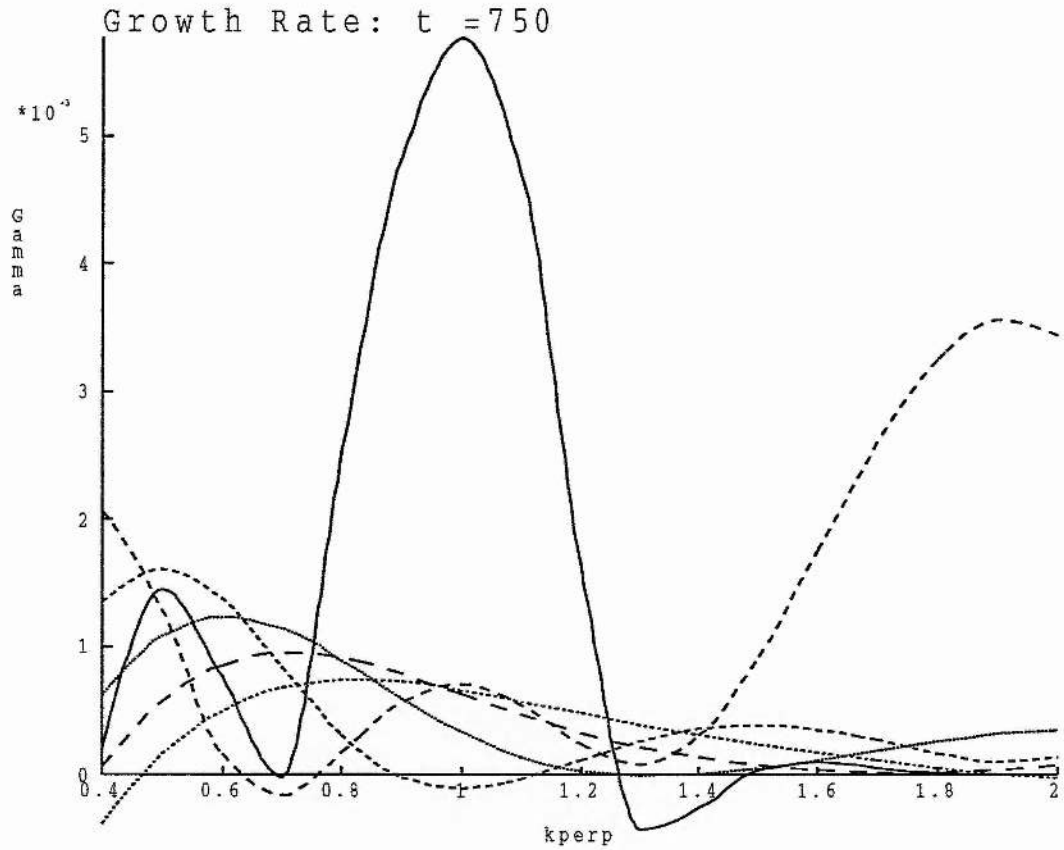

KEY			
———	kpar =0.50D-01	———	kpar =0.20D+00
- - - - -	kpar =0.20D+00	— — —	kpar =0.25D+00
-------	kpar =0.15D+00	----------	kpar =0.30D+00

Figure 5.2: Parallel thermal velocity versus time

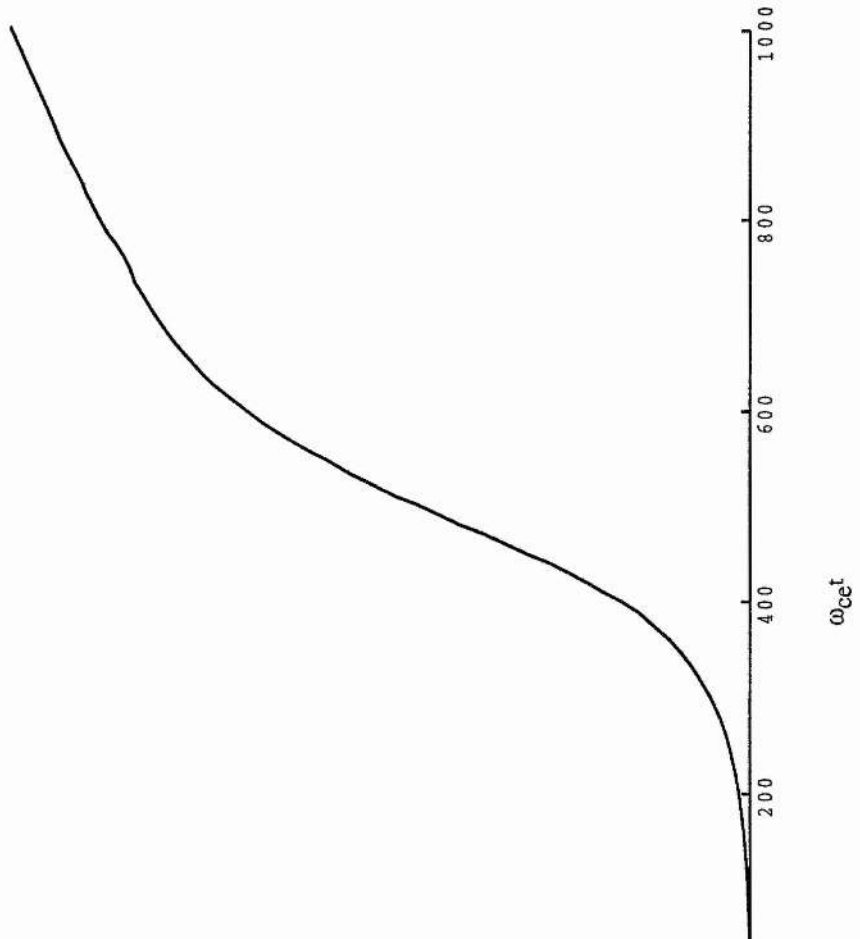

Figure 5.3: Maximum growth rate versus time

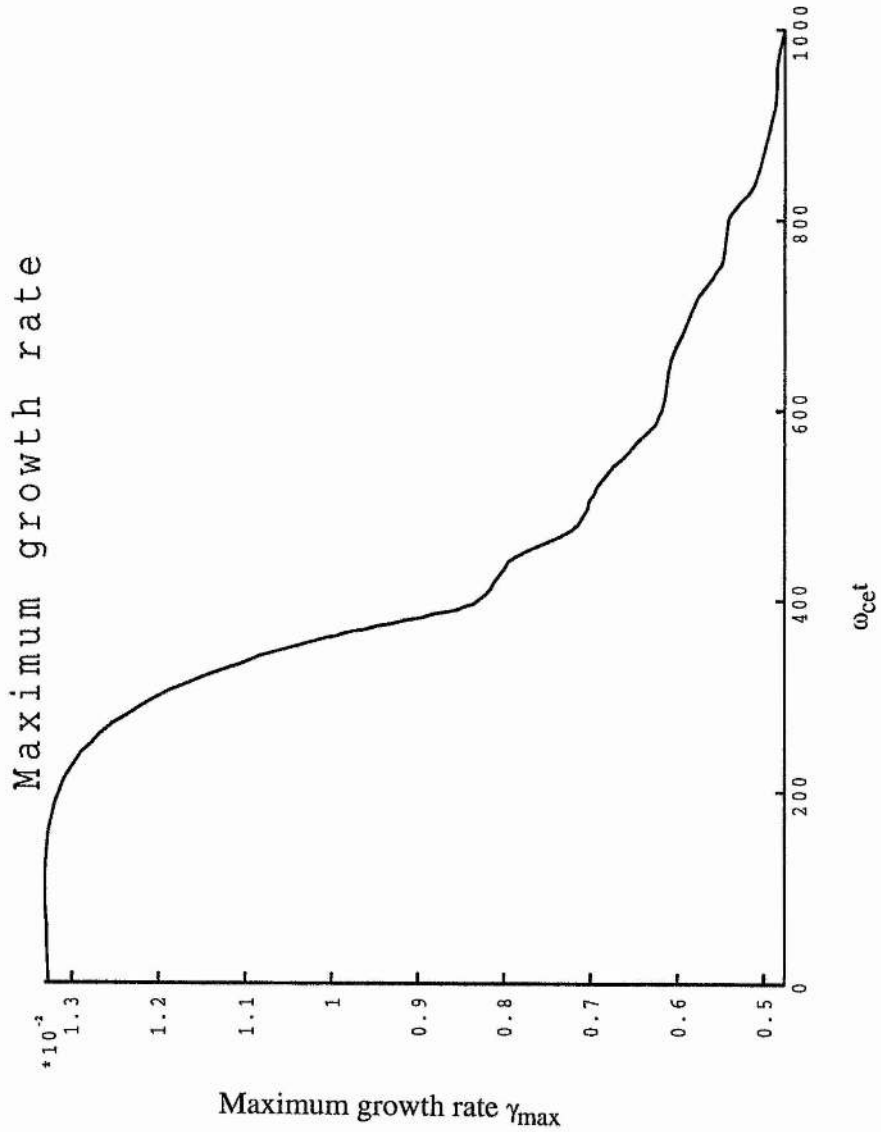

Run 2

Parameter	*description*	*value*
$\epsilon_B a_{the}$	Inverse magnetic field scale	0.02
α	ω_{pe}/ω_{ce}	68
β_e	Electron beta	0.1
δ	Electron/ion mass ration	1/1836
T_i	Ion temperature	0

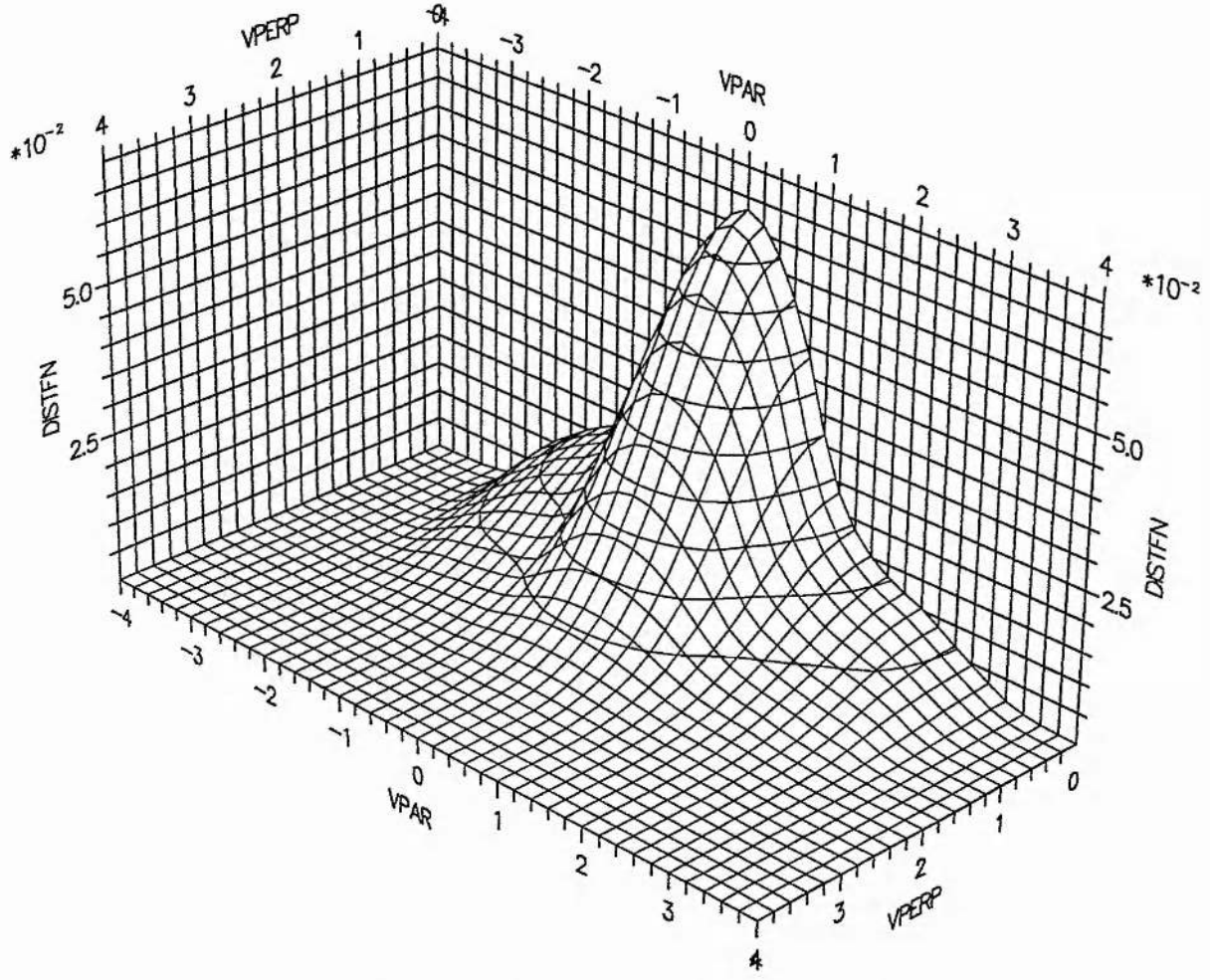

TIME = $300\omega_{ce}^{-1}$ ELECTRON DISTRIBUTION FUNCTION.

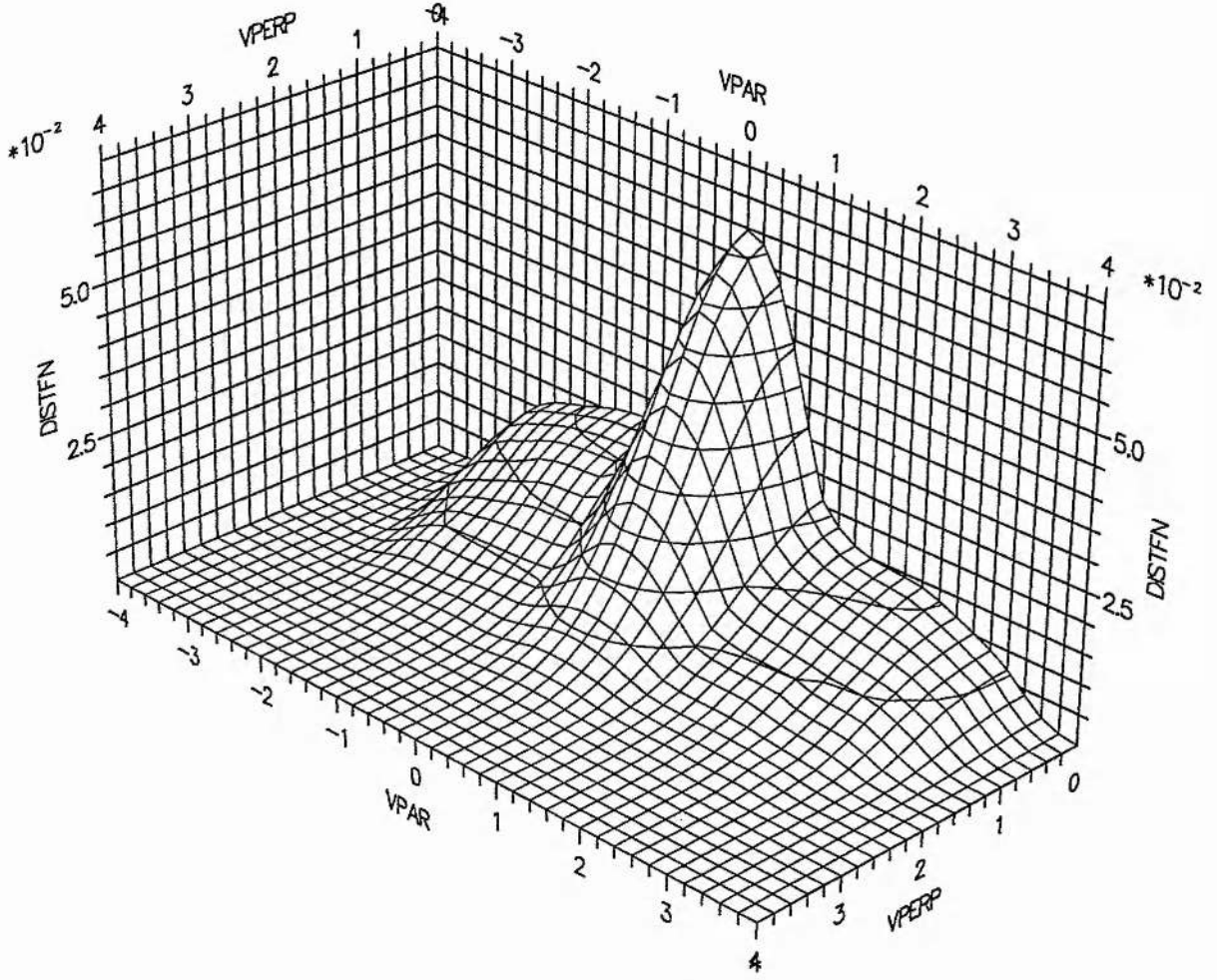

TIME = $400\omega_{ce}^{-1}$ ELECTRON DISTRIBUTION FUNCTION.

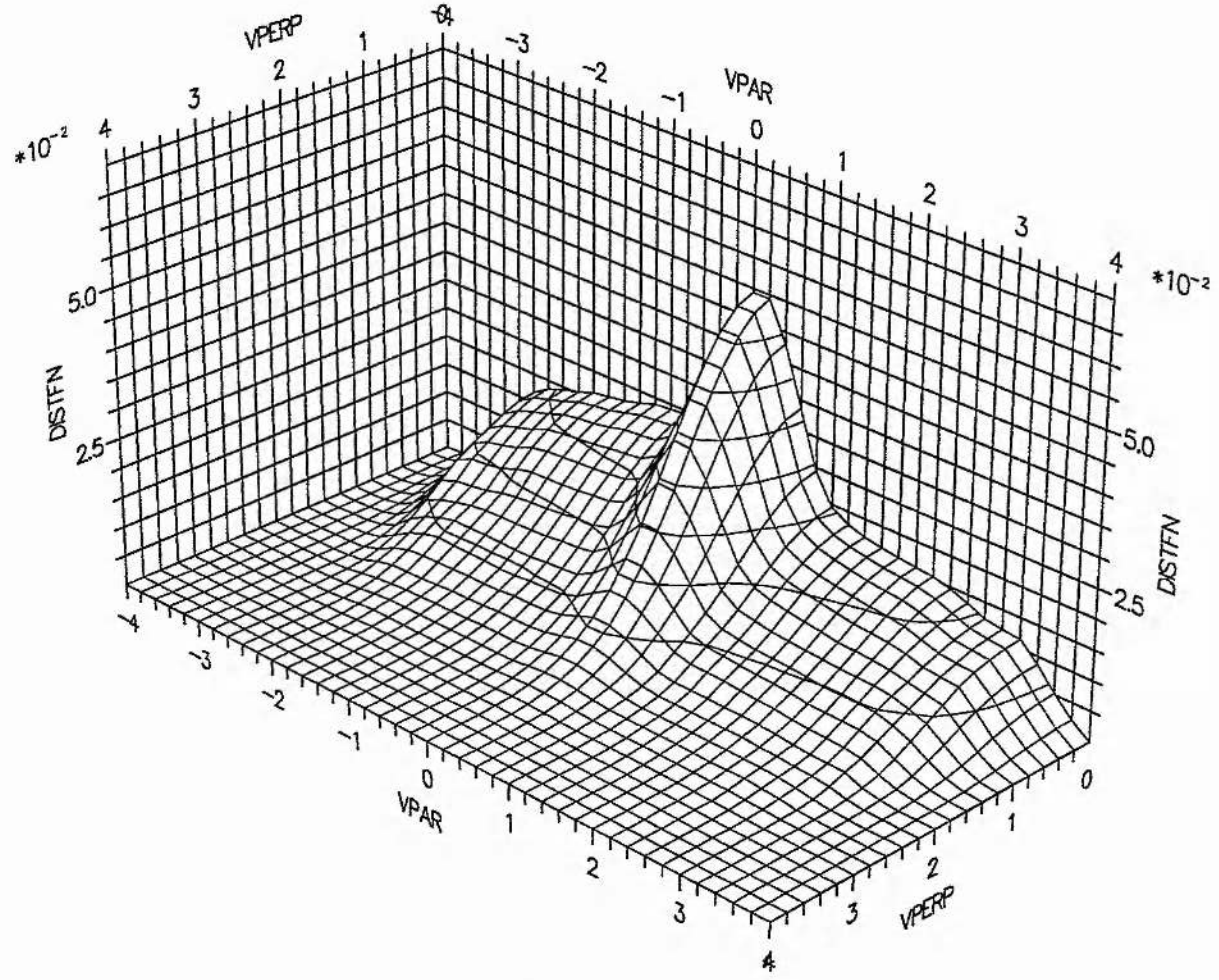

TIME = $500\omega_{ce}^{-1}$ ELECTRON DISTRIBUTION FUNCTION.

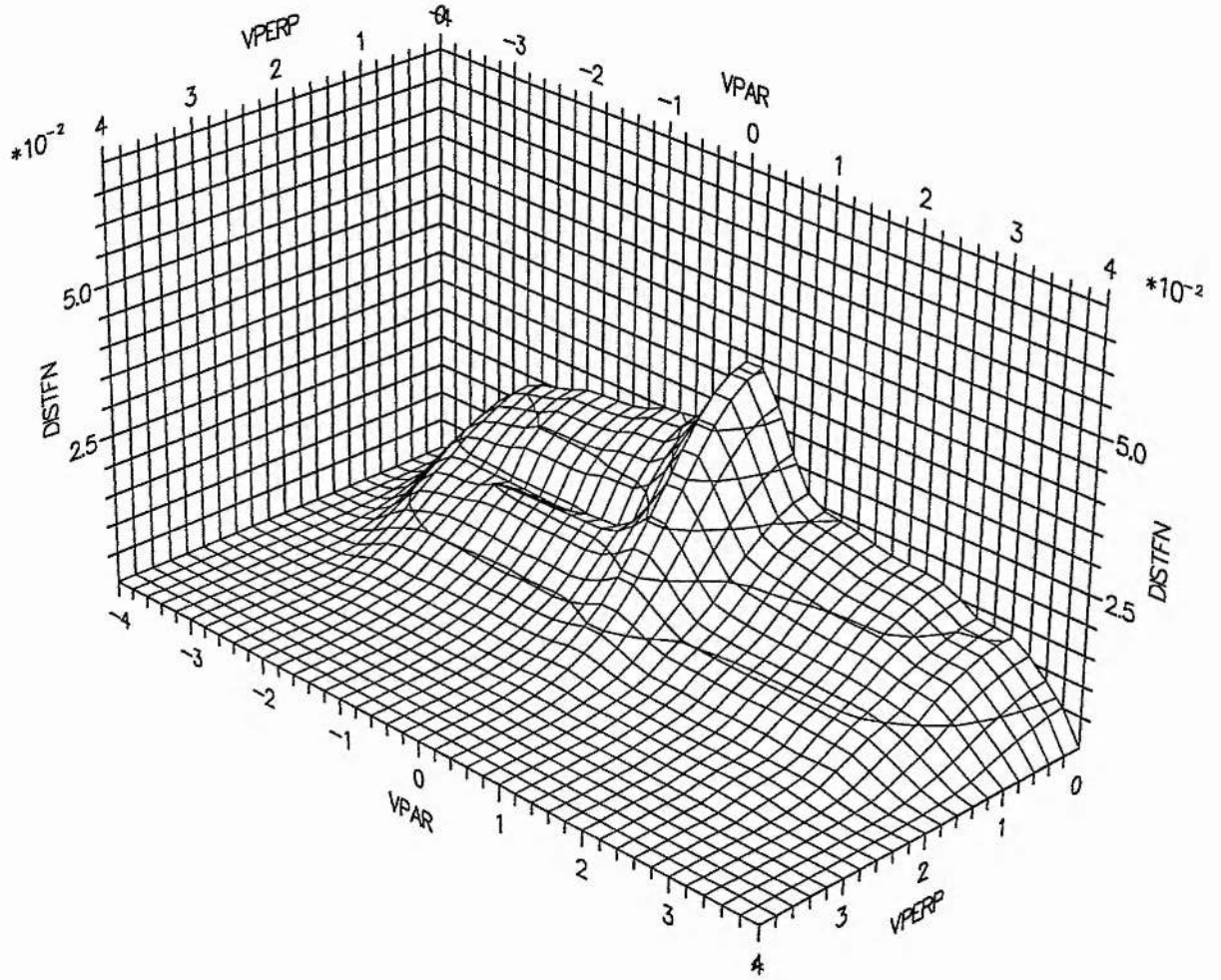

TIME = $600\omega_{ce}^{-1}$ ELECTRON DISTRIBUTION FUNCTION.

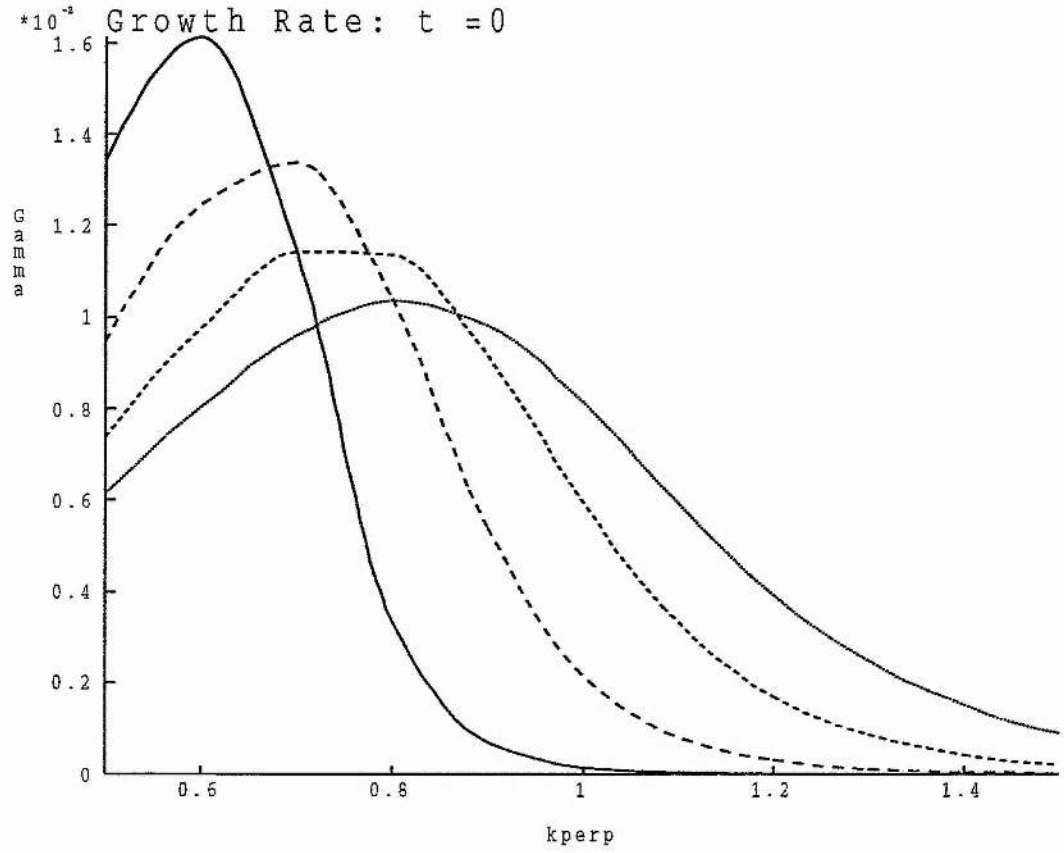
*10^-2 Growth Rate: t =0
Gamma
1.6
1.4
1.2
1
0.8
0.6
0.4
0.2
0
0.6
0.8
1
1.2
1.4
kperp
KEY
kpar =0.100+00
kpar =0.130+00
kpar =0.160+00
kpar =0.200+00

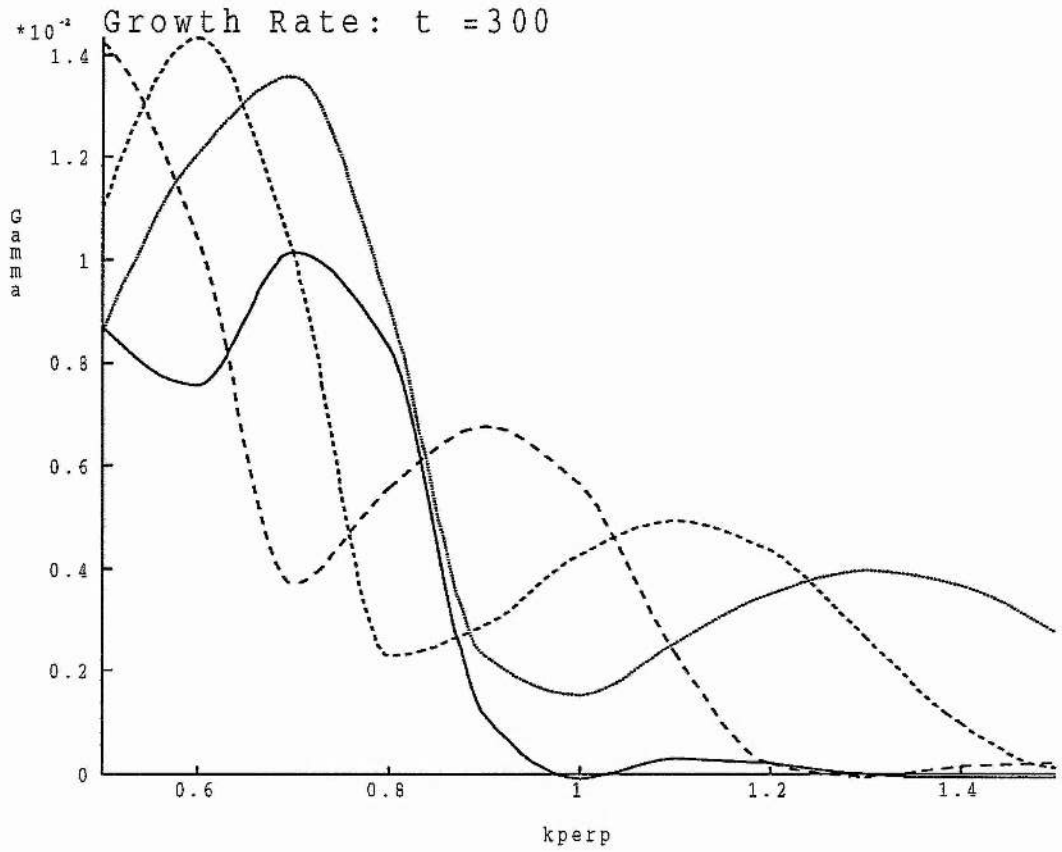

KEY			
———	kpar =0.10D+00	- - - - - -	kpar =0.16D+00
- - - -	kpar =0.13D+00	———	kpar =0.20D+00

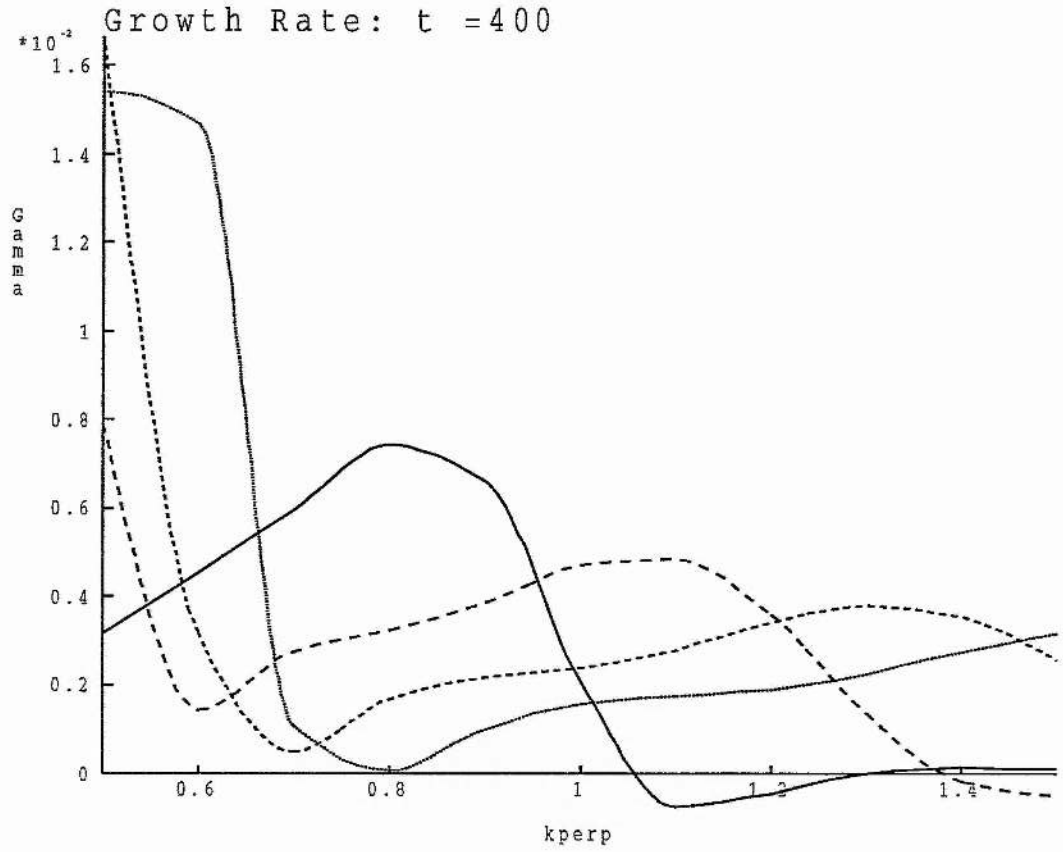
Growth Rate: t =400
*10^-2
1.6
1.4
1.2
1
0.8
0.6
0.4
0.2
0
Gamma
0.6
0.8
1
1.2
1.4
kperp

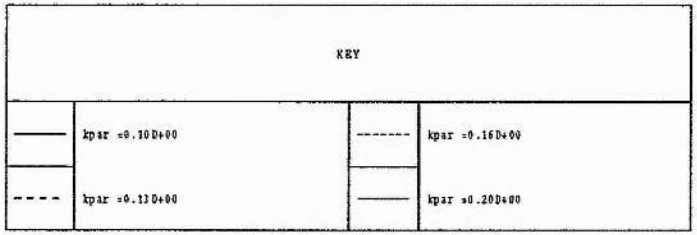
KEY
kpar =0.10D+00
kpar =0.16D+00
kpar =0.13D+00
kpar =0.20D+00

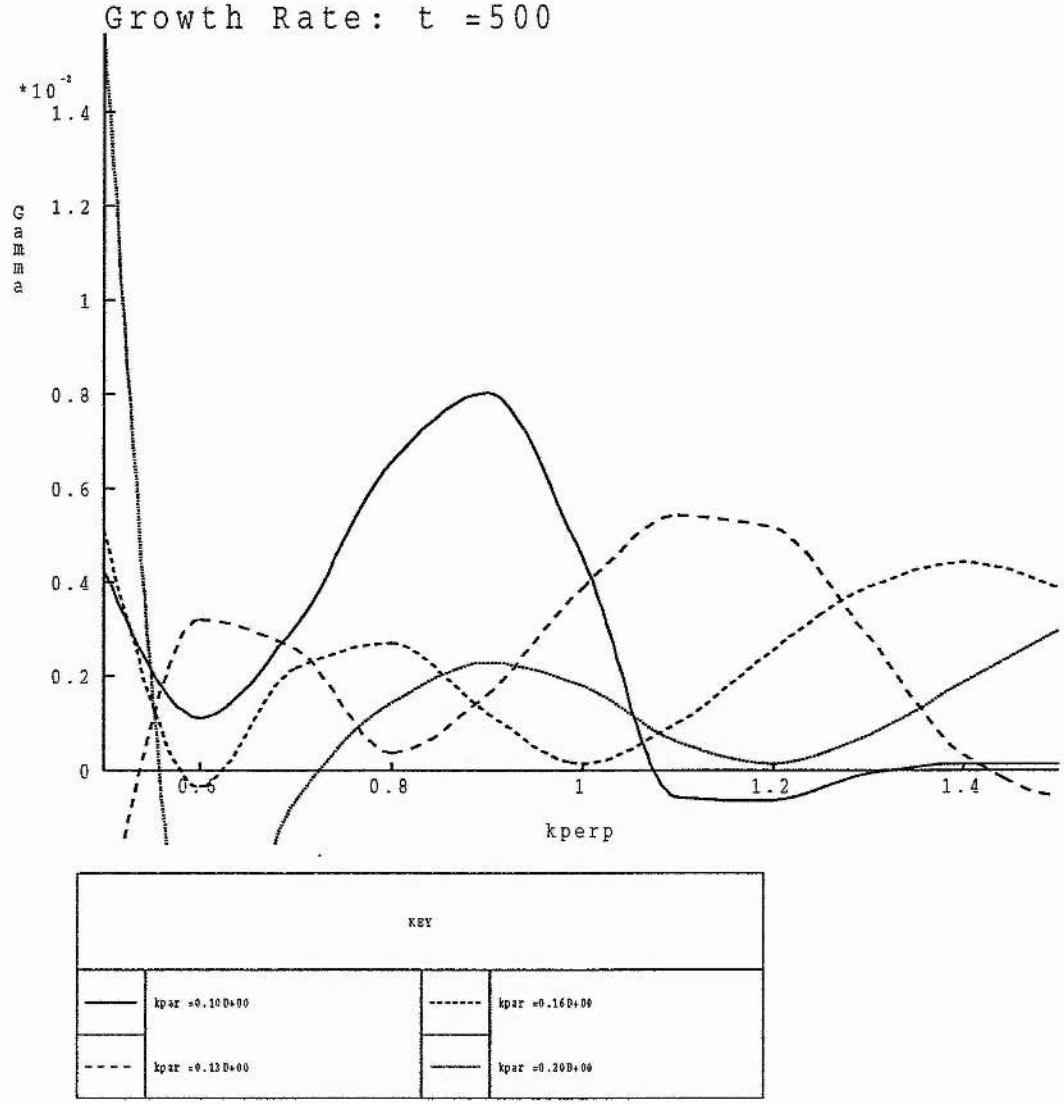
Growth Rate: t =500
*10^-2
1.4
1.2
1
0.8
0.6
0.4
0.2
0
Gamma
0.6
0.8
1
1.2
1.4
kperp
KEY
kpar =0.100+00
kpar =0.130+00
kpar =0.160+00
kpar =0.200+00

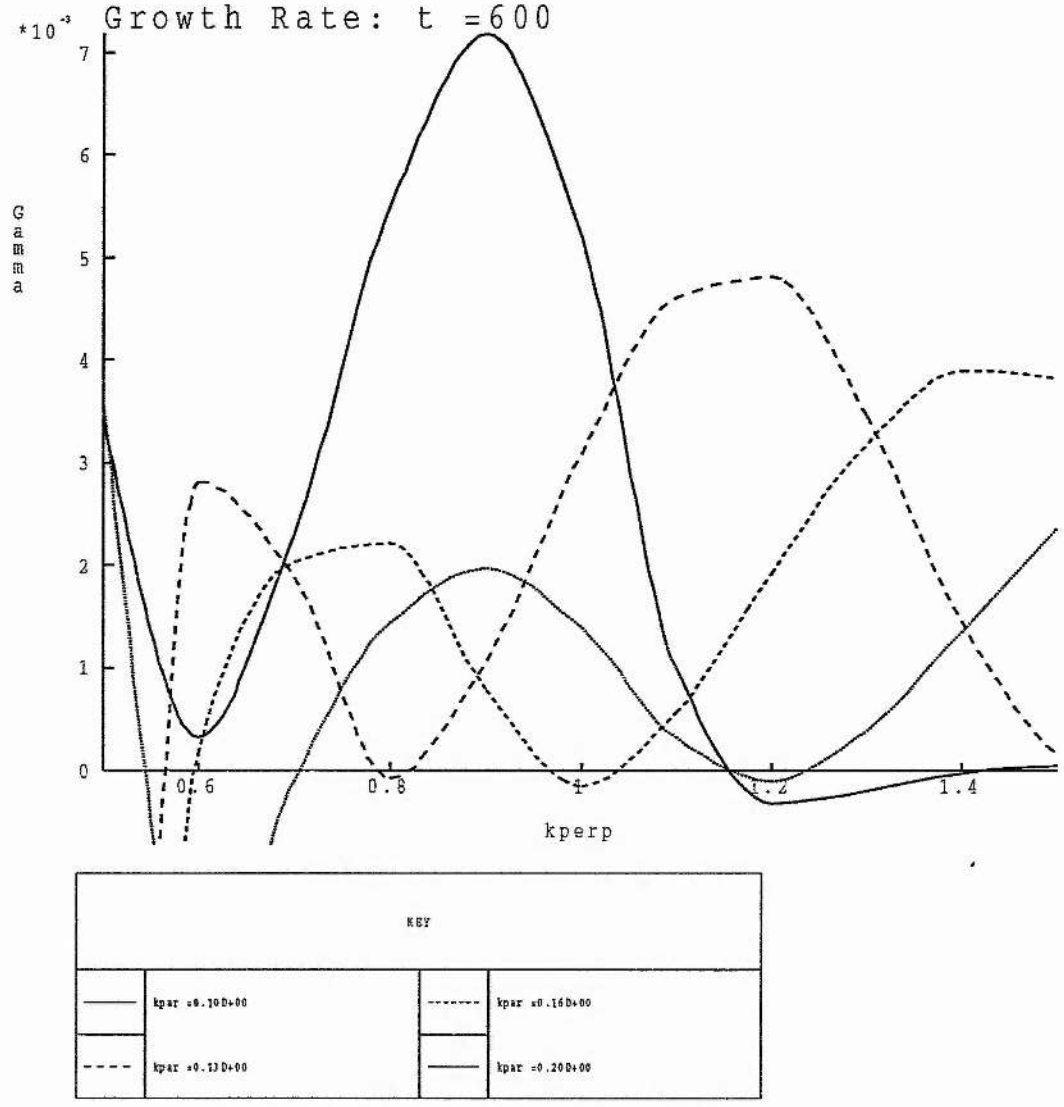
Growth Rate: t =600
*10^-3
Gamma
7
6
5
4
3
2
1
0
0.6
0.8
1
1.2
1.4
kperp
KEY
kpar =0.10D+00
kpar =0.16D+00
kpar =0.13D+00
kpar =0.20D+00

Figure 5.4: Parallel thermal velocity versus time

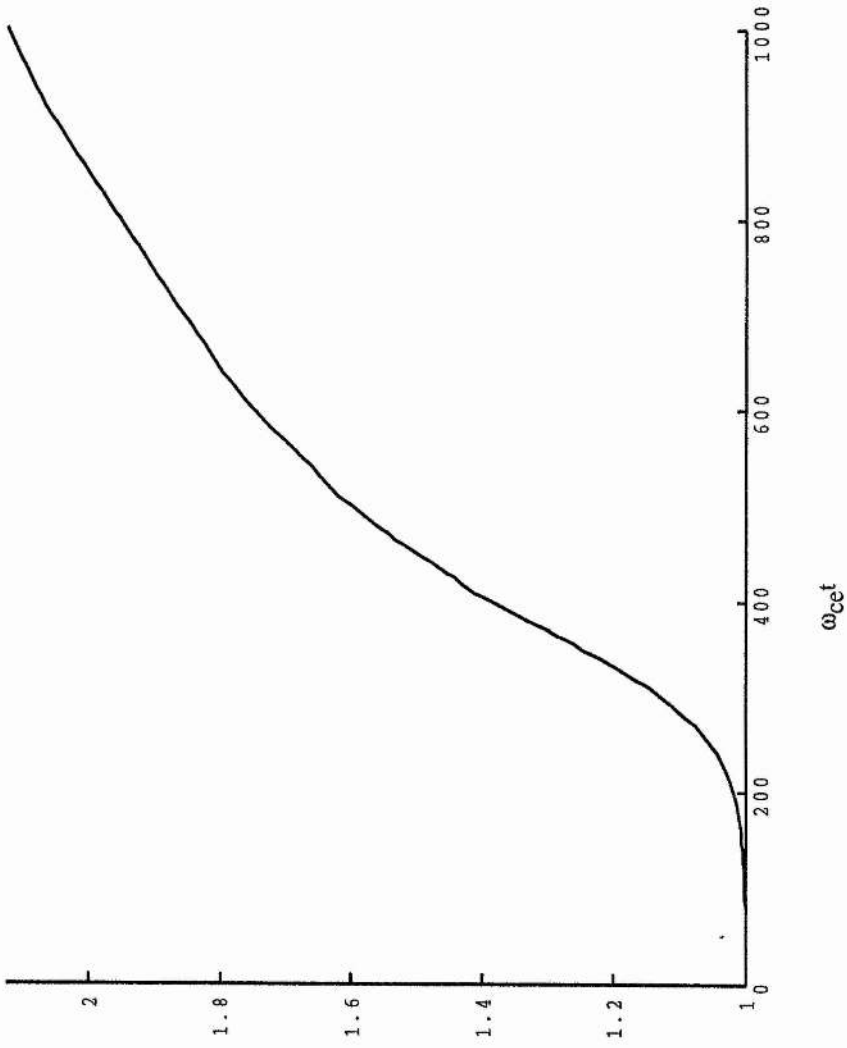

Figure 5.5: Maximum growth rate versus time

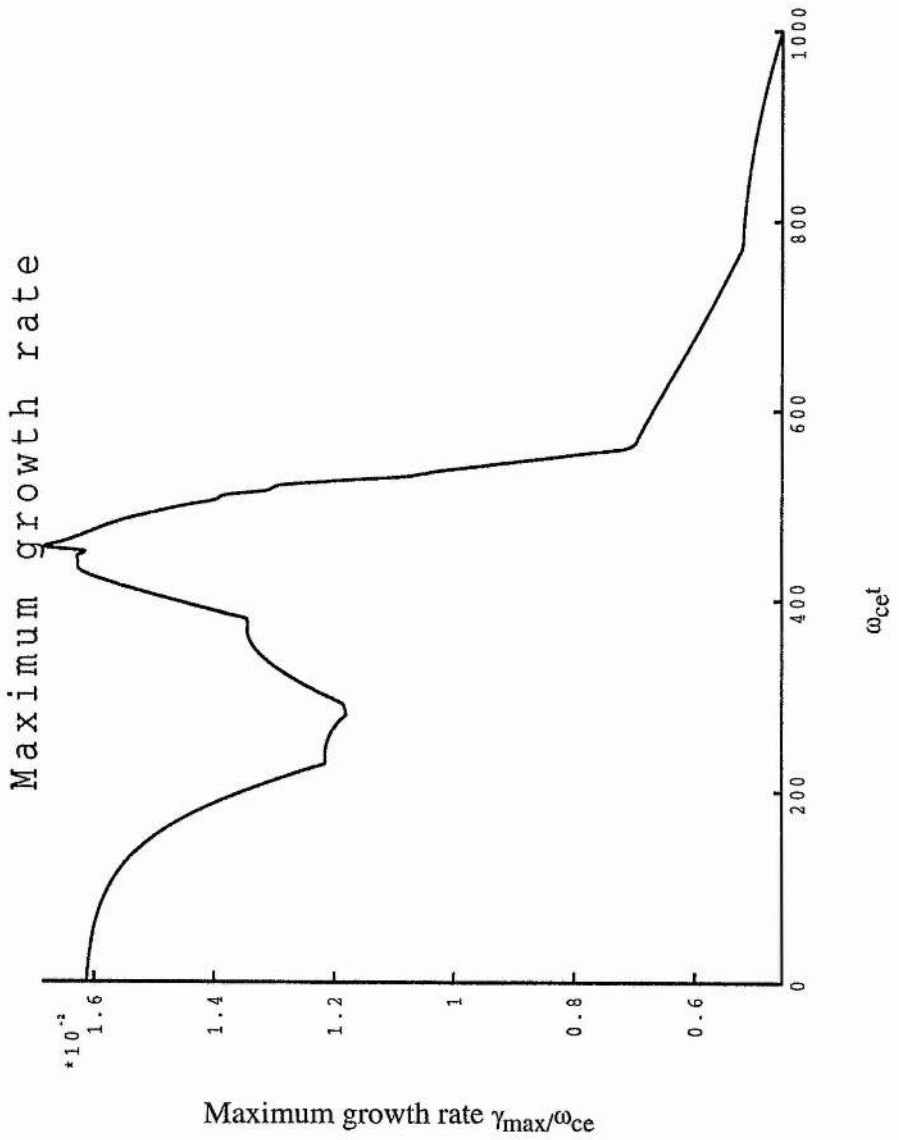

Figure 5.6: Parallel thermal velocity versus time

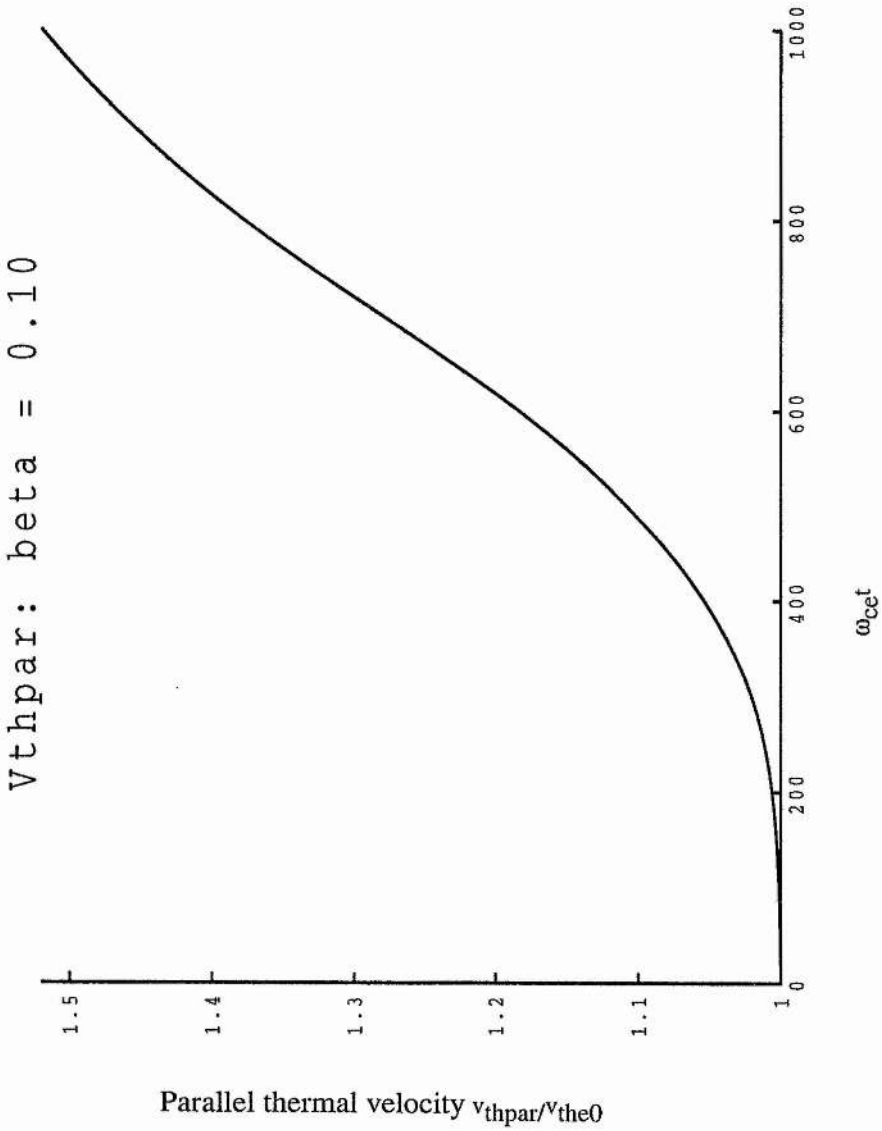

Figure 5.7: Parallel thermal velocity versus time

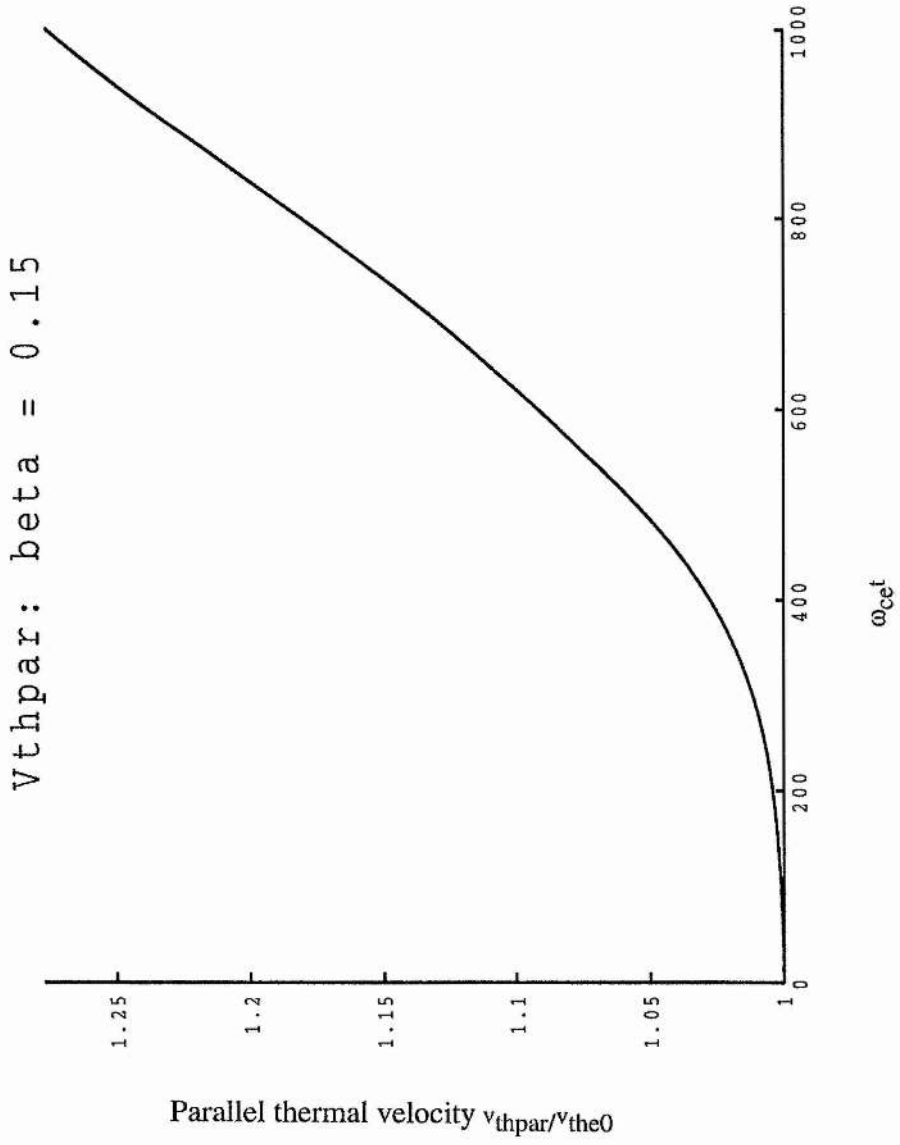

Figure 5.8: Parallel thermal velocity versus time

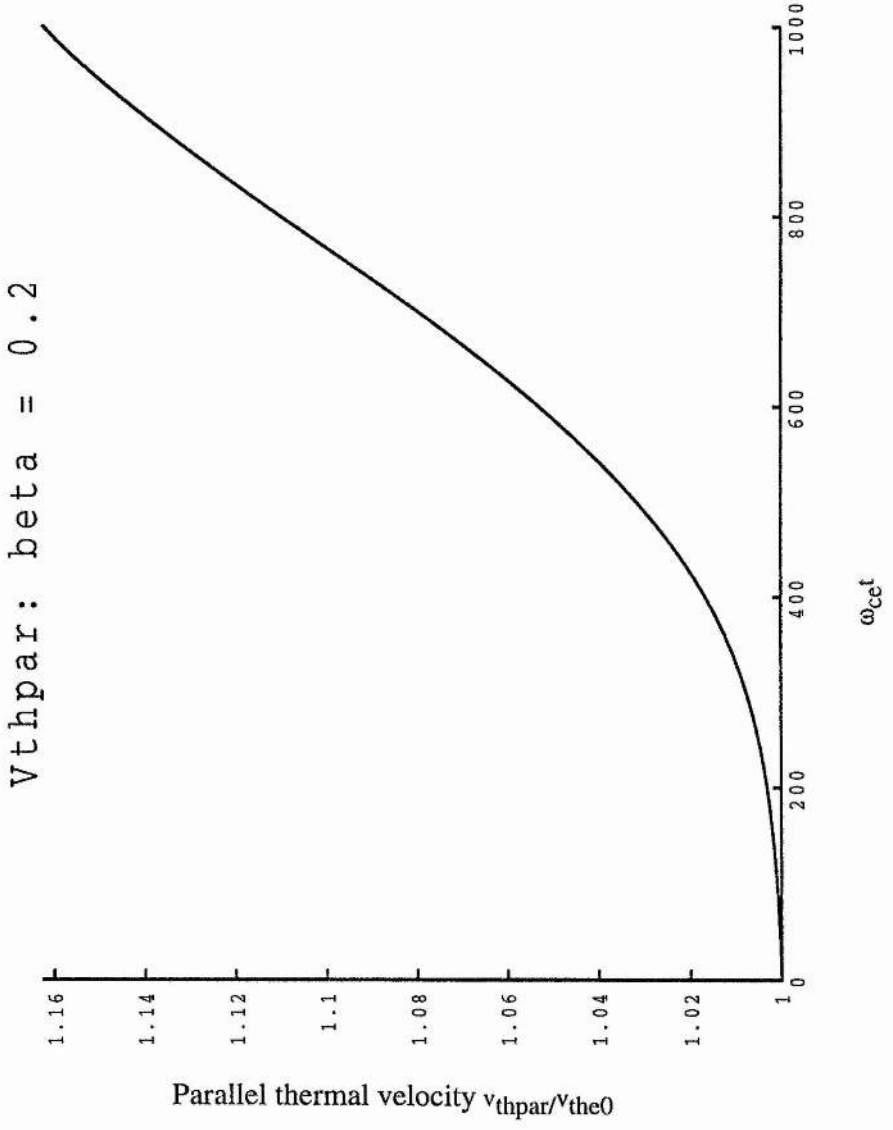

Figure 5.9: Parallel thermal velocity versus time

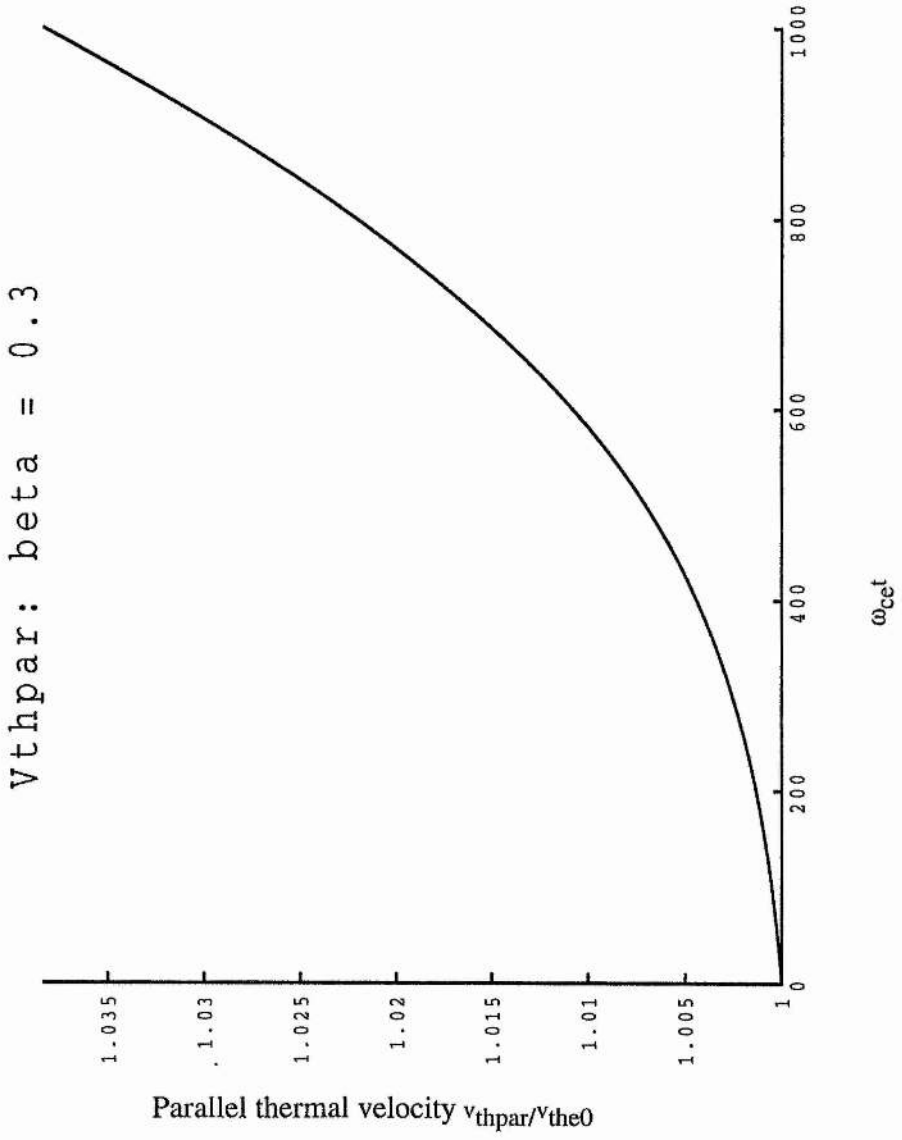

Run 3

Parameter	*description*	*value*
α	ω_{pe}/ω_{ce}	68
β_e	Electron beta	0.1
δ	Electron/ion mass ration	1/1836
T_i	Ion temperature	0
M_{A1}	Upstream Mach Number	2
$\frac{L_s c}{\omega_{pi}}$	Dimensionless shock width	1
$\frac{L_s}{a_{the}}$	Shock width	192

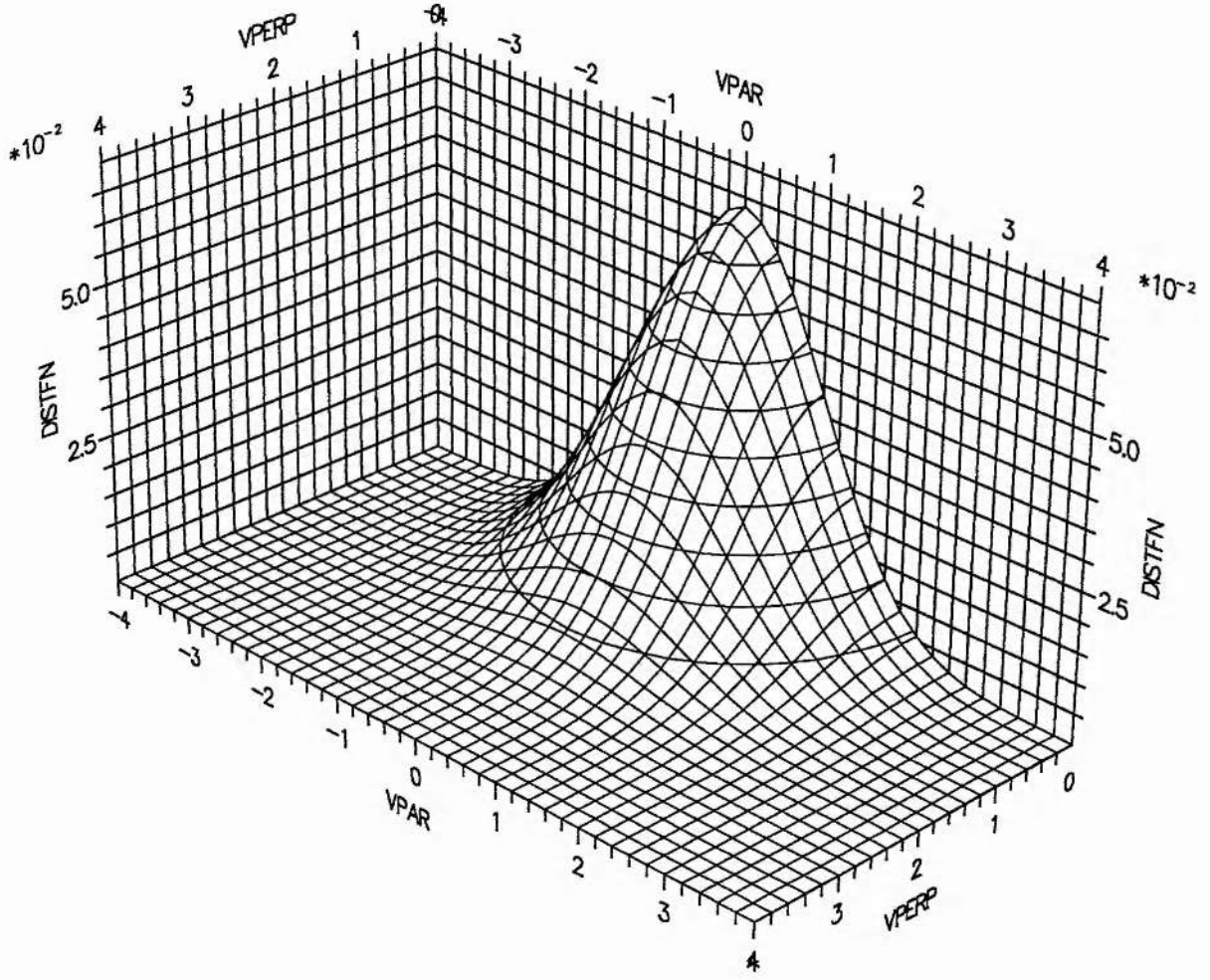

x = $0a_{the\ 1}$ ELECTRON DISTRIBUTION FUNCTION.

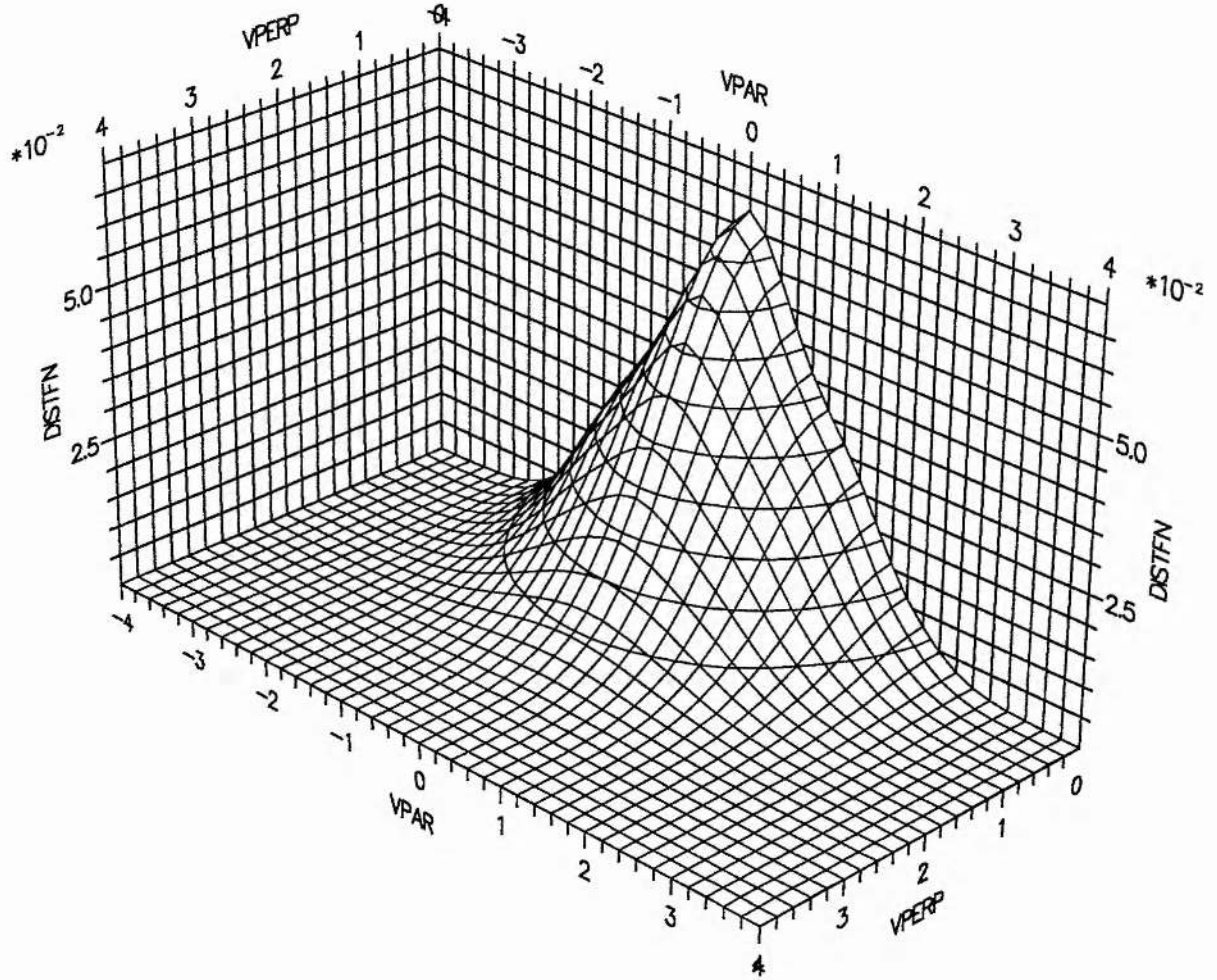

x = 96$a_{the\ 1}$ ELECTRON DISTRIBUTION FUNCTION.

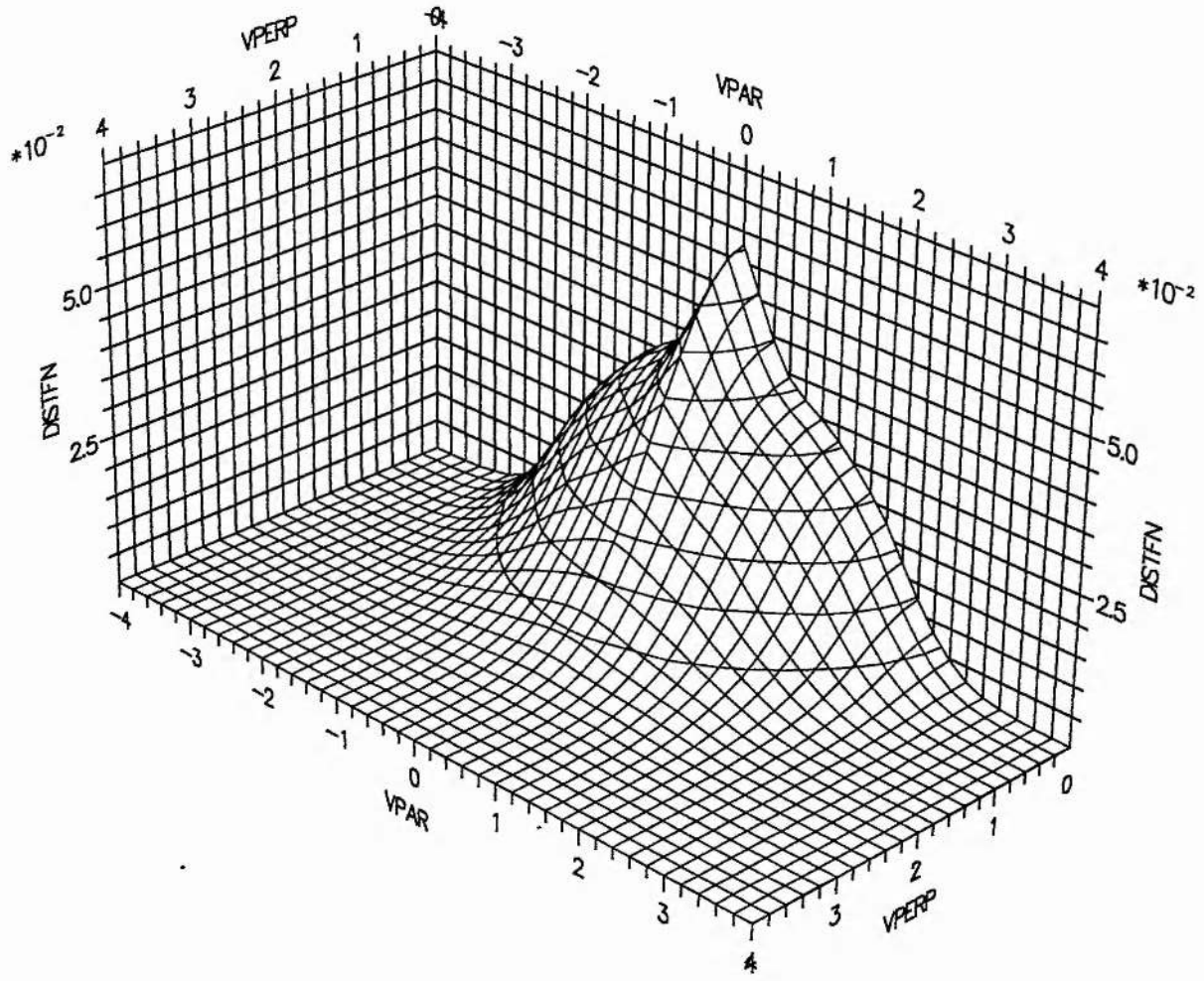

x = $120a_{the\ 1}$ ELECTRON DISTRIBUTION FUNCTION.

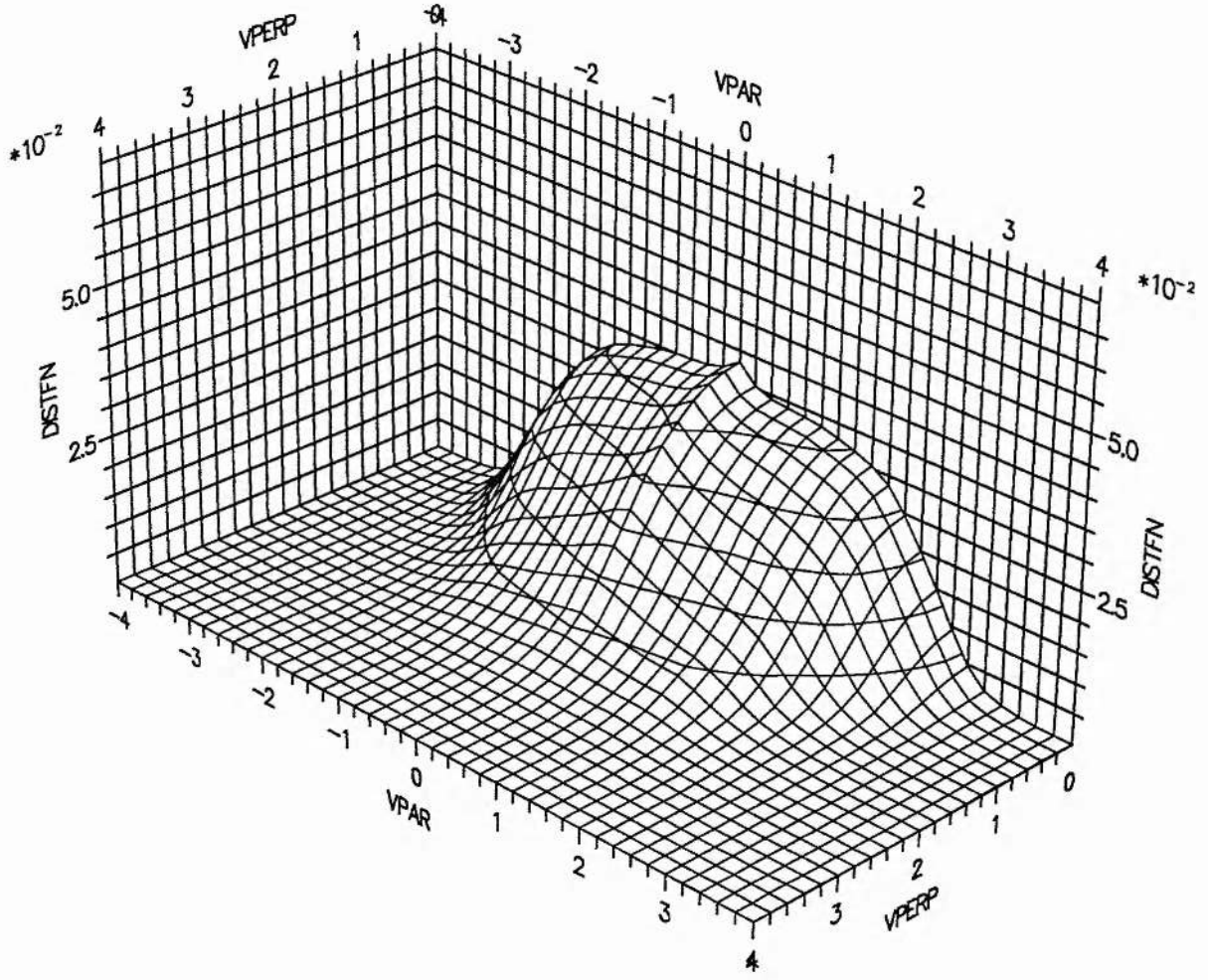

x = 144$a_{the\ 1}$ ELECTRON DISTRIBUTION FUNCTION.

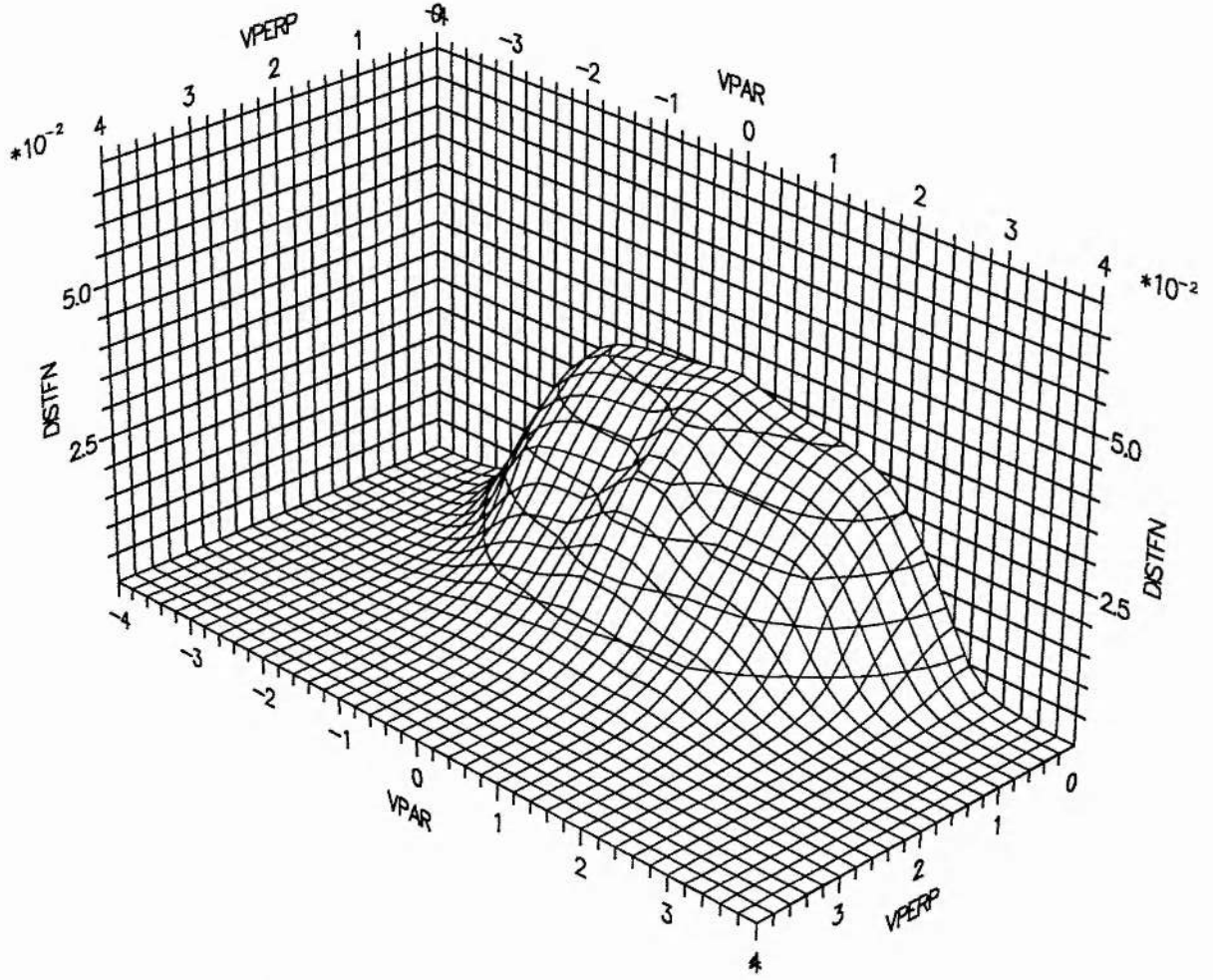

x = 168$a_{the\ 1}$ ELECTRON DISTRIBUTION FUNCTION.

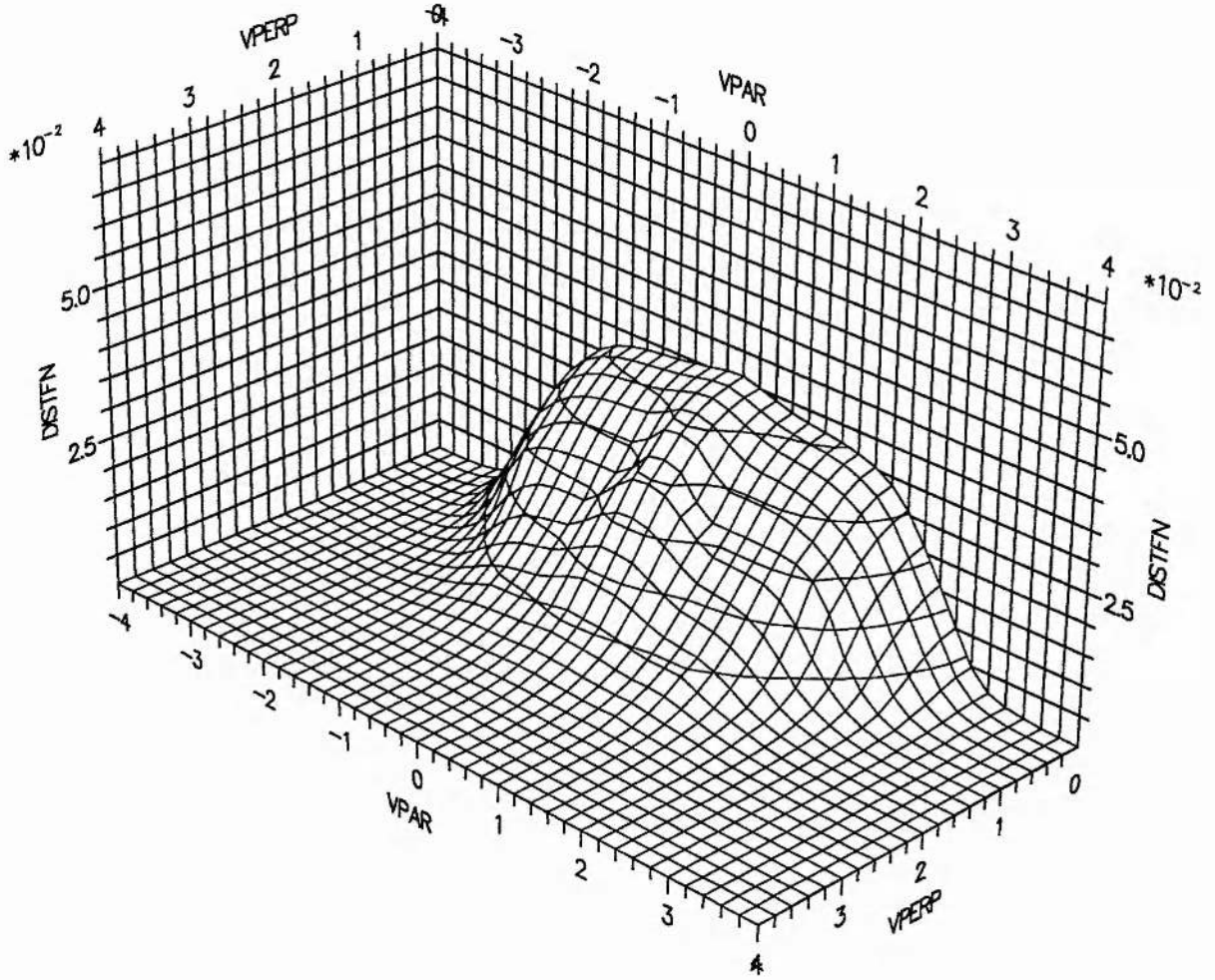

x = 192$a_{the\ 1}$ ELECTRON DISTRIBUTION FUNCTION.

Figure 5.10: Parallel temperature (in units of upstream temperature) versus distance through shock (in units of upstream thermal electron gyroradius).

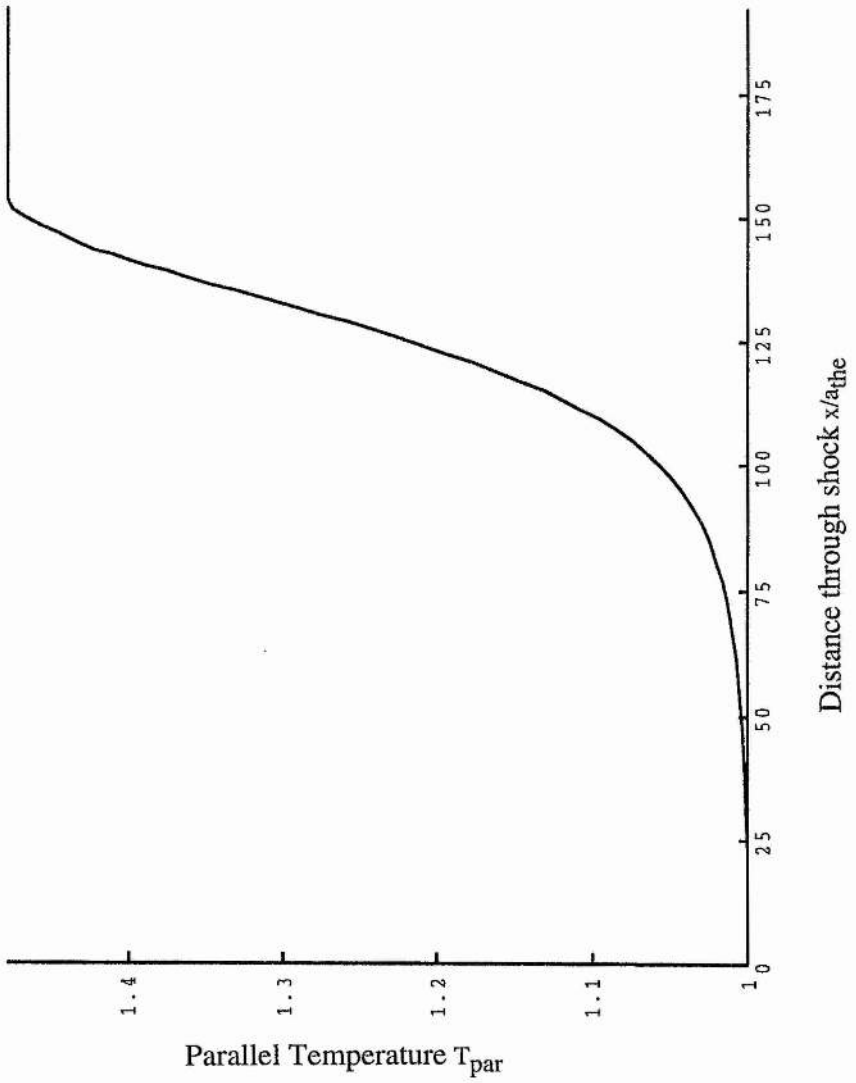

Figure 5.11: Total field energy versus distance through shock (in units of upstream thermal electron gyroradius).

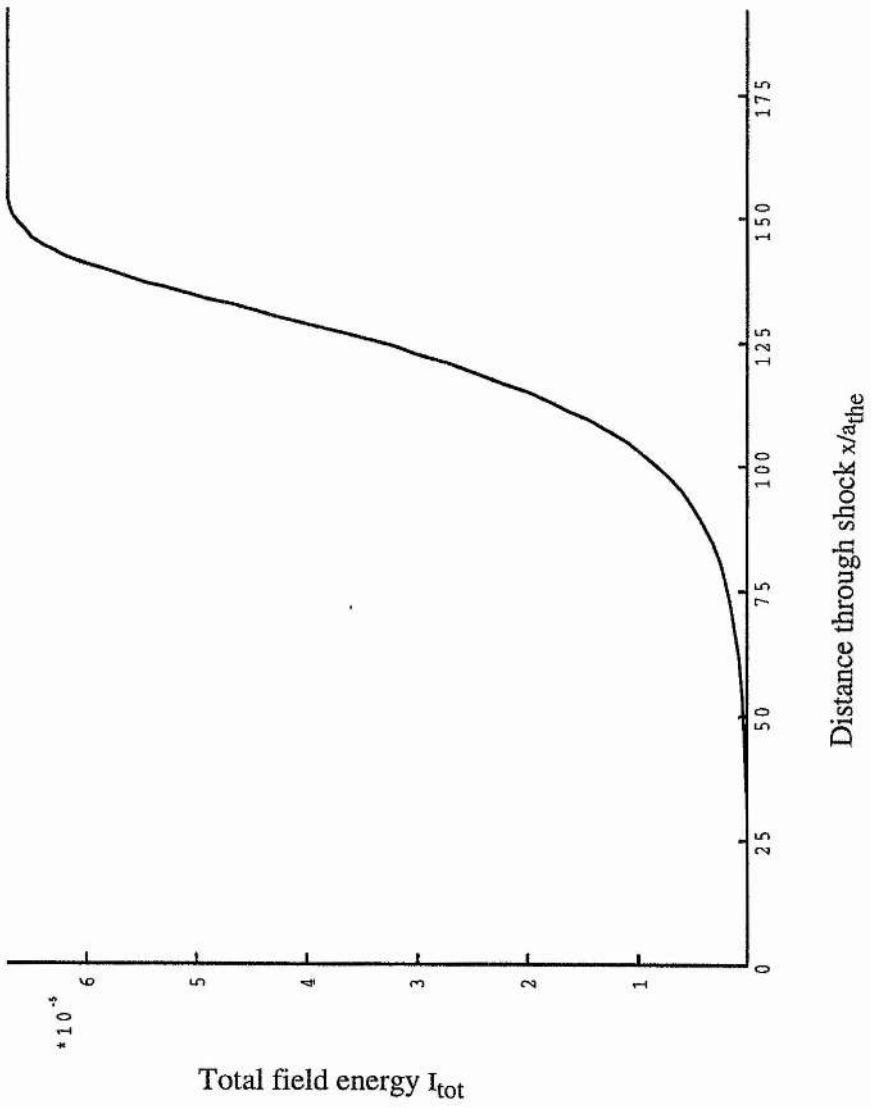

Figure 5.12: Maximum growth rate (in units of upstream gyrofrequency) versus distance through shock (in units of upstream thermal electron gyroradius).

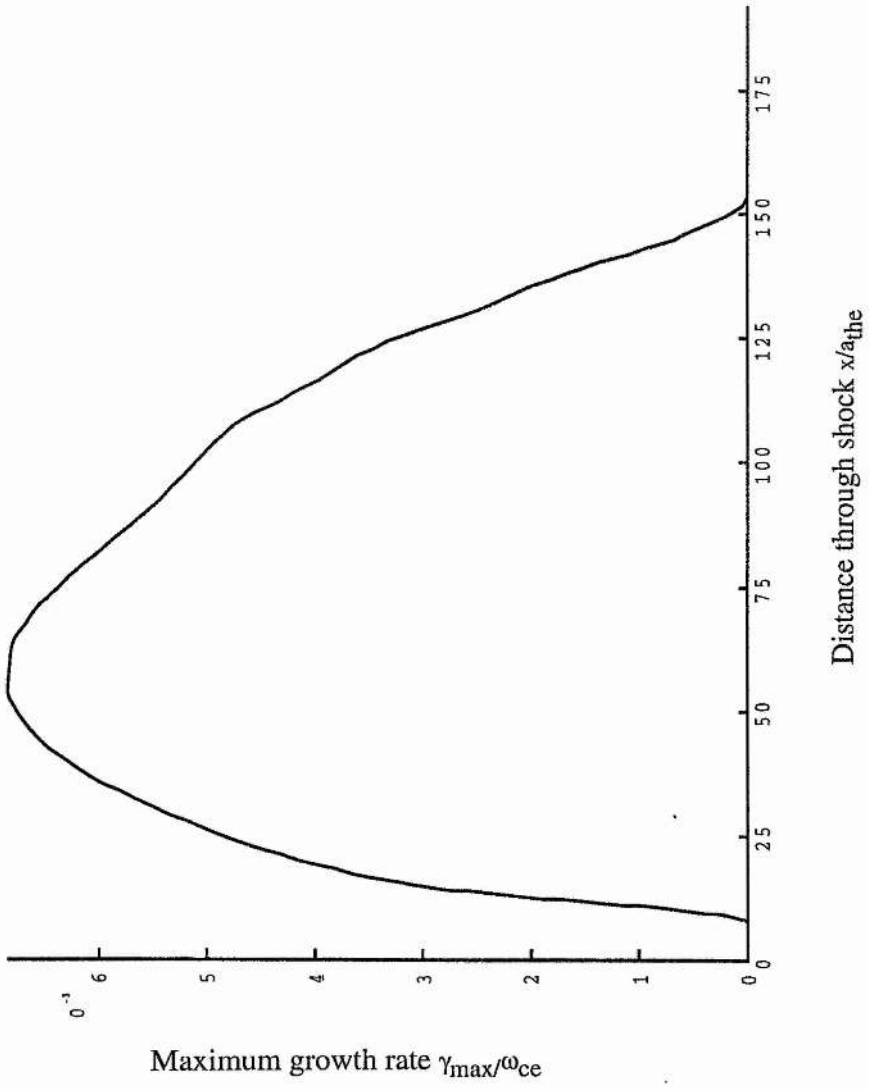

Appendix A

Conservation properties of the quasilinear equations

A.1 Conservation of energy

It is a property of quasilinear equations in general that they conserve matter and energy. In this section we will show that the equations derived in this thesis do possess these properties. The quasilinear diffusion equation is

$$\frac{\partial f_e}{\partial t} = \frac{\partial}{\partial \mu} \cdot \left[\mathsf{D_e} \cdot \frac{\partial}{\partial \mu} \mathbf{f_e} \right] \tag{A.1}$$

$$\mathsf{D_e} = \Re \left\{ i \frac{e^2}{m_e} \sum_n \sum_{\mathbf{k}} \mathbf{a}^*_{n,\mathbf{k}} \Omega^{-1}_{n,\mathbf{k}} \mathbf{a}_{n,\mathbf{k}} \right\} \tag{A.2}$$

The quantities $\mathbf{a}_{n,\mathbf{k}}$ and $\Omega^{-1}_{n,\mathbf{k}}$ are defined in equations and (3.35) (2.22) respectively. The electric and magnetic field amplitudes evolve according to

$$\frac{\partial \left| \delta \tilde{E}_{\mathbf{k}} \right|^2}{\partial t} = 2\gamma_{\mathbf{k}} \left| \delta \tilde{E}_{\mathbf{k}} \right|^2 \tag{A.3}$$

$$\frac{\partial \left| \delta \tilde{B}_{\mathbf{k}} \right|^2}{\partial t} = 2\gamma_{\mathbf{k}} \left| \delta \tilde{B}_{\mathbf{k}} \right|^2 \tag{A.4}$$

In this section, we will not take the ions into account at all. Equation (A.1) must conserve the total number of electrons since the right-hand side will dis-

appear when integrated over μ by Gauss's theorem, as long as the boundary conditions are right.

To prove that energy is conserved, we multiply (A.1) by $\frac{1}{2}m_e v^2 - e\varphi_0$, where $\varphi_0(x)$ is the potential of the background electric field, and integrate over $\mathbf{v}$ and Λ to give:

$$\begin{aligned}
\int\int \left[\frac{1}{2}m_e v^2 - e\varphi_0\right] \frac{\partial f_e}{\partial t} d\mathbf{v} d\Lambda &= \int \left[\frac{1}{2}m_e v^2 - e\varphi_0\right] \frac{\partial}{\partial \mu} \cdot \left[\mathsf{D_e} \cdot \frac{\partial}{\partial \mu}\mathbf{f_e}\right] d\mu \\
&= -\int \left[m_e \mathbf{v} - e\frac{\partial}{\partial \mu}\varphi_0\right] \cdot \mathsf{D_e} \cdot \frac{\partial}{\partial \mu}\mathbf{f_e} d\mu \\
&= \Re\left\{-i\frac{e^2}{m_e}\sum_n \sum_{\mathbf{k}} [\mathbf{v} - v_E \omega_{ce}\hat{\mathbf{e}}_x] \cdot \mathbf{a}^{\star}_{n,\mathbf{k}} \Omega^{-1}_{n,\mathbf{k}} \right. \\
&\qquad \left. \mathbf{a}_{n,\mathbf{k}} \cdot \frac{\partial}{\partial \mu} f_e \right\} \qquad \text{(A.5)}
\end{aligned}$$

Where we have used the fact that $\frac{\partial}{\partial \mu}\varphi_0 = -E_x = v_E B_0$. This term represents the rate of change of energy due to the evolution of the background distribution function. Now,

$$\begin{aligned}
[\mathbf{v} - v_E\hat{\mathbf{e}}_\Lambda] \cdot \mathbf{a}_{n,\mathbf{k}} &= -v_E a_{n,\Lambda,\mathbf{k}} + v_\perp a_{n,\perp,\mathbf{k}} + v_{||} a_{n,||,\mathbf{k}} \\
&= \frac{v_E}{\Omega_{\mathbf{k}}}\left[ik_\perp v_\perp J_n' \delta\tilde{E}_{x,\mathbf{k}} + \left(\Omega_{\mathbf{k}} - k_{||}v_{||}\right) J_n \delta\tilde{E}_{y,\mathbf{k}} \right. \\
&\qquad \left. + k_\perp v_{||} J_n \delta\tilde{E}_{||,\mathbf{k}}\right] \\
&\quad + i\frac{v_\perp}{\Omega_{\mathbf{k}}}\left(\Omega_{\mathbf{k}} - k_\perp v_E - k_{||}v_{||}\right) J_n' \delta\tilde{E}_{x,\mathbf{k}} \\
&\quad + \frac{(n\omega_{ce} + k_\perp v_B)}{k_\perp}\frac{\left(\Omega_{\mathbf{k}} - k_{||}v_{||}\right)}{\Omega_{\mathbf{k}}} J_n \delta\tilde{E}_{y,\mathbf{k}} \\
&\quad + \frac{v_{||}}{\Omega_{\mathbf{k}}}\left(n\omega_{ce} + k_\perp v_B\right) J_n \delta\tilde{E}_{||,\mathbf{k}} \\
&\quad + iv_\perp \frac{k_{||}v_{||}}{\Omega_{\mathbf{k}}} J_n' \delta\tilde{E}_{x,\mathbf{k}} + \frac{(n\omega_{ce} + k_\perp v_D)}{\Omega_{\mathbf{k}}}\frac{k_{||}v_{||}}{k_\perp} J_n \delta\tilde{E}_{y,\mathbf{k}} \\
&\quad + \left(\Omega_{\mathbf{k}} - k_\perp v_D - k_{||}v_{||}\right)\frac{v_{||}}{\Omega_{\mathbf{k}}} J_n \delta\tilde{E}_{||,\mathbf{k}} \\
&= iv_\perp J_n' \delta\tilde{E}_{x,\mathbf{k}} + \frac{(n\omega_{ce} + k_\perp v_B)}{k_\perp} J_n \delta\tilde{E}_{y,\mathbf{k}} + v_{||} J_n \delta\tilde{E}_{||,\mathbf{k}}
\end{aligned} \qquad \text{(A.6)}$$

on collecting together terms in $\delta\tilde{E}_{x,\mathbf{k}}$, $\delta\tilde{E}_{y,\mathbf{k}}$ and $\delta\tilde{E}_{\|,\mathbf{k}}$, and performing the necessary cancellations.

The current density of the $\mathbf{k}^{th}$ mode is:

$$\delta\tilde{\mathbf{j}}_{\mathbf{k}} = -i\frac{e^2}{m_e}\sum_n \int \left(-iv_\perp J_n', \frac{(n\omega_{ce}+k_\perp v_D)}{k_\perp} J_n, v_\| J_n\right) \Omega_{n,\mathbf{k}}^{-1}\mathbf{a}_{n,\mathbf{k}} d\mathbf{v} \qquad (A.7)$$

so that (A.5) with (A.6) and (A.7) gives:

$$\frac{\partial}{\partial t}\int \left[\frac{1}{2}m_e v^2 - e\varphi_0\right] f_e d\mu = \Re\left\{\sum_{\mathbf{k}} \tilde{\mathbf{E}}_{\mathbf{k}}^\star \cdot \tilde{\mathbf{j}}_{\mathbf{k}}\right\} = \int \langle \delta\mathbf{E}\cdot\delta\mathbf{j}\rangle \, d\Lambda \qquad (A.8)$$

The rate of change of the energy of the particle distribution is thus balanced by the averaged power in the waves excited in the system.

We now use the Fourier transformed versions of Maxwell's equations to write the right-hand side of A.8 in terms of the amplitudes of the rapidly varying wave fields:

$$i\mathbf{k}\wedge\delta\tilde{\mathbf{B}}_{\mathbf{k}} = \mu_0\delta\tilde{\mathbf{j}}_{\mathbf{k}} - i\mu_0\varepsilon_0\Omega_{\mathbf{k}}\delta\tilde{\mathbf{E}}_{\mathbf{k}} \qquad (A.9)$$

$$\mathbf{k}\wedge\delta\tilde{\mathbf{k}}_{\mathbf{k}} = \Omega_{\mathbf{k}}\delta\tilde{\mathbf{B}}_{\mathbf{k}} \qquad (A.10)$$

Multiplying (A.9) by $\delta\tilde{\mathbf{B}}_{\mathbf{k}}^\star$ and (A.10) by $\delta\tilde{\mathbf{E}}_{\mathbf{k}}^\star$ and eliminating the term proportional to $\delta\tilde{\mathbf{E}}_{\mathbf{k}}\wedge\delta\tilde{\mathbf{B}}_{\mathbf{k}}$ gives

$$\delta\tilde{\mathbf{E}}_{\mathbf{k}}^\star\cdot\delta\tilde{\mathbf{j}}_{\mathbf{k}} - i\varepsilon_0\Omega_{\mathbf{k}}\left|\delta\tilde{\mathbf{E}}_{\mathbf{k}}\right|^2 + \frac{\Omega_{\mathbf{k}}^\star}{\mu_0}\left|\delta\tilde{\mathbf{B}}_{\mathbf{k}}\right|^2 = 0 \qquad (A.11)$$

If we sum (A.11) over $\mathbf{k}$ and use the symmetry properties (3.7) to (3.9), we can deduce that:

$$\sum_{\mathbf{k}}\left[\delta\tilde{\mathbf{E}}_{\mathbf{k}}^\star\cdot\delta\tilde{\mathbf{j}}_{\mathbf{k}} + \varepsilon_0\gamma_{\mathbf{k}}\left|\delta\tilde{\mathbf{E}}_{\mathbf{k}}\right|^2 + \frac{1}{\mu_0}\gamma_{\mathbf{k}}\left|\delta\tilde{\mathbf{B}}_{\mathbf{k}}\right|^2\right] = 0$$

$$\Rightarrow \quad \sum_{\mathbf{k}}\left[\delta\tilde{\mathbf{E}}_{\mathbf{k}}^\star\cdot\delta\tilde{\mathbf{j}}_{\mathbf{k}} + \frac{1}{2}\varepsilon_0\frac{\partial}{\partial t}\left|\delta\tilde{\mathbf{E}}_{\mathbf{k}}\right|^2 + \frac{1}{2\mu_0}\frac{\partial}{\partial t}\left|\delta\tilde{\mathbf{B}}_{\mathbf{k}}\right|^2\right] = 0 \qquad (A.12)$$

Using (A.8) we obtain:

$$\frac{\partial}{\partial t}\int\left[\frac{1}{2}m_e v^2 - e\varphi_0\right] f_e d\mu + \frac{\partial}{\partial t}\int\sum_{\mathbf{k}}\left[\frac{1}{2}\varepsilon_0\left|\delta\tilde{\mathbf{E}}_{\mathbf{k}}\right|^2 + \frac{1}{2\mu_0}\left|\delta\tilde{\mathbf{B}}_{\mathbf{k}}\right|^2\right] d\Lambda = 0 \qquad (A.13)$$

Therefore, on integrating:

$$\int \left[\frac{1}{2}m_e v^2 - e\varphi_0\right] f_e d\mu + \sum_{\mathbf{k}} \int \left[\frac{1}{2}\varepsilon_0 \left|\delta\tilde{\mathbf{E}}_{\mathbf{k}}\right|^2 + \frac{1}{2\mu_0}\left|\delta\tilde{\mathbf{B}}_{\mathbf{k}}\right|^2\right] d\Lambda = T \qquad \text{(A.14)}$$

where T is the total (wave plus particle) energy of the system. The first term is the particle energy. The other term represents the total (electric plus magnetic) energy of the waves. These equations have all been derived for a discrete wave spectrum: however, similar expressions will hold for the continuous spectrum case, with the summations becoming integrations.

A.2 Conservation of momentum

In the case of electrostatic waves, it is also easy to show that the parallel component of the electron momentum is conserved. The diffusion equation is:-

$$\frac{\partial f_e}{\partial t} = \frac{\partial}{\partial \mu} \cdot \left[\mathsf{D}_\mathbf{e} \cdot \frac{\partial}{\partial \mu}\mathbf{f_e}\right] \qquad \text{(A.15)}$$

where

$$\mathsf{D}_\mathbf{e} = \Re\left\{-i\frac{e^2}{m_e^2}\sum_n\sum_{\mathbf{k}} \mathbf{b}_{n,\mathbf{k}} \frac{J_n^2(a_\perp) I_{\mathbf{k}}}{(\Omega_{\mathbf{k}} - k_\perp v_D - k_{||} v_{||} - n\omega_{ce})} \mathbf{b}_{n,\mathbf{k}}\right\} \qquad \text{(A.16)}$$

$$\mathbf{b}_{n,\mathbf{k}} = -k_\perp \hat{\mathbf{e}}_\Lambda + \frac{(n\omega_{ce} + k_\perp v_B)}{v_\perp}\hat{\mathbf{e}}_\perp + k_{||}\hat{\mathbf{e}}_{||} \qquad \text{(A.17)}$$

$$I_{\mathbf{k}}(t) = \left|\delta\tilde{\varphi}_{\mathbf{k}}(t)\right|^2 \qquad \text{(A.18)}$$

and the frequency $\Omega_{\mathbf{k}} = \omega_{\mathbf{k}} + i\gamma_{\mathbf{k}}$ is related to the wavelength by the dispersion relation:

$$\begin{aligned} K &= 1 + \frac{e^2}{m_e\varepsilon_0 k^2}\sum_n\sum_{\mathbf{k}}\int \frac{J_n^2(a_\perp)}{\left(\Omega_{\mathbf{k}} - k_\perp v_D - k_{||}v_{||} - n\omega_{ce}\right)} \\ &\quad \times \left[-k_\perp\frac{\partial}{\partial\Lambda} + \frac{(n\omega_{ce} + k_\perp v_B)}{v_\perp}\frac{\partial}{\partial v_\perp} + k_{||}\frac{\partial}{\partial v_{||}}\right] f_e d\mathbf{v} \\ &= 0 \end{aligned} \qquad \text{(A.19)}$$

We multiply (A.15) by $m_e v_\parallel$ and integrate over μ. Thus:

$$\begin{aligned}
\int m_e v_\parallel \frac{\partial f_e}{\partial t} d\mu &= \int m_e v_\parallel \frac{\partial}{\partial \mu} \cdot \left[\mathsf{D}_\mathbf{e} \cdot \frac{\partial}{\partial \mu} \mathbf{f_e} \right] d\mu \\
&= \Re \left\{ -i \frac{e^2}{m_e} \sum_n \sum_\mathbf{k} \int \hat{\mathbf{e}}_\parallel \cdot \mathbf{a}_{n,\mathbf{k}} J_n^2 \Omega_{n,\mathbf{k}}^{-1} I_\mathbf{k} \mathbf{a}_{n,\mathbf{k}} \cdot \frac{\partial}{\partial \mu} f_e d\mu \right\} \\
&= \sum_\mathbf{k} \varepsilon_0 k^2 I_\mathbf{k} \Im\{K\} \\
&= 0 \qquad \text{(A.20)}
\end{aligned}$$

by virtue of the dispersion relation (A.19). Thus we see that

$$\int m_e v_\parallel f_e d\mathbf{v} = p_\parallel = \text{constant} \qquad \text{(A.21)}$$

as required.

Bibliography

[1] **Abramowitz, M. and Stegun, I.A.** *Handbook of Mathematical Functions* Dover 1965

[2] **Armstrong, T.P.** *Phys. Fluids* 10,1269,(1967)

[3] **Armstrong T.P. and Montgomery, D.** *J. Plas. Phys.* 1,425,(1967)

[4] **Berk, H.L.** *J. Plas. Phys.* 20,205,(1978)

[5] **Bernstein, I.B.** *Phys. Rev.* 109,10,(1958)

[6] **Cairns, R.A.** *Il Nuovo Cimento* 2C,712,(1979)

[7] **Colgate, S.A. and Hartman, C.W.** *Ann. Physics* 10,1288,(1967)

[8] **Davidson, R.C., Gladd, N.T., Wu, C.S. and Huba, J.D.** *Phys. Fluids* 20,301,(1971)

[9] **Dawson, J.** *Phys. Fluids* 5,445,(1962)

[10] **Drummond, W.E., and Pines, D.** *Ann. Physics* 28,478,(1964)

[11] **Feldman, W.C., Bame, S.J., Gary. S.P., Gosling, J.T., McComas, D. and Thomsen, M.F.** *Phys. Rev. Lett.* 49,199,(1982)

[12] **Fried, B.D. and Conte, S.D.** *The Plasma Dispersion Function* Academic Press 1961

[13] **Gary, S.P.** *Plasma Physics* 15,399,(1973)

[14] **Gary, S.P.** *J. Plas. Phys.* 4,753,(1970)

[15] **Gary, S.P. and Paul, J.W.M.** *Phys. Rev. Lett.* 26,1097,(1971)

[16] **Gary, S.P. and Sanderson, J.J.** *J. Plas. Phys.* 4,739,(1970)

[17] **Gladd, N.T.** *Plasma Physics* 18,27,(1976)

[18] **Goodrich, L.C., Durney, C.H. and Grow. R.W.** *Plasma Physics* 14,715,(1972)

[19] **Gourlay,A.R.** *J.Inst.Maths.Applics.* 6,375,(1970)

[20] **Gourlay,A.R. and McGuire, G.R.** *J.Inst.Maths.Applics.* 7,216,(1971)

[21] **Gourlay,A.R. and McKee, S.** *J. Comp. Appl. Math.* 3,201,1987

[22] **Grant, F.C. and Feix, M.R.** *Phys. Fluids* 10,696,(1967)

[23] **Hockney, R.W. and Eastwood, J.W.** *Computer Simulation using Particles* Adam Hilger 1988

[24] **Hsia, J.B., Chiu, S.M., Hsia, M.F., Chou, R.L. and Wu C.S.** *Physics of Fluids* 22,1737,(1979)

[25] **Kennel, C.F. and Engelmann, F.** *Phys. Fluids* 9,2377,(1966)

[26] **Krall, N.A. and Book, D.L.** *Phys. Fluids* 12,347,(1969)

[27] **Krall, N.A. and Book, D.L.** *Phys. Rev. Lett.* 23,574,(1969)

[28] **Krall, N.A. and Liewer, P.C.** *Phys. Rev.* A4,2094,(1971)

[29] **Lamb, H.** *Hydrodynamics,* §*282* Cambridge University Press 1945 (Sixth Edition)

[30] **Lampe, M., Manheimer, W.M., Orens, J.H., Papadopoulos,K., Shanny, R., Sudan, R.N.** *Phys. Fluids* 15,662,(1972)

[31] **Lampe, M., Manheimer, W.M., Orens, J.H., Papadopoulos,K., Shanny, R., Sudan, R.N.** *Phys. Rev. Lett.* 26,1221,(1972)

[32] **Lashmore-Davies, C.N.** *J. Phys.* 3A,L40,(1970)

[33] **Lashmore-Davies, C.N.** *Phys. Fluids* 14,1481,(1971)

[34] **Lembege,B.** in *Physical Processes in Hot Cosmic Plasma* Eds. Brinkman, W., Fabian, A.C., and Giovanelli, F. Kluwer Academic Publishers (1990)

[35] **McBride, J.B., Ott, E., Boris, J.P. and Orens, J.H.** *Phys. Fluids* 15,2367,(1972)

[36] **Manheimer, W.M. and Boris, J.P.** *Phys. Rev. Lett.* 28,659,(1972)

[37] **Mitchell, A.R. and Griffiths, D.F.** *Finite Difference Methods in Partial Differential Equations* Wiley-Interscience 1980

[38] **Morawetz, C.S.** *Phys. Fluids* 4,988,(1961)

[39] **Morawetz, C.S.** *Phys. Fluids* 5,1447,(1962)

[40] **Ness, N.F., Scearce, C.S. and Seek, J.B.** *J. Geo. Res.*,69,3531,(1964)

[41] **Papadopoulos, K.** in *Proceedings of a Workshop on Plasma Astrophysics held at Varenna, Italy* p. 409 (1981)

[42] **Press, W.H., Flannery, B.P., Teukolsky, S.A. and Vetterling, W.T.** *Numerical Recipes: The Art of Scientific Computing* Cambridge University Press, 1989.

[43] **Revathy, P. and Lakhina, G.S.** *J. Plas. Phys.* 17,133,(1977)

[44] **Rodman, R.D.** *Comm. A.C.M.* 6,441,(1963)

[45] **Sagdeev, R.Z.** *Rev. Mod. Phys.* 51,11,(1979)

[46] **Thomsen, M.F., Barr, H.C., Gary, S.P., Feldman, W.C. and Cole, T.E.** *J. Geo. Res.*,88,3035,(1983)

[47] **Thomsen, M.F., Gosling, J.T., Bame, S.J. and Mellott, M.M.** *J. Geo. Res.*,90,,(1985)

[48] **Tidman, D. and Krall, N.A.** *Shock Waves in Collisionless Plasmas* Wiley-Interscience 1971

[49] **Vedenov,A., Velikov,E. and Sagdeev,R.Z.** *Nuclear Fusion* 1,82,(1961)

[50] **Whitley, V.W.** *Comm. A.C.M.* 11,12,(1968)

[51] **Winske, D., Giacolone, J. Thomsen, M.F., and Mellott, M.M.** *J. Geo. Res.* 92,4411,(1987)